DOKUZ EYLÜL UNIVERSITY
GRADUATE SCHOOL OF NATURAL AND APPLIED SCIENCES

# ELECTRONIC STRUCTURE OF QUANTUM DOTS

by

Serpil ŞAKİROĞLU

January, 2009
İZMİR

# ELECTRONIC STRUCTURE OF QUANTUM DOTS

**A Thesis Submitted to the**
**Graduate School of Natural and Applied Sciences of Dokuz Eylül University**
**In Partial Fulfillment of the Requirements for the Degree**
**of Doctor of Philosophy in**
**Physics**

**by**

**Serpil ŞAKİROĞLU**

**January, 2009**
**İZMİR**

**Ph.D. THESIS EXAMINATION RESULT FORM**

We have read the thesis entitled **"ELECTRONIC STRUCTURE OF QUANTUM DOTS"** completed by **SERPİL ŞAKİROĞLU** under supervision of **PROF. DR. İSMAİL SÖKMEN** and we certify that in our opinion it is fully adequate, in scope and in quality, as a thesis for the degree of Doctor of Philosophy.

.....

Prof. Dr. İsmail SÖKMEN

Supervisor

| | |
|---|---|
| ..... | ..... |
| Prof. Dr. Kadir YURDAKOÇ | Prof. Dr. Doğan DEMİRHAN |
| Thesis Committee Member | Thesis Committee Member |
| ..... | ..... |
| Prof. Dr. Yüksel ERGÜN | Yard. Doç. Dr. Kadir AKGÜNGÖR |
| Examining Committee Member | Examining Committee Member |

Prof. Dr. Cahit HELVACI
Director
Graduate School of Natural and Applied Sciences

## ACKNOWLEDGEMENTS

It is a great pleasure for me to be at this point of my work when I have the opportunity to acknowledge and thank all the people who brought his contribution in a way or another during my PhD works.

First of all, I would like to express my deepest gratitude to my supervisor Prof. Dr. İsmail SÖKMEN for his excellent guidance, endless patience, continual encouragement and insightful suggestions throughout this work. His invaluable scientific contributions and enlightening on several physical concepts related to the theory and methods are irreplaceable for my further scientific carriers. I have greatly benefited from his thorough knowledge and expertise in semiconductor and computational physics. Professor SÖKMEN taught me not only his precious knowledge, but also his responsibility and strict attitude.

I am indebted to Assis. Prof. Dr. Kadir AKGÜNGÖR for much support, excellent motivation, fruitful discussions, valuable recommendations and contributions especially in preparation of the publications. This work would not been possible without his assistance in providing and administering excellent computer facilities.

At this point, I am also grateful to Assoc. Prof. Dr. Ceyhun BULUTAY at the Bilkent University for the successful collaboration and for the hospitality during my three months visit.

This last paragraph I devote to people whom I am deeply emotionally connected with, my wonderful and loving family. Without their love and constant support nothing of this would be possible. SEVİNÇ thank you for being such a nice sister. I have no words to express my gratitude to my parents, FATMA and SELİM for their confidence in me all through my journey of life. They always encouraged me to pursue my goals and never to give up. And I certainly will not to !

Serpil ŞAKİROĞLU

*This thesis is dedicated to my mother and father.*

## ELECTRONIC STRUCTURE OF QUANTUM DOTS


### ABSTRACT

In this thesis, an efficient method for reducing the computational effort of variational calculations with Hylleraas-like wavefunctions is introduced. The method consists in introducing integral transforms for the terms as $r_{12}^k \exp(-\lambda r_{12})$ arising out from the explicitly correlated wavefunctions. Introduced integral transforms provide the calculation of expectation value of energy and the related matrix elements to be done analytically over single-particle coordinates instead of Hylleraas coordinates.

We have applied the method to calculate the ground state energies of different types of two-particle systems (atomic systems and artificial atoms). The first application of the present method has been done on atomic two-particle systems. The ground state energies of helium and a few helium-like ions with nuclear charge $Z = 1 - 6$ were computed by four-parameters wavefunction, satisfying the boundary conditions for coalescence points and combined with Hylleraas-like basis set. To further the investigation of the applicability of the method, we have studied the ground state energies of electron-hole pair and two electrons in zero-dimensional semiconductor systems. The effects of quantum confinement on the ground state energy of a correlated electron-hole pair in a spherical and in a disk-like quantum dot have been investigated as a function of quantum dot size. Moreover, under parabolic confinement potential and within effective mass approximation, size and shape effects of quantum dots on the ground state energy of two electrons have been studied.

The results show that, the method proposed in this thesis provides powerful tool to obtain the ground state energy of two-particle systems. With a properly chosen trial wavefunctions, variational determination of the ground state energy of two-particle systems were achieved without time-consuming numerical calculations. The results of calculations even with a small number of basis sets are in good agreement with previous theoretical works given in literature.



**Keywords:** quantum dot, exciton, Hylleraas basis, Ritz's method

## KUANTUM NOKTALARIN ELEKTRONİK YAPISI

## ÖZ

Bu tezde, Hylleraas-benzeri deneme dalgafonksiyonlarını kullanan varyasonel hesaplamalardaki sayısal uğraşıları azaltmak için etkin bir yöntem sunulmaktadır. Yöntem, açıkça bağlantılı olan dalgafonksiyonlarından ortaya çıkan $r_{12}^k \exp(-\lambda r_{12})$ gibi terimler için integral dönüşümlerinin takdim edilmesine dayanmaktadır. Sunulan integral temsilleri, enerjinin beklenen değerinin ve ilgili matris elemanlarının Hylleraas koordinatları yerine tek-parçacık koordinatları üzerinden analitik olarak hesaplanabilmesini sağlamaktadır.

Bu yöntemi farklı tipte iki-parçacıklı sistemlerin (atomik sistemler ve yapay atomlar) taban durum enerjilerini hesaplamak için uyguladık. Sunulan yöntemin ilk uygulaması iki-parçacıklı atomik sistemler üzerine gerçeklenmiştir. Çekirdek yükü $Z = 1 - 6$ olan Helyum ve birkaç helyum-benzeri iyonların taban durum enerjileri, birleşim noktalarında sınır koşullarını sağlayan ve Hylleraas benzeri baz seti ile birleştirilmiş dört-parametreli dalgafonksiyonu kullanarak hesaplanmıştır. Yöntemin uygulanabilirliği üzerindeki incelemeleri daha ileri götürmek için sıfır boyutlu yarıiletken sistemlerdeki elektron-deşik çifti ve iki elektronun taban durum enerjisini inceledik. Kuantum kuşatmanın küresel ve disk-benzeri kuantum noktasındaki korele elektron-deşik çiftinin taban durum enerjisi üzerindeki etkileri, kuantum noktanın büyüklüğünün fonksiyonu olarak araştırılmıştır. Ayrıca parabolik hapsetme potansiyeli altında ve etkin kütle yaklaşımı içerisinde, iki elektronun taban durum enerjisi üzerindeki kuantum noktanın büyüklük ve biçim etkileri incelenmiştir.

Sonuçlar, bu çalışmada önerilen yöntemin iki-parçacıklı sistemlerin taban durum enerjisinin elde edilmesi için güçlü bir araç olduğunu göstermektedir. Seçilen uygun deneme dalgafonksiyonu ile iki-parçacıklı sistemlerin taban durum enerjisinin varyasyonel belirlenmesi zaman alan nümerik hesaplar kullanmaksızın gerçeklenmektedir. Sonuçlar, az sayıda baz seti ile bile, literatürde verilen daha önceki teorik çalışmalarla uyum içindedir.

**Anahtar sözcükler:** kuantum nokta, ekziton, Hylleraas bazı, Ritz's yöntemi

**CONTENTS**

# CHAPTER ONE
# INTRODUCTION

*"A journey of a thousand miles starts with one single step..."*
An old Buddhist saying

In the rapidly expanding field of nanotechnology, semiconductor quantum dots have proven to be a fascinating laboratory to observe interesting phenomena with profound implications on the basic solid state physics and great potential for application in future technology (Masumoto, & Takagahara, 2002; Bellucci, 2005; Michler, 2003; Jacak, Hawrylak, & Wojs, 1998). They have dimensions from nanometers to a few microns and contain a controlled number of electrons, typically from one to several thousands. The tunable shape, size, and electron number of these "artificial atoms", as well as their pronounced electron-electron correlation effects, make them excellent objects for studying various many-electron phenomena.

The aim in this work is to study the electronic structure and the correlation picture in regimes of parabolically confining spherical quantum dot potential. In general the calculation of the electronic structure of a system of many electrons cannot be solved exactly. Variational methods are powerful tool for studying the Coulomb-three body bound-state problems. This well-known and effective method builds very accurate solutions of the Schrödinger equation and has numerous applications in many field of physics. Approximate calculations based on basis sets are standard practice. The approach using basis sets, which has been adopted in this work, usually has an advantage of analytical calculation of the required single- and double-electron integrals. The disadvantage in the approach however is the incompleteness of the desired basis set.

In this work, we proposed an efficient method for reducing the computational effort of variational calculation with Hylleraas-like trial wavefunction. The method consists in introducing integral transforms for the terms as $r_{12}^k \exp(-\lambda r_{12})$. This leads to the significant simplification of the calculation of expectation value of energy and the related matrix elements.

For this study two-electron atomic systems have been used as starting point of the method adopted here. Numerical calculations for the ground state energies for Helium-like ions with the nuclear charge up to $Z = 6$ have been performed. Relatively simple wavefunction for obtaining the ground state energy of two-electron atoms is constructed in terms of exponential and power series. In order to fulfill conditions for coalescence points special care is taken. Our work, with low number of parameters, is based on modifying and extending the wavefunction proposed by (Bhattacharyya, Bahttacharyya, Talukdar, & Deb, 1996) with Hylleraas-like basis set to get improved accuracy than the work done by them for He atom and apply the same wavefunction for He-like ions. Variational parameters for improved versions of ground state wavefunction have been determined.

The present work also focuses on calculation of ground state energies of two-particle systems, electron-electron pair and correlated electron-hole pair, in spherically and cylindrically symmetric quantum dots subjected to isotropic harmonic potential. Within the framework of Ritz's variational approach and effective-mass approximation, trial wavefunctions constructed by extending the harmonic oscillator basis to the fully correlated Hylleraas-like one have been used as a trial functions. The basic assumptions here is that charge carriers are subjected to the unscreened confining potential and distortion of Coulomb interaction formed due to the difference between dielectric constants of quantum dot and matrix material is neglected.

A two-particle quantum dot is first nontrivial case of many particle systems. Analytical and approximate solutions for the two-electron quantum dot problem have been reported. The harmonic oscillator potential has been extensively used as a model potential for real quantum dots in the calculation of the energies of low lying states (Halonen, Chakraborty, & Pietilainen, 1992; Elsaid, 2002; Zhu, Li, Yu, Ohno, & Kawazoe, 1997; Xie, 2000; Pino, & Villalba, 2001; Harju, Siljamaki & Nieminen, 2002; Ciftja, & Kumar, 2002). In the second and third stage of the present work, benefits derived from explicitly correlated wavefunction and analytical convenience provided by the profile of confining potential have been used. The harmonic oscillator model has of course undeniable merits with regard to the analytic form of the one-particle energies and wavefunctions and assistance to the analytical calculation of the matrix elements when expanded in basis of harmonic oscillator functions (Kimani, 2008). This is particularly convenient for the calculation of the integrations over single-particle coordinates. The effects of quantum confinement and many-body interactions on the ground state energies of semiconductor quantum dots are investigated.

Optical properties of three-dimensionally confined electrons and holes in semiconductor quantum dots have been extensively studied in recent years from the interest in the fundamental physics of finite systems as well as in their potential use as efficient nonlinear optical and laser materials (Masumoto, & Takagahara, 2002). The interaction between confined electrons and holes is more effective than their bulk counterparts and confined exciton binding energy is enhanced. In the present work the size and shape effects on the ground state energy for parabolically confined heavy- and light-hole excitons in QDs have been studied.

This work is organized as follows: In Chapter 2 we give a brief overview of quantum dots and their fabrication techniques. We present the fundamental

electronic structure methods and explicitly correlated wavefunctions in Chapter 3. Chapter 4 is devoted to introduce the method and formalism used in this work. Application of the method and results obtained for the systems with two -distinguishable and -indistinguishable particles is given in Chapter 5. A short concluding chapter summarizes our findings.

# CHAPTER TWO
# QUANTUM DOTS

## 2.1 Artificial Atoms: An overview

Bulk crystalline semiconductors started a new era in the development of science and technology. Their optical and electronic properties constitute the basis of an entire industry including electronics, telecommunications, microprocessors, computers and many other components of modern technology. Further innovation was brought by reducing the semiconductor's spatial dimensions, leading to huge enhancement in their optical nonlinearities due to confinement of the carriers (Babocsi, 2005). A semiconductor heterostructure is called to be of reduced dimensionality, when the motion of at least one type of charge carriers is confined in at least one direction within a spatial extent comparable to the de-Broglie wavelength of the carriers. The carriers momentum in that direction is quantized and its energy spectrum is given by the discrete solutions of the Schröodinger equation, the eigenenergies. As a consequence the carrier has a non-vanishing minimum kinetic energy, the quantum confinement energy. For confinement in one, two, and three dimensions the expressions quantum well (QW), quantum wire (QWR) and quantum dot (QD) have been established, as shown in Figure 2.1.

Semiconductor quantum dots (QDs) are very small three-dimensional (3D) artificial semiconductor based structures whose dimension ranges from nanometers to tens of nanometers in all three directions (Mlinar, 2007; Masumoto, & Tagahara, 2002). Their confinement, smaller than de Broglie wavelength in semiconductors, leads to a discrete energy spectrum and a delta function atomic-like density of states, which enables the analogy with real atoms.

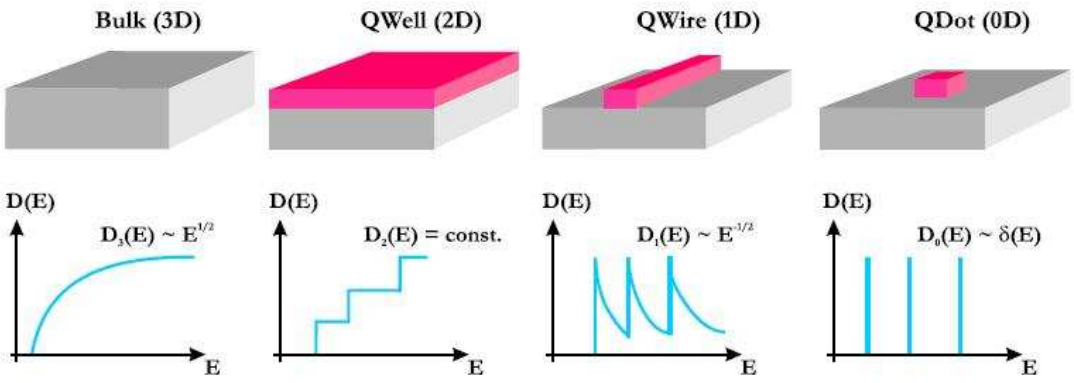


Figure 2.1 Density of states of the bulk, quantum well, quantum wire, and quantum dot.

Therefore, QDs are often referred to as artificial atoms although containing from $10^3$ to $10^5$ atoms. Furthermore, the coupling between QDs to obtain new functional units, leads to a formation of quantum dot molecules (Michler, 2003). With respect to to system sizes, these structures are intermediate between molecular and bulk systems so the structure of dot shows both molecular and bulk features (Kouwenhoven, Austing, & Tarucha, 2001).

The interior of the quantum dot contains a crystal structure which resembles a bulk crystal. However, the periodicity of the crystal is violated near the dot surface before the dot size reaches an infinite volume limit. The electronic properties of QDs show many analogies with those of atoms; the most relevant is their discrete energy spectrum resulting from confinement: electrons and holes occupy discrete quantum levels, similarly to the physical situation in atoms (Bellucci, 2005). A characteristic quantity for QDs is the addiction energy, analogous to the ionization energy of an atom, which is the energy required to add or remove one electron from the dot. The addiction energy is a finite quantity, experimentally measurable injecting carriers one by one on to the QD in Single-Electron Tunnelling Spectroscopy (SETS) or capacitance experiments (Kouwenhoven et al., 2001; Reusch, 2003). Shell structure for the correlated electron system, magic numbers, singlet-triplet transitions and fine corrections to

the energy due to exchange interactions (Hund's rule) (Bellucci, 2005).

However, quantum dots show important differences with respect to natural atoms: for example in QDs the number of charge carriers N is tunable starting from N = 0, and the characteristic lengths of the system corresponding to external confinement potential, electron-electron interaction, and an applied magnetic field are of comparable size. Even if electrons are free to move in a quantum dot, the mass of electrons is different from a free electron mass due to the surrounding host semiconductor material (Helle, 2006). Usually the electrons in the QD devices can be described with an effective-mass approximation. Some of these factors are favorable to explore the fundamentals of few-body interacting systems: for example, the relatively large dimensions of QDs make that experimentally accessible magnetic field regimes (up to s 20 T) correspond to regimes of the order 106 T for real atoms. Therefore, applying external fields generated by standard laboratory sources, transitions never observed in the spectra of natural atoms can be seen in the artificial ones (Siljamaki, 2003). Moreover, due to the increased role of electron-electron interactions, these systems exhibit new physics which has no analogue in real atoms. In addition to the fact that QDs are excellent laboratory to investigate the properties of few-body strongly interacting systems, the basic technological motivation to study QDs is that smaller electronic components should be faster and may also dissipate less heat; besides, quantum-mechanical effects are so important in such systems that devices with fundamentally new properties could be obtained. In this perspective relevant examples are single-electron transistors, or micro-heaters and micro-refrigerators based on thermoelectric effects. Otherwise, since QDs absorb and emit light in a very narrow spectral range, they might find application in the realization of more efficient and more controllable semiconductor lasers. The strong quantization of electron energy, with parameters suitable for laser action, will probably allow QD-based lasers to operate at higher temperatures and lower injection currents

(Bellucci, 2005; Mlinar, 2007). The small dimensions and the possibility of dense packing of QD matrices could also permit them to be used for computer memory media of huge capacity; furthermore, recent advances in nanoscale fabrication techniques have raised hopes for the possible realization of QD-based scalable quantum computing devices. Indeed, the demonstration of spin effects in QDs and the unusually long spin dephasing times make the electron spin in QDs a natural candidate for the quantum bit (qubit), the fundamental unit of quantum information processing. Some years ago, in a famous proposal, it have been shown that spin qubits in QDs satisfy all requirements for realizing a scalable quantum computer (Rasanen, 2004; Saarikoski, 2003).

The optical excitation of quantum dots is a process of creating electron-hole pairs in the quantum dots. The created electron-hole pair forms a bound state due to the attractive Coulomb interaction between the electron and hole. The bound state is called an exciton. To create excitons requires meeting two conditions. First, a photon energy of an optical excitation source should match the energy required to create an exciton due to the conservation of energies. Second, the total angular momentum of an exciton should be the same as that of an absorbed photon, i.e. one, due to the conservation of angular momenta. Therefore, the measurement of the response of quantum dots to the optical excitation such as absorption and emission measurements reveals the exciton level structures of the dots.

The energy band structure forms the basis of understanding the most optical properties of semiconductors. The conditions for a nanocrystal to be considered as a quantum dot are related to their spatial dimensions. From the theoretical point of view, the ground state property of an electron and hole confined in nanocrystal poses a fundamental problem of quantum mechanics: The competition between the attractive Coulomb force and the repulsive confinement force gives rise to a distinct size-dependent change of motional state

of the electron-hole pair. This is in contrast to the electron system with repulsive interaction alone, where the main concern is the occurrence of shell structures and the emergence of collective movements (Uozumi, & Kayanuma, 2002). It can be readily inferred that there are two limiting situations according to the ratio of characteristic length R indicating the size of the nanocrystal to the effective Bohr radius $a_x^*$ of the exciton in the bulk material. In the limit $R/a_x^* \gg 1$, the exciton can be envisaged as a *quasiparticle* moving around the quantum dot with only little energy increment due to confinement (Marin, Riera, & Cruz, 1998). In opposite limit $R/a_x^* \ll 1$, the confinement effect dominates and the electron and hole should be viewed as individual particles predominantly in their respective lowest eigenstate of quantum dot with only little spatial correlation between them (Kayanuma, 1988). In this regime (called the strong-confinement regime), the exciton in the quantum dot feels the boundary effects strongly.

## 2.2 Fabrication Techniques

Various techniques have been developed to obtain QDs, leading to systems with different shape and characteristics (Figure 2.2).

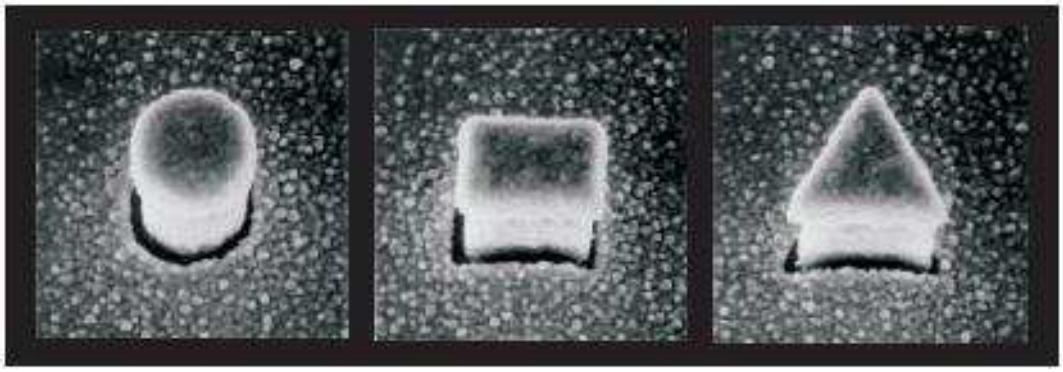

Figure 2.2 Scanning electron micrographs of quantum dot pillars with various shapes. The pillars have widths of about $0.5\,\mu m$. (from Ref. Kouwenhoven et al. (2001))

The reliable production of QDs offers outstanding opportunities for optical and electronic technologies as well as the development of new technologies. First attempts to produce QD systems with sufficient optical quality were based on conventional post-growth lithography and etching methods or epitaxy on patterned substrates. The main problem with these techniques are introduction of interface damages and impurities, and relatively poor resolution of post-growth lithography methods. The more successful techniques are based on in-situ growth of self-assembled QDs, where nucleation at desired sites is promoted introducing nonplanar features or strained patterns. In general, demands in the fabrication of QD systems are ranging from precise position control i.e. to achieve ordered QD systems, or tailored optical emission and absorption, to effective integration with photonic devices such as optical cavities, waveguides, and photonic crystals. In what follows, we briefly introduce various techniques used in QD fabrication without going into the details.

### *2.2.1 Lithographic Techniques*

Method frequently used to create quantum confinement in a semiconductor heterostructure is the lithographic patterning of gates (Figure 2.3), i.e. nanoscale electrodes are created on the surface of a heterostructure (Mlinar, 2007). The widely used lithographic techniques are: optical lithography and holography, X-ray lithography, electron and focused ion beam lithography, and scanning tunnelling microscopy. The application of appropriate electric voltages over the electrodes then produces a suitable confining potential, thus creating areas where electrons have been pushed away at desired locations (depletion areas). The typical size of this kind of dot, with currently available lithographic techniques, is generally large (Bellucci, 2005). These quantum dots are better suited to electrical rather than optical manipulation (Bianucci, 2007).

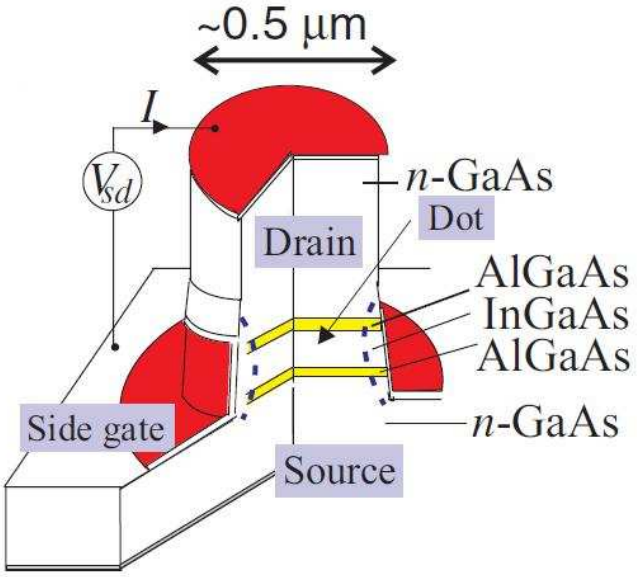


Figure 2.3 Schematic diagram of a semiconductor heterostructure. The dot is located between the two AlGaAs tunnel barriers(from Ref. Kouwenhoven et al. (2001)).

### *2.2.2 Epitaxial Growth*

Epitaxial growth techniques are currently the best choice to grow high-quality crystalline films. Molecular Beam Epitaxy, in particular, is noted for its ability to grow crystalline materials one atomic layer at a time and is predominantly used to make nanostructures such as Quantum Wells (QW), where a thin layer (a few nm high) of a low bandgap semiconductor sits between two layers of a higher bandgap one (Bianucci, 2007). MOCVD is a chemical vapour deposition method of epitaxial growth of materials, especially compound semiconductors from the surface reaction of metalorganics compounds or metal hydrides containing the required chemical elements. In contrast to MBE, the growth of crystals is by chemical reaction and not physical deposition, where formation of the epitaxial layer occurs by final pyrolisis of the constituent chemicals at the substrate surface (Mlinar, 2007).

### Self-assembled quantum dots

When growing epitaxial layers of a material on top of a substrate with a different lattice constant, the mismatch causes strain that accumulates as the material is deposited. When the crystal thickness exceeds certain value, a significant strain is accumulated in the layer which leads to the break-down of such an ordered structure and to the spontaneous creation of randomly distributed islands of regular shape and similar sizes (Mlinar, 2007). The growth conditions, the misfit of the lattice constants (strain) and the growth temperature determine the form of self assembled dots, which, for example, can be pyramidal, disk shaped or lens shaped. Self-assembled QDs are the best candidates to realize lasers and to perform photoluminescence spectroscopy (Bellucci, 2005).

# CHAPTER THREE
# THEORETICAL BASIS

## 3.1 Motivation

Computational physics is based on theoretical models describing the interactions between particles in specific material. Different models vary significantly in their accuracy and computational cost, both of which are important factors to be considered when modeling is undertaken (Lehtonen, 2007). Some models include all electrons explicitly, others consider particles classically. To choose the right model for a particular problem is not always straightforward, and often different models yield complimentary information. However, more often the computational resources are the limiting factor in determining which model can be used.

The aim of all electronic structure methods is to solve the Schrödinger equation. Usually the solution is obtained within some well defined approximations. There are two main approaches to describe electronic structure of systems: the wavefunction and density based methods (Kohanoff, 2006). In the wavefunction based methods an approximation for the actual wavefunction is constructed and the structural properties are calculated based on it. In the other approach the electron density is taken as the fundamental variable.

In the following the most common electronic structure methods are described. Some of the methods are described, not because they are applied in this work, but to provide a consistent overview on available methods and to show the similarities and differences between the methods.

The time independent Schrödinger equation for a system of $N$ particles interacting via the Coulomb interaction is (Kent Thesis)

$$\hat{H}\,\Psi(\vec{r}_1,\vec{r}_2,...,r_N,\sigma_1,\sigma_2,...,\sigma_N) = E\,\Psi(\vec{r}_1,\vec{r}_2,...,r_N,\sigma_1,\sigma_2,...,\sigma_N)$$

where

$$\hat{H} = \sum_{i=1}^{N}\left(-\frac{\hbar^2}{2\,m_i}\vec{\nabla}_i^2 + V(\vec{r}_i)\right) + \frac{1}{2}\sum_{i=1}^{N}\sum_{j\neq 1}^{N}\frac{1}{4\pi\epsilon|\vec{r}_i-\vec{r}_j|}$$

and $\Psi$ is an N-body wavefunction. $\vec{r}$ denotes spatial positions of particles and $V(r)$ the external potential applied to the individual particles. $E$ denotes the energy of either the ground or an excited state of the system. The solutions to the above equation would provide a detailed theoretical description of multi electron quantum dots, in particular, their energy structures.

If the electrons were assumed to not interact with each other, the above equation could be reduced to a single electron Schrödinger equation which can be solved by any method. These electrons would then sequentially fill the single electron energy levels starting from the lowest state according to the Pauli's exclusion principle. The total energy of a multi-electron quantum dot would be a simple sum of the energies of individual electron in the quantum dot.

However, the Coulomb interactions between the electrons are significant, especially when they are comparable with the confinement potential imposed by external electrods, and therefore cannot be ignored. Several computational schemes have been developed to deal with the interacting electrons in quantum mechanically confined systems, such as atoms and molecules. These methods have been extended to study the electronic structure of quantum dots and other nanosystems. Their strengths and limitations are reviewed in this section.

### 3.2 The Born-Oppenheimer Approximation

A common and very reasonable approximation used in the solution of Schrödinger equation is the Born-Oppenheimer Approximation. In a system of interacting electrons and nuclei there will usually be little momentum transfer between the two types of particles due to their greatly differing masses. The forces between the particles are od similar magnitude due to their similar charge. If one then assumes that the momenta of the particles are also similar, then the nuclei must have much smaller velocities than the electrons due to their far great mass. On the time-scale of nuclear motion, one can therefore consider the electrons to relax to a ground state given by the Hamiltonian written above with the nuclei at fixed locations (Saarikoski, 2003). This separation of the electronic and nuclear degrees of freedom is known as the Born-Oppenheimer Approximation.

### 3.3 Effective-Mass Approximation

The effective-mass approximation models a single-particle Hamiltonian with the dispersion relations of bulk bands near the minimum and maximum. The kinetic energy of the single-particle Hamiltonian is described by replacing a bare electron mass with an effective mass (Saarikoski, 2003). The effective mass $m^*$ is obtained from the band curvature near the minimum and maximum when the dispersion relation $E(k)$ of the band is given:

$$\frac{1}{m^*} = \frac{1}{\hbar^2} \left. \frac{\partial^2 E(k)}{\partial k^2} \right|_{k=0} \tag{3.3.1}$$

In the simplest case where the coupling between the lowest conduction and the highest valence bands is negligible, the effective Hamiltonians of low-lying electron

and hole levels in quantum dots can be separately written as

$$\hat{H}_e = -\frac{\hbar^2}{2m_e^*}\vec{\nabla}^2 + V_e(r) + E_g, \tag{3.3.2}$$

$$\hat{H}_h = -\frac{\hbar^2}{2m_h^*}\vec{\nabla}^2 + V_h(r), \tag{3.3.3}$$

where $m_e^*$ and $m_h^*$ are the electron and hole effective masses. $E_g$ is a bulk band gap, i.e. the energy difference between the bottom of the lowest conduction band and the top of the highest valance band. The confinement of the quantum dot is imposed in the potential $V(r)$.

The single-band effective-mass approximation can be improved by including more bands and by allowing couplings between different bands. Since the Hamiltonian is constructed based on the parabolic dispersion relations of bands near $\Gamma$, this approximation is valid only if relevant bands near $\Gamma$ can be approximated as parabolic curves, and relevant properties are attributed to single particle levels near $\Gamma$. The low-lying electron and holes states of quantum dots appear near $\Gamma$ as the dot size increases. Therefore, the effective-mass approximation is applicable to relatively large quantum dots with interior properties outweighing surface properties (Lee, 2002).

## 3.4 Electronic Structure Methods

### *3.4.1 Hartree-Fock Theory*

Hartree-Fock theory is one the simplest approximation theories for solving the many-body Hamiltonian. In this mean-field model for quantum systems each electron is assumed to experience an averaged repulsive potential due to all the other electrons in the system. It is based on a simple approximation to the

true many-body wavefunction: that the wavefunction is given by a single Slater determinant of N spin-orbitals

$$\Psi(\mathbf{x}_1, \mathbf{x}_2, \cdot, \mathbf{x}_N) = \frac{1}{\sqrt{N!}} \begin{vmatrix} \psi_\lambda(\mathbf{x}_1) & \psi_\lambda(\mathbf{x}_2) & \cdots & \psi_\lambda(\mathbf{x}_N) \\ \psi_\beta(\mathbf{x}_1) & \psi_\beta(\mathbf{x}_2) & \cdots & \psi_\beta(\mathbf{x}_N) \\ \vdots & \vdots & \vdots & \vdots \\ \psi_\nu(\mathbf{x}_1) & \psi_\nu(\mathbf{x}_2) & \cdots & \psi_\nu(\mathbf{x}_N) \end{vmatrix} \tag{3.4.1}$$

where the variables $\mathbf{x} \equiv (\vec{r}_i, \sigma_i)$ include the coordinates of space and spin. $\psi_\lambda(\mathbf{x}_i) = u_\lambda(\vec{r}_i)\chi_\lambda$ is the spin-orbital of the $i$th electron with a collective quantum number $\lambda$, and $u$ and $\chi$ are respectively the spatial and spin wavefunction. This definition, in conjuction with the requirement of orthogonality, i.e.

$$< \psi_\mu | \psi_\lambda >= \delta_{\mu,\lambda} \tag{3.4.2}$$

ensures that the total wavefunction is antisymmetric. Proceeding with the variation leads to the system of equations

$$\begin{aligned} &\hat{H}_i\psi_\lambda(\mathbf{x}_i) + \sum_{\mu=1}^{N} \int \psi_\mu^*(\mathbf{x}_j)\frac{1}{r_{ij}}\psi_\mu(\mathbf{x}_j)d\mathbf{x}_j\psi_\lambda(\mathbf{x}_i) - \sum_{\mu=1}^{N} \int \psi_\mu^*(\mathbf{x}_j)\frac{1}{r_{ij}}\psi_\lambda(\mathbf{x}_j)d\mathbf{x}_j\psi_\mu(\mathbf{x}_i) \\ &= E_\lambda\psi_\lambda(\mathbf{x}_i) \end{aligned} \tag{3.4.3}$$

known as Hartree-Fock equations (Szabo, & Ostlund, 1989). To solve this set of one electron equations, an iterative procedure is adopted. At the $n$th iteration, one has an estimate for each spin-orbitals denoted by $\psi_\lambda^n$. Then we can write Hartree-Fock equations as follows:

$$\begin{aligned} &\hat{H}_i\psi_\lambda^{n+1}(\mathbf{x}_i) + \sum_{\mu=1}^{N} \int \psi_\mu^{n*}(\mathbf{x}_j)\frac{1}{r_{ij}}\psi_\mu^n(\mathbf{x}_j)d\mathbf{x}_j\psi_\lambda^{n+1}(\mathbf{x}_i) \\ &= -\sum_{\mu=1}^{N} \int \psi_\mu^{n*}(\mathbf{x}_j)\frac{1}{r_{ij}}\psi_\lambda^{n+1}(\mathbf{x}_j)d\mathbf{x}_j\psi_\mu^n(\mathbf{x}_i)E_\lambda^{n+1}\psi_\lambda^{n+1}(\mathbf{x}_i) \end{aligned} \tag{3.4.4}$$

Self-consistency is obtained by repeating this procedure iteratively until the difference between $\psi_\lambda^{n+1}$ and $\psi_\lambda^n$ is negligibly small.

Hartree-Fock theory, by assuming a single-determinant form for the wavefunction, neglects correlation between electrons. The electrons are subject to an *average* non-local potential arising from the other electrons, which can lead to a poor description of the electronic structure.

### *3.4.2 Density Functional Theory*

Density Functional Theory (DFT) is formally exact one-electron theory based on the charge density of a system (Williamson, 1996). The number of degrees of freedom is reduced from $3N$ to 3, and the problem is drastically simplified. Working within the Born-Oppenheimer approximation, the many-body Schrödinger equation is replaced by a set of $N$ one-electron equations in the from (in a.u.)

$$\left(-\frac{1}{2}\vec{\nabla}^2 + V(\vec{r})\right)\psi_i(\vec{r}) = \varepsilon\psi_i(\vec{r}) \tag{3.4.5}$$

where $\psi_i(\vec{r})$ is a single-electron wavefunction. These one-electron equations contain a potential $V(\vec{r})$ produced by all the ions and the electrons. DFT properly includes all parts of the electron-electron interaction, i.e. the Hartree potential

$$V_H(\vec{r}) = \int d\vec{r}' \frac{\rho(\vec{r}')}{|\vec{r} - \vec{r}'|} \tag{3.4.6}$$

where $\rho$ is the charge density of all the electrons, a potential due to exchange and correlation effects, $V_{XC}(\vec{r})$, and the external potential due to the ions, $V_{\text{ext}}(\vec{r})$,

$$V(\vec{r}) = V_{\text{ext}}(\vec{r}) + V_H(\vec{r}) + V_{XC}(\vec{r}). \tag{3.4.7}$$

Hohenberg and Kohn originally developed DFT theory for application to the ground state of a system of spinless fermions. In such a system the particle

density is given by

$$\rho(\vec{r}) = N \int |\Psi_0(\vec{r}, \vec{r}_2, \cdots, \vec{r}_N)|^2 d\vec{r}_2 \cdots d\vec{r}_N \tag{3.4.8}$$

with $\Psi_0$ being the many-body ground state wavefunction of the system. Total ground state energy of the system is a functional of the density, $E[\rho(\vec{r})]$, and if the energy due to the electron-ion interactions is excluded the remainder of the energy is a universal functional of the density, $F[\rho(\vec{r})]$.

**Kohn-Sham equations**

Kohn and Sham introduced a method based on the Hohenberg-Kohn theorem that enables one to minimize the functional $E[\rho(\vec{r})]$ by varying $\rho(\vec{r})$ over all densities containing N electrons (Rasanen, 2004). Kohn and Sham chose to separate $F[\rho(\vec{r})]$ into three parts, so that $E[\rho(\vec{r})]$ becomes

$$E[\rho(\vec{r})] = T_s[\rho(\vec{r})] + \frac{1}{2} \int \int \frac{\rho(\vec{r})\rho(\vec{r}')}{|\vec{r} - \vec{r}'|} r\vec{r} d\vec{r}' + E_{XC}[\rho(\vec{r})] + \int \rho(\vec{r}) V_{\text{ext}}(\vec{r}) d\vec{r} \tag{3.4.9}$$

where $T_s[\rho(\vec{r})]$ is defined as the kinetic energy of a *non-interacting* electron gas with density $\rho(\vec{r})$,

$$T_s[\rho(\vec{r})] = -\frac{1}{2} \sum_{i=1}^{N} \int \psi_i^*(\vec{r}) \vec{\nabla}^2 \psi_i(\vec{r}) d\vec{r}. \tag{3.4.10}$$

Expression for the energy functional also acts as definition for the *exchange correlation energy functional*, $E_{XC}[\rho(\vec{r})]$,

$$V_{XC}[\rho(\vec{r})] = \frac{\delta E_{XC}[\rho(\vec{r})]}{\delta \rho(\vec{r})}. \tag{3.4.11}$$

If one considers a system that really contained *non-interacting* electrons moving

in an external potential equal to $V_{\text{eff}}(\vec{r})$

$$V_{\text{eff}}(\vec{r}) = V_{\text{ext}}(\vec{r}) + \int d\vec{r}' \frac{\rho(\vec{r}')}{|\vec{r} - \vec{r}'|} + V_{XC}(\vec{r}). \tag{3.4.12}$$

then the ground state energy and density, $E_0$ and $\rho_0(\vec{r})$ can be find by solving the one-electron equations

$$\left( -\frac{1}{2}\vec{\nabla}_i^2 + V_{\text{eff}}(\vec{r}) - \varepsilon_i \right) \psi_i(\vec{r}) = 0. \tag{3.4.13}$$

As the density is constructed according to

$$\rho(\vec{r}) = \sum_{i=1}^{N} |\psi_i(\vec{r})|^2 \tag{3.4.14}$$

complete solution can be obtained by self-consistent procedure.

The simplest approximation for $E_{XC}$ is the *Local Density Approximation* (LDA) where the the properties of the homogeneous electron gas (EG) are extrapolated to inhomogeneous systems (Torsti, 2003; Dreizler, & Gross, 1990),

$$E_{XC}^{LDA} = \int d\vec{r} \rho(\vec{r}) \varepsilon_{XC}^{EG}(\rho(\vec{r})), \tag{3.4.15}$$

where $\varepsilon_{XC}^{EG}(\rho(\vec{r}))$ denotes the exchange-correlation energy per electron of a uniform electron gas with density $\rho$.

### *3.4.3 Configuration Interaction*

Configuration Interaction (CI) methods are one of the conceptually simplest methods for solving the many-body Hamiltonian. Although theoretically elegant, in principle exact, and relatively simple to implement, in practice *full* CI can be applied to only the smallest systems (Pauncz, 1979). In order to take into

account the electron correlation, wavefunction of the system is construct as a linear combination of multiple Slater determinants orthogonal to each other. Such determinants can be constructed using the orthonormal orbitals obtained from the canonical HF orbitals by exciting electrons from the occupied to unoccupied orbitals, i.e. replacing an occupied orbital with an unoccupied one in the determinant. This approach is called the configuration interaction (CI) method. Based on the variational principle, the solution is found by minimizing the energy with respect to the expansion coefficients in front of the determinants. A general CI wavefunction can be written as

$$|CI>=\sum_i c_i|i> \tag{3.4.16}$$

where $|i>$ are configuration state functionals and $c_i$ are expansion coefficients to be determined by variational principle. The linear variation problem reduces into solving a secular equation, i.e. finding the eigenvalues and eigenvectors of a matrix equation (Lehtonen, 2007)

$$\mathbf{H}\,\mathbf{C} = \mathbf{C}\,\mathbf{E} \tag{3.4.17}$$

where $\mathbf{H}$ is a matrix having the expectation values $< i|\hat{H}|j >$ between different configurational state functions, $\mathbf{C}$ has the eigenvectors as columns and $\mathbf{E}$ the eigenenergies on its diagonal. The matrix elements of $\mathbf{H}$ can be expressed in terms of one- and two-electron integrals using Slater-Condon rules (Szabo, & Ostlund, 1989). In this method a very large number of configurations is required to yield energies and wavefunctions approaching the exact many-body wavefunction. In practice the expansion must be limited on physical grounds, as the total number of determinants is

$$k_{max} = \frac{M!}{N!(M-N)!}, \tag{3.4.18}$$

where the length of the expansion $k_{max}$ is given in terms of the number of electrons, $N$, and the number of basis sets, $M$, in the expansion ($M \gg N$). The scientific

problem in adapting the CI method in to a practical one is to obtain the best wavefunction with the shortest expansion length due to the computational costs. Although truncation of the expansion can be applied performing within a finite reference space, an additional problem, lack of "size-extensivity", with the method becomes apparent.

### 3.5 Explicitly Correlated Wavefunctions

The methods described above are based on one-electron orbitals. Although these methods are easier to deal with, they ignore the fact that the position of an electron is correlated to the position of all the other electrons. This is recovered in by constructing combinations of products of one-electron orbitals which requires many number of combinations. A more efficient approach would be to try and build the correlation directly into the trial wavefunction (Kohanoff, 2006). Explicit inclusion of an $r_{12}$ dependent term into wave function improves significantly convergence of energy as compared with other functions not having such correlation term. Today, the methods based on explicitly correlated wave functions are able to achieve the spectroscopic accuracy in atomic and molecular energy calculations (errors of the order of one $\mu$hartree).

Several methods using different expressions of $r_{12}$ dependence have been developed. They can be divided into two groups depending on the form of the correlation factor used (Rychlewski, 2004). In the first group the correlation factor has the form of $r_{12}^{u}$ whereas in the second one, the correlation factor has the exponential form of $\exp(-\alpha r_{12}^2)$ or less often $\exp(-\alpha r_{12})$. An extension of approaches are to introduce an explicit dependence on the interelectronic dependence such that the cusp conditions are verified (cusp at the origin, $r_{12} = 0$ meaning a discontinuous first derivative, and nuclear cusp due to the electron-nuclear distance). A general approach is to propose a

wavefunction of the form $\Phi_{R12} = \gamma(\{r_{ij}\})\Phi_{CI}$, where $\gamma$ is an appropriate correlating function. Possible expressions are (Kohanoff, 2006)

$$\gamma = 1 + \beta \sum_{i>j} r_{ij} \tag{3.5.1}$$

$$\gamma = \prod_{i>j} (1 + \beta r_{ij}) \tag{3.5.2}$$

$$\gamma = e^{\beta \sum_{i>j} r_{ij}} \tag{3.5.3}$$

Correlating functions which can be handled more easily are also used in variational quantum Monte Carlo calculations.

Although explicitly correlated methods are potentially more accurate than the usual one-electron approaches, they have not yet reached the efficiency required to become widely adopted as a standard tool.

### *3.5.1 Hylleraas-type Wavefunctions*

Hylleraas wave function can be described as composed of three factors: exponential (Slater type), power expansion of the coordinates and correlation factor. Therefore this function is not based on the one-electron approximation. The Hylleraas method is very accurate, and only a few terms in the expansion are required. Unfortunately it is only applicable to atomic systems with a few electrons. The explicitly correlated wave functions, i.e. wave functions containing an interelectron distance, $r_{12} = |\vec{r}_2 - \vec{r}_1|$, have been introduced at the end of 1920s. Successful construction of an accurate wave function for the singlet S state helium and its isoelectronic series had been done by Hylleraas

(1929). His original ansatz reads

$$\begin{aligned} \Psi &= \Phi(ks, kt, ky) \\ \Phi &= \exp(-s/2) \sum_{n,l,m=0} c_{n,2l,m}\, s^n t^{2l} u^m \end{aligned} \tag{3.5.4}$$

with

$$s = r_1 + r_2, \quad t = -r_1 + r_2, \quad u = r_{12} \tag{3.5.5}$$

Hylleraas determined the scaling factor, k, and the expansion coefficients, $c_i$ for the sets of non-negative integers $\{n, l, m\}$. The breakthrough work was the six term expansion which lead to the energy only by $0.0005 E_H$ higher than the exact value. Koga (1990) followed the method applied by Hylleraas and studied optimal selections of terms in longer (up to 20-term) Hylleraas expansions and found a much better set on integers of the six-term expansion that improves the energy.

The original definition of the Hylleraas wave function was generalized in two directions (Rychlewski, 2004). Half-integer powers of the Hylleraas variables have been introduced in 1956 by H.M.Schwartz (Schwartz, 1956)

$$\Phi = \exp(-s/2) \sum_{n,l,m=0} c_{n,2l,m} s^{n/2}\, t^{2l}\, u^{m/2} \tag{3.5.6}$$

and in 1957 the domain of $\{n, l, m\}$ to negative integers have been extended by Kinoshita (1957)

$$\Phi = \exp(-s/2) \sum_{n,l,m=0} c_{n,2l,m} s^{n-m}\, t^{2l}\, u^{m-2l} \tag{3.5.7}$$

Both modifications significantly increased the flexibility of the wave function. Bartlett et al. (1935) introduced another modification of the the Hylleraas wave function by suggesting the inclusion of terms with logarithmic dependence on the

$s$ variable

$$\Phi = \exp\left(-s/2\right) \sum_{n,l,m,i,j=0} c_{n,l,m,i,j} s^n \, t^{2l} \, u^m \left(s^2 + t^2\right)^{i/2} (\ln s)^j \tag{3.5.8}$$

This form of the helium wave function was fully exploited by (Frankowski, et al.,1966). Pekeris (1959) applied the atomic wavefunction introduced by Coolidge and James (Coolidge, & James, 1936) to calculate the ground and excited states of two-electron atoms which is closely related to the Hylleraas ansatz. This wave function depends on perimetric coordinates

$$u = \varepsilon\left(r_2 + r_{12} - r_1\right), \; \upsilon = \varepsilon\left(r_1 + r_{12} - r_2\right), \; \omega = \varepsilon\left(r_1 + r_2 - r_{12}\right); \tag{3.5.9}$$

and has the form

$$\Phi = \exp\left[-\left(u + \upsilon + \omega\right)/2\right] \sum_{l,m,n} A_{l,m,n} L_l(u) L_m(\upsilon) L_n(\omega) \tag{3.5.10}$$

$L_l$ being the normalized Laguerre polynomial of order $l$.

In search of better description of the electron shell structure, wave functions expanded in a doubled basis set were later used in high precision calculations on two-electron atoms (Coolidge, & James, 1936). Recently, there are many works with triple basis set in Hylleraas coordinates. The Hylleraas-type wave functions was generalized also towards systems with more than two electrons. Coolidge, & James (1936) expressed their 3-electron wave function in terms of the following spatial basis set (Rychlewski, 2004)

$$\Phi = r_{ij} \exp\left[-\left(\delta\, r_1 + \delta\, r_2 + \gamma\, r_3\right)\right] r_3^k r_2^m r_1^n \tag{3.5.11}$$

later on generalized to

$$\Phi = \exp\left[-\left(\alpha\, r_1 + \beta\, r_2 + \gamma\, r_3\right)\right] r_1^i r_2^j r_3^k r_{23}^l r_{13}^m r_{12}^n \tag{3.5.12}$$

Over the years, many authors have used the last form, augmented by proper angular and spin functions to calculate energies of the ground and excited states of lithium-like atoms.

# CHAPTER FOUR
# THEORETICAL METHOD

In this chapter we would like to present some of the necessary details to obtain the results of this thesis.

## 4.1 Variational Calculations

The work presented in this thesis relies heavily on the Rayleigh-Ritz variational principle. With the availability of computers this method has become an important tool. Typically the necessary expectation values are computed analytically or numerically by means of appropriate approach to the proposed trial wavefunction. We defer the discussion about the choose of wavefunction is actually done to Chapter Five and concentrate here on the physically important aspects of the method.

### *4.1.1 Variational Principle*

The application of quantum mechanics to a physical system in principle is a simple process, easily accomplished by writing and solving the Shrödinger wave equation for the given system. In practice, however, this differential equation is usually too difficult or impossible to be solved analytically. But with the "Variational Methods", often used to approximate solutions to problems, mathematical complexity is no longer a deterrent. Moreover, these methods provide a framework for numerical computations that can harness the power and efficiency of of modern day workstations (Nistor, 2004). The variational principle provides the starting point for almost all methods whose objective to find an approximate solution to Schrödinger equation. It is also possible to use

variational methods to study excited states, but the real strength of this principle lies in finding ground state energies (Williamson, 1996).

The key theorem of the calculus of variations is the Euler-Lagrange equation (Inci, 2004). This corresponds to the stationary condition on a functional

$$J = \int_{x_1}^{x_2} f(x, y, y_x)\, dx, \tag{4.1.1}$$

where $f(x, y, y_x)$ is a function of indicated variables $x$, $y$ and $y_x = \frac{dy}{dx}$. $x_1$ and $x_2$ are fixed end points, but the dependence of $y$ on $x$ is not fixed. It means that the exact path of integration is not known. The variational principle is that we choose the path of integration from points $(x_1, y_1)$ to $(x_2, y_2)$ to minimize $J$ subject to the fixed endpoints constraint. The method of solution is to consider small deviations of actual path $y(x)$ requiring that the variations $\delta J$ introduced in $J$ vanish. This is presented as in Figure 4.1. Here $\eta(x)$ is the arbitrary deformation of the path

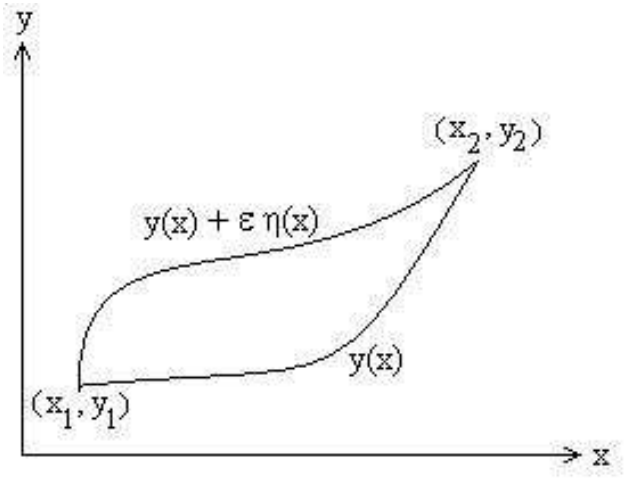


Figure 4.1 Illustration of the actual path $y(x)$ and the varied path connecting fixed end points.

and $\epsilon$ is a scale factor. Applying the variational principle to the equation gives

$$\left[\frac{\partial J(\epsilon)}{\partial \epsilon}\right]_{\epsilon=0} = 0 \tag{4.1.2}$$

The condition for the existence of a stationary value can be satisfied only if,

$$\frac{\partial f}{\partial y} - \frac{df}{dx}\frac{\partial f}{\partial y_x} = 0 \tag{4.1.3}$$

known as the Euler-Lagrange equation (İnci, 2004).

Equivalently, the problem is to find the path $y(x)$ that minimizes the value of the integral $J$; or, find the path $y(x)$ such that the value of the integral is made stationary with respect to variations in $y(x)$.

As an extension of the above considerations, applying the variational principle to stationary states (i.e. time independent states) in quantum mechanics, results in the energy of the system being stationary (i.e. variationally stable) with respect to the first order variations in the wavefunction. The foundations of the variational calculations in this work is in principle that the energy is stationary with respect to first order variations in the wavefunction.

The expression for the expectation value of the Hamiltonian $\hat{H}$ is

$$E = \frac{\left\langle \Psi \left| \hat{H} \right| \Psi \right\rangle}{\langle \Psi | \Psi \rangle} \tag{4.1.4}$$

The expectation value of the Hamiltonian $\langle \hat{H} \rangle = E[\Psi]$ that is a functional of the wavefunction. Small variation to the state vector can be defined as:

$$| \Psi \rangle \rightarrow | \Psi \rangle + | \delta\Psi \rangle \tag{4.1.5}$$

Then the variation in the trial energy $E$ is then given by

$$\begin{aligned} \delta E &= E[\Psi + \delta\Psi] - E[\Psi] \\ &= \frac{1}{\langle \Psi | \Psi \rangle} \left[ \left\langle \delta\Psi \left| \hat{H} - E[\Psi] \right| \Psi \right\rangle + \left\langle \Psi \left| \hat{H} - E[\Psi] \right| \delta\Psi \right\rangle \right] \end{aligned} \tag{4.1.6}$$

where $O[\delta\Psi^2]$ represents the higher order in $\delta\Psi$ that are ignorable.

Thus $\delta E[\Psi] = 0$, when $|\Psi\rangle$ is an eigenstate of Hamiltonian and $E[\Psi]$ is eigenvalue (Cassar, 2004).

### *4.1.2 Matrix Equivalency*

In this section, we show that the variational principle is equivalent to the solution to a matrix eigenvalue problem. In practice, we write a trial wavefunction in the form

$$|\Psi_{tr}\rangle = \sum_{i=1}^{N} a_i |\phi_{tr}\rangle, \tag{4.1.7}$$

where the arbitrary basis set of functions $\phi_k$ (subject to integrability and suitable boundary conditions) becomes complete only when the summation is carried out over an infinite number of terms. The linear expansion coefficients $a_i$ are determined according to the variational principle such that the resultant energy should be a minimum.

According to the variational principle, where the energy $E$ depends on any given set of linear parameters $a_i$, we can write

$$\delta E = \sum_i \frac{\partial E}{\partial a_i} \delta a_i = 0 \tag{4.1.8}$$

For arbitrary nonzero variations $\delta a_i$, requiring $\delta E = 0$, implies

$$\frac{\partial E}{\partial a_i} = 0$$

identically for all $i$. Applying this condition to the energy leads to a system of N homogeneous linear equations ($k$ has the same range as $i$)

$$\frac{\partial E_{tr}}{\partial a_k} = 0, \qquad \text{for all } a_k. \tag{4.1.9}$$

Using the equation for trial wavefunction, we may rewrite quotient for the energy as

$$\begin{aligned} E_{tr} &= \frac{\left\langle \Psi_{tr} \left| \hat{H} \right| \Psi_{tr} \right\rangle}{\langle \Psi_{tr} | \Psi_{tr} \rangle} \\ &= \frac{\sum\limits_{ij} a_i^* a_j H_{ij}}{\sum\limits_{ij} a_i^* a_j S_{ij}} \end{aligned} \tag{4.1.10}$$

where $H_{ij} = \left\langle \phi_i \left| \hat{H} \right| \phi_j \right\rangle$ and $S_{ij} = \langle \phi_i | \phi_j \rangle$. Then taking the derivative with respect to $a_k$, we can write as

$$\begin{aligned} \frac{\partial E_{tr}}{\partial a_k} &= \frac{\left( \sum\limits_{ij}^{N} a_i^* a_j S_{ij} \right) \left( \sum\limits_{ij}^{N} a_i^* H_{ij} \delta_{jk} \right) - \left( \sum\limits_{ij}^{N} a_i^* a_j H_{ij} \right) \left( \sum\limits_{ij}^{N} a_i^* S_{ij} \delta_{jk} \right)}{\left( \sum\limits_{ij}^{N} a_i^* a_j S_{ij} \right)^2} \\ &= \frac{\sum\limits_{ij}^{N} a_i^* H_{ik}}{\left( \sum\limits_{ij}^{N} a_i^* a_j S_{ij} \right)} - \frac{\left( \sum\limits_{ij}^{N} a_i^* a_j H_{ij} \right) \left( \sum\limits_{ij}^{N} a_i^* S_{ik} \right)}{\left( \sum\limits_{ij}^{N} a_i^* a_j S_{ij} \right)^2} \end{aligned} \tag{4.1.11}$$

Using the equation for the energy quotient we can write the last equation in the

form

$$\frac{\partial E_{tr}}{\partial a_k} = \frac{\sum_i^N a_i^* H_{ik}}{\sum_{ij}^N a_i^* a_j S_{ij}} - (E_{tr}) \frac{\sum_i^N a_i^* S_{ik}}{\sum_{ij}^N a_i a_j S_{ij}} \tag{4.1.12}$$

From the variational principle this should be zero, so that

$$\begin{aligned} \frac{\sum_i^N a_i^* H_{ik}}{\sum_{ij}^N a_i^* a_j S_{ij}} - (E_{tr}) \frac{\sum_i^N a_i^* S_{ik}}{\sum_{ij}^N a_i^* a_j S_{ij}} &= 0 \\ \sum_i^N a_i^* H_{ik} - (E_{tr}) \sum_i^N a_i^* S_{ik} &= 0 \\ \sum_i^N a_i^* \left(H_{ik} - E_{tr}\, S_{ik}\right) &= 0 \end{aligned} \tag{4.1.13}$$

Taking the complex conjugate of the last line, we get

$$\sum_i a_i \left[H_{ik} - E_{tr}\, S_{ik}\right] = 0 \tag{4.1.14}$$

where $H_{ik}^* = H_{ki}$, $S_{ik}^* = S_{ki}$ and $E_{tr} = E_{tr}^*$. If we write this expression in matrix form, we obtain

$$\begin{bmatrix} H_{11} & H_{12} & ... & H_{1N} \\ H_{21} & H_{22} & ... & H_{2N} \\ . & . & ... & . \\ . & . & ... & . \\ . & . & ... & . \\ H_{N1} & H_{N2} & ... & H_{NN} \end{bmatrix} \begin{bmatrix} a_1 \\ a_2 \\ . \\ . \\ . \\ a_N \end{bmatrix} = E_{tr} \begin{bmatrix} S_{11} & S_{12} & ... & S_{1N} \\ S_{21} & S_{22} & ... & S_{2N} \\ . & . & ... & . \\ . & . & ... & . \\ . & . & ... & . \\ S_{N1} & S_{N2} & ... & S_{NN} \end{bmatrix} \begin{bmatrix} a_1 \\ a_2 \\ . \\ . \\ . \\ a_N \end{bmatrix} \tag{4.1.15}$$

We write the equivalent, yet more compact and in more convenient way, equation:

$$\mathbf{H}\,\mathbf{a} = E_{tr}\mathbf{S}\,\mathbf{a} \tag{4.1.16}$$

where $H_{ij}$ denote the matrix elements of $H$, and similarly for $S_{ij}$. Diagonalizing $\mathbf{H}$ yield to $N$ eigenvalues $E_{tr}^{j}\,(j = 1, 2, 3, ..., N)$. The $j^{th}$ column vector of $\mathbf{a}$ represents $\Psi_{tr}$ in the chosen basis.

### *4.1.3 Rayleigh-Ritz's Variational Principle*

The Rayleigh-Ritz variational principle is one of the most powerful nonperturbative methods in quantum mechanics (Baym, 1974). It may be stated as follows: *" The expectation value of a Hamiltonian, $\hat{H}$, calculated using a trial wavefunction, $\Psi_T$, is never lower in value than the true ground state energy, $\varepsilon_0$, which is the expectation value of $\hat{H}$ calculated using the true ground state wavefunction, $\Psi_0$."*(Williamson,1996, p.15)

This statement means that it is always possible to find an upper bound for the ground state energy. Variational calculations rely on making a physically plausible guess at the form of the ground state wavefunction of the Hamiltonian. The trial wavefunction depends on a number of variable parameters which can be adjusted to minimize the energy expectation value. If the guessed values of these parameters are good and the chosen functional form has an enough variational freedom to adequately describe the the system, then very accurate estimates of the ground state energy can be obtained.

Even if $\Psi$ is not an exact eigenfunction of $\hat{H}$, the Schrödinger variational principle is still useful because the corresponding energy eigenvalue of the function $\Psi$ is an upper bound to the exact eigenvalue. The proof of this theorem is relatively straightforward. We can expand an arbitrary trial wavefunction $\Psi_{tr}$ in terms of the exact eigenfunctions $\phi_i$, according to $\Psi_{tr} = \sum_{i=1}^{\infty} a_i \phi_i$,

where $\hat{H}\,\phi_i = E_i\,\phi_i$. Considering the Rayleigh quotient,

$$E_{tr} = \frac{\left\langle \Psi_{tr} \left| \hat{H} \right| \Psi_{tr} \right\rangle}{\left\langle \Psi_{tr} \left| \Psi_{tr} \right. \right\rangle}$$

and using the fact that $\langle \phi_i \left| \phi_j \right. \rangle = \delta_{ij}$, substitution of the trial wavefunction leads to

$$\begin{aligned} E_{tr} &= \frac{\left\langle \Psi_{tr} \left| \hat{H} \right| \Psi_{tr} \right\rangle}{\left\langle \Psi_{tr} \right| \left. \Psi_{tr} \right\rangle} \\ &= \frac{\sum\limits_{ij} a_i^* a_j \left\langle \phi_i \left| \hat{H} \right| \phi_j \right\rangle}{\sum\limits_{ij} a_i^* a_j \left\langle \phi_i \right| \left. \phi_j \right\rangle} \\ &= \sum_{ij} a_i^* a_j E_i \delta_{ij} = \sum_{i=0}^{\infty} |a_i|^2 E_j \end{aligned} \tag{4.1.17}$$

Note that $\sum\limits_{i=0}^{\infty} |a_i|^2 = 1$ and we can write this in the form

$$|a_0|^2 = 1 - \sum_{i=1}^{\infty} |a_i|^2$$

Using this equation along with the Rayleigh quotient for the energy proves that the trial energy is no lower than the exact eigenenergy

$$\begin{gathered} E_{tr} = E_0 + \sum_{i=1}^{\infty} |a_i|^2 \left(E_i - E_0\right) \\ E_{tr} \geq E_0 \end{gathered} \tag{4.1.18}$$

If we have a set of states we can choose the "best" approximation to the ground state as the one with the lowest expectation value for the energy. However, we should keep in mind that the only rigorous result is the upper bound to the ground state energy. (Heeb, 1994).

## 4.2 The Method and Formalism

### *4.2.1 Hamiltonian and Trial Wavefunction*

The aim of this thesis is to investigate the ground state of the two-particle spherical symmetric systems such as excitons in quantum dots, two-electron quantum dots, He atom and its isoelectronic sequence. The Hamiltonian of such systems includes six independent electronic spherical coordinates. In order to take the electron-electron correlation effects, it is convenient to use the coordinate system that explicitly includes $r_{12}$ interelectronic distance. The most used is $r_1$, $r_2$, $r_{12}$, $\alpha$, $\beta$ and $\gamma$ basis set where $\alpha$, $\beta$ and $\gamma$ are three Euler angles that define the rotation from space-fixed axis to the body-fixed axis (Forrey, 2004). Due to the spherical symmetry of the system, after removing Euler angles three independent coordinates, i.e. the sides of the triangle constructed by the distances of position vectors, $r_1$ and $r_2$, of two particles and $r_{12}$ distance between two particles, are sufficient enough to describe completely the S-states (Ancarani et al., 2007; Myers et al., 1991). Thus the Hamiltonian of the system expressed in Hylleraas coordinates should be written in Hylleraas coordinates (Aquino et al., 2006).

We can express symbolically the total wavefunction of N-particle system as a function of relative and independent coordinates as follows

$$\Psi = \Psi(r_1, r_2, ..., r_N; r_{12}, r_{13}, ..., r_{1N}; r_{23}, ..., r_{2N}; ...; r_{N-1,N})$$

$$\Psi = \Psi\left[\{r_i\}, \{r_{jk}\}\right]$$

The kinetic energy terms in Hamiltonian should be expressed in new defined

coordinates. Let's firstly define the gradient and divergence expressions.

$$\vec{\nabla}_i \Psi = \sum_{j=1}^{N} (\vec{\nabla}_i r_j) \frac{\partial \Psi}{\partial r_j} + \sum_{j<k} (\vec{\nabla}_i r_{jk}) \frac{\partial \Psi}{\partial r_{jk}} \tag{4.2.1}$$

$$\vec{\nabla}_i r_j = \hat{x} \frac{\partial r_j}{\partial x_i} + \hat{y} \frac{\partial r_j}{\partial y_i} + \hat{z} \frac{\partial r_j}{\partial z_i} = \delta_{ij} \frac{\vec{r}_j}{r_j} \tag{4.2.2}$$

$$r_j = (x_j^2 + y_j^2 + z_j^2)^{1/2}$$

$$\frac{\partial r_j}{\partial x_i} = \delta_{ij} . \frac{1}{2} . 2 x_j . r_j^{-1/2} \Rightarrow \frac{x_j}{r_j}$$

$$\Rightarrow \vec{\nabla}_i r_j = \delta_{ij} \hat{r}_j$$

$$\vec{\nabla}_i r_{jk} = \hat{x} \frac{\partial r_{jk}}{\partial x_i} + \hat{y} \frac{\partial r_{jk}}{\partial y_i} + \hat{z} \frac{\partial r_{jk}}{\partial z_i}$$

$$r_{jk} = \left[ (x_j - x_k)^2 + (y_j - y_k)^2 + (z_j - z_k)^2 \right]^{1/2}$$

$$\frac{\partial r_{jk}}{\partial x_i} = \delta_{ij} . \frac{1}{2} . 2 . (x_j - x_k) r_{jk}^{-1/2} - \delta_{ik} (x_j - x_k) r_{jk}^{-1/2}$$

$$\frac{\partial r_{jk}}{\partial x_i} = (\delta_{ij} - \delta_{ik}) \frac{(x_j - x_k)}{r_{jk}}$$

$$\Rightarrow \vec{\nabla}_i r_{jk} = (\delta_{ij} - \delta_{ik}) \frac{\vec{r}_{jk}}{r_{jk}} = (\delta_{ij} - \delta_{ik}) \hat{r_{jk}}$$

Arrangement of the expression for derivative according to the $i^{th}$ coordinate gives

$$\begin{aligned}
\vec{\nabla}_i\Psi &= \hat{r}_i\frac{\partial\Psi}{\partial r_i} + \sum_{i<k}\hat{r}_{ik}\frac{\partial\Psi}{\partial r_{ik}} - \sum_{j<i}\hat{r}_{ji}\underbrace{\frac{\partial\Psi}{\partial r_{ji}}}_{=\partial r_{ij}} \\
\vec{\nabla}_i\Psi &= \hat{r}_i\frac{\partial\Psi}{\partial r_i} + \sum_{i<j}\hat{r}_{ij}\frac{\partial\Psi}{\partial r_{ij}} + \sum_{j<i}\hat{r}_{ij}\frac{\partial\Psi}{\partial r_{ij}} \qquad (4.2.3) \\
\Rightarrow \quad \tilde{\nabla}_{\mathbf{i}}\mathbf{\Psi} &= \hat{\mathbf{r}}_{\mathbf{i}}\frac{\partial\mathbf{\Psi}}{\partial\mathbf{r_i}} + \sum_{\mathbf{j}\neq\mathbf{i}}\hat{\mathbf{r}}_{\mathbf{ij}}\frac{\partial\mathbf{\Psi}}{\partial\mathbf{r_{ij}}}
\end{aligned}$$

Similarly we can define the Laplacian

$$\begin{aligned}
\vec{\nabla}_i^2\Psi &= \vec{\nabla}_i(\vec{\nabla}_i\Psi) = \vec{\nabla}_i\left[\hat{r}_i\frac{\partial\Psi}{\partial r_i} + \sum_{j\neq i}\hat{r}_{ij}\frac{\partial\Psi}{\partial r_{ij}}\right] \\
&= (\vec{\nabla}_i\hat{r}_i)\frac{\partial\Psi}{\partial r_i} + \hat{r}_i\vec{\nabla}_i(\frac{\partial\Psi}{\partial r_i}) + \sum_{j\neq i}\left[(\vec{\nabla}_i\hat{r}_{ij})\frac{\partial\Psi}{\partial r_{ij}} + \hat{r}_{ij}\vec{\nabla}_i(\frac{\partial\Psi}{\partial r_{ij}})\right]
\end{aligned} \qquad (4.2.4)$$

Let's look at the effect of operator $\nabla$ on the unit vectors and extend this derivation to the D-dimension

$$\begin{aligned}
\vec{\nabla}_i\hat{r}_i &= \vec{\nabla}_i\frac{\vec{r}_i}{r_i} = \frac{\vec{\nabla}_i\vec{r}_i}{r_i} - \frac{1}{r_i^2}\vec{r}_i\cdot(\vec{\nabla}\vec{r}_i) \\
&= \frac{D}{r_i} - \frac{1}{r_i^2}\vec{r}_i\cdot\hat{r}_i = \frac{(D-1)}{r_i}
\end{aligned} \qquad (4.2.5)$$

$$\begin{aligned}
\vec{\nabla}_i\hat{r}_{ij} &= \frac{\vec{\nabla}_i\vec{r}_i - \vec{\nabla}_i\vec{r}_j}{r_{ij}} - \frac{1}{r_{ij}^2}(\vec{r}_i - \vec{r}_j)(\vec{\nabla}_i r_{ij}) \\
&= \frac{D}{r_{ij}} - \frac{1}{r_{ij}^2}\vec{r}_{ij}.\hat{r}_{ij} = \frac{(D-1)}{r_{ij}}
\end{aligned} \qquad (4.2.6)$$

$$\begin{aligned}\vec{\nabla}_i(\frac{\partial\Psi}{\partial r_i}) &= \hat{r}_i\frac{\partial^2\Psi}{\partial r_i^2}+\sum_{k\neq i}\hat{r}_{ik}\frac{\partial^2\Psi}{\partial r_i\partial r_{ik}}\\ \vec{\nabla}_i(\frac{\partial\Psi}{\partial r_{ij}}) &= \hat{r}_i\frac{\partial^2\Psi}{\partial r_i\partial r_{ij}}+\sum_{k\neq i}\hat{r}_{ik}\frac{\partial^2\Psi}{\partial r_{ij}\partial r_{ik}}\end{aligned} \tag{4.2.7}$$

Rearrangement of all expressions leads to the general formula for Laplacian

$$\begin{aligned}\vec{\nabla}_i^2\Psi &= \frac{(D-1)}{r_i}\frac{\partial\Psi}{\partial r_i}+\hat{r}_i\left[\hat{r}_i\frac{\partial^2\Psi}{\partial r_i^2}+\sum_{k\neq i}\hat{r}_{ik}\frac{\partial^2\Psi}{\partial r_i\partial r_{ik}}\right]\\ &+ \sum_{j\neq i}\left[\frac{(D-1)}{r_{ij}}\frac{\partial\Psi}{\partial r_{ij}}+\hat{r}_{ij}\left(\hat{r}_i\frac{\partial^2\Psi}{\partial r_i\partial r_{ij}}+\sum_{k\neq i}\hat{r}_{ik}\frac{\partial^2\Psi}{\partial r_{ij}\partial r_{ik}}\right)\right]\end{aligned} \tag{4.2.8}$$

$$\begin{aligned}\vec{\nabla}_i^2\Psi &= \frac{\partial^2\Psi}{\partial r_i^2}+\frac{(D-1)}{r_i}\frac{\partial\Psi}{\partial r_i}+\sum_{j\neq i}2\hat{r}_i.\hat{r}_{ij}\frac{\partial^2\Psi}{\partial r_i\partial r_{ij}}\\ &+ \sum_{j\neq i}\left(\frac{\partial^2\Psi}{\partial r_{ij}^2}+\frac{(D-1)}{r_{ij}}\frac{\partial\Psi}{\partial r_{ij}}\right)+\underbrace{\sum_{j\neq i}\sum_{k\neq i}}_{j\neq k}\hat{r}_{ij}.\hat{r}_{ik}\frac{\partial^2\Psi}{\partial r_{ij}\partial r_{ik}}\end{aligned} \tag{4.2.9}$$

Products of unit vectors are evaluated as follows:

$$\hat{r}_i\cdot\hat{r}_{ij} = \frac{\vec{r}_i}{r_i}.\frac{\vec{r}_i-\vec{r}_j}{r_{ij}}=\frac{r_i^2-\vec{r}_i.\vec{r}_{ij}}{r_ir_{ij}}$$

$$r_{ij}^2 = r_i^2+r_j^2-2\vec{r}_i.\vec{r}_j$$

$$\hat{r}_i\cdot\hat{r}_{ij} = \frac{1}{r_ir_{ij}}\left[r_i^2-\frac{1}{2}(r_i^2+r_j^2-r_{ij}^2)\right]$$

$$\hat{r}_i\cdot\hat{r}_{ij} = \frac{r_i^2-r_j^2+r_{ij}^2}{2r_ir_{ij}}$$

Similarly the dot products of other interparticle unit vectors can be defined as

$$\begin{aligned}
\hat{r}_{ij}\cdot\hat{r}_{ik} &= \frac{(\vec{r}_i-\vec{r}_j)}{r_{ij}}.\frac{(\vec{r}_i-\vec{r}_k)}{r_{ik}} = \frac{(r_i^2-\vec{r}_i.\vec{r}_j-\vec{r}_i.\vec{r}_k+\vec{r}_j.\vec{r}_k)}{r_{ij}r_{ik}} \\
&= \frac{1}{r_{ij}r_{ik}}\left[r_i^2-\frac{1}{2}(r_i^2+r_j^2-r_{ij}^2)-\frac{1}{2}(r_i^2+r_k^2-r_{ik}^2)+\frac{1}{2}(r_j^2+r_k^2-r_{jk}^2)\right] \\
\hat{r}_{ij}\cdot\hat{r}_{ik} &= \frac{1}{2r_{ij}r_{ik}}\left[r_{ij}^2+r_{ik}^2+r_{jk}^2\right]
\end{aligned}$$

Hamiltonian expressed in Hylleraas coordinates in D-dimensional space can be rewritten as

$$\hat{H}=\sum_{i=1}^{N}\hat{H}_i+\sum_{i<j}V_{ij}$$

$$\begin{aligned}
\hat{H} &= \sum_{i=1}^{N}\left\{-\frac{\hbar^2}{2m_i^\star}\left(\frac{\partial^2}{\partial r_i^2}+\frac{(D-1)}{r_i}\frac{\partial}{\partial r_i}\right)+V(r_i)\right\} \\
&+\sum_{i=1}^{N}(-\frac{\hbar^2}{2m_i^\star})\sum_{j\neq i}^{N}\frac{(r_i^2-r_j^2+r_{ij}^2)}{r_ir_j}\frac{\partial^2}{\partial r_i\partial r_{ij}} \\
&+\sum_{i<j}\left[-\frac{\hbar^2}{2}\left(\frac{1}{m_i}+\frac{1}{m_j}\right)\left(\frac{\partial^2}{\partial r_{ij}^2}+\frac{(D-1)}{r_{ij}}\frac{\partial}{\partial r_{ij}}\right)+U(r_{ij})\right] \\
&+\underbrace{\sum_{i}^{N}\sum_{j}^{N}\sum_{k}^{N}}_{j\neq k\neq i}\frac{(r_{ij}^2+r_{ik}^2-r_{jk}^2)}{2r_{ij}r_{ik}}\frac{\partial^2}{\partial r_{ij}\partial r_{ik}}
\end{aligned} \tag{4.2.10}$$

If "D" stands for the dimension of space, Hamiltonian of system with two-particle interacting via Coulomb force in central field can be written in

Hylleraas coordinates as follows

$$
\begin{aligned}
H &= -\frac{\hbar^2}{2m_1}\frac{1}{r_1^{(D-1)}}\frac{\partial}{\partial r_1}(r_1^{(D-1)}\frac{\partial}{\partial r_1}) + V(r_1) \\
&\quad -\frac{\hbar^2}{2m_2}\frac{1}{r_h^{(D-1)}}\frac{\partial}{\partial r_2}(r_2^{(D-1)}\frac{\partial}{\partial r_2}) + V(r_2) \\
&\quad -\frac{\hbar^2}{2}\left(\frac{1}{m_1}+\frac{1}{m_2}\right)\frac{1}{r_{12}^{(D-1)}}\frac{\partial}{\partial r_{12}}(r_{12}^{(D-1)}\frac{\partial}{\partial r_{12}}) \pm \frac{e^2}{4\pi\epsilon}\frac{1}{r_{12}} \\
&\quad -\frac{\hbar^2}{2m_1}\frac{(r_1^2-r_2^2+r_{12}^2)}{r_1 r_{12}}\cdot\frac{\partial^2}{\partial r_1 \partial r_{12}} \\
&\quad -\frac{\hbar^2}{2m_2}\frac{(r_2^2-r_1^2+r_{12}^2)}{r_2 r_{12}}\cdot\frac{\partial^2}{\partial r_2 \partial r_{12}}
\end{aligned}
\tag{4.2.11}
$$

Under this circumstances the basis set for the trial wavefunction for investigation of two-particle systems can be proposed as

$$\Psi^{(p)}(r_1, r_2, r_{12}) = \psi_1(\vec{r}_1)\psi_2(\vec{r}_2)F^{(p)}(r_{12}) \tag{4.2.12}$$

In order to take into account the correlation effects we define ($p \in Z$)

$$F^{(p)}(r_{12}) = e^{-\lambda r_{12}}\, r_{12}^p \tag{4.2.13}$$

Total wavefunction describing the system is proposed as a linear combination of 4.2.12

$$\Psi(r_1, r_2, r_{12}) = \sum_{p=0}^{N_p} C_p \Psi^{(p)}(r_1, r_2, r_{12}) \tag{4.2.14}$$

According to the Ritz's variational principle energy of the system is minimized over the subsets of the $\Psi(r_1, r_2, r_{12})$ constructed as a linear combination of $N_p$ number of basis:

$$E = \min \frac{\langle \Psi \,|H|\, \Psi \rangle}{\langle \Psi |\, \Psi \rangle}$$

Optimization with respect to the $C_p$ coefficients leads to the generalized eigenvalue problem:

$$\mathbf{H}\,\mathbf{C} = \mathbf{E}\,\mathbf{S}\,\mathbf{C} \tag{4.2.15}$$

Here matrix **H** involves kinetic energy terms, energy from Coulomb effects and the other potentials while matrix **S** is the norm with respect to the basis function. Elements of **S** overlap matrix are

$$S_{p'p} = \int d\tau \Psi^{(p')}(r_1, r_2, r_{12}) \Psi^{(p)}(r_1, r_2, r_{12})$$

whereas elements of matrix **H** are calculated as

$$H_{p'p} = \int d\tau \Psi^{(p')}(r_1, r_2, r_{12})\, H\, \Psi^{(p)}(r_1, r_2, r_{12})$$

There are some useful steps which are helpful in the evaluation of various expectation values. For the calculation of the expectation value of the kinetic energy for a product wavefunction, one can use an identity deduced by Le Sech (1997)

$$\int (f\,g)\nabla^2(f\,g)\,d\tau = \int [f\,g^2\nabla^2 f - f^2(\vec{\nabla}g)\cdot(\vec{\nabla}g)]\,d\tau$$

Another useful step is that the integrals of type

$$I = \int F(r_1, r_2)\, f(r_{12}) d^3r_1 d^3r_2$$

as are greatly simplified by taking the angular orientation of $\vec{r}_2$ with respect to $\vec{r}_1$, as variables, so that

$$d^3r_2 = r_2^2 dr_2 \sin\theta_{12} d\theta_{12} d\phi_{12}.$$

Then with

$$r_{12}^2 = r_1^2 + r_2^2 - 2r_1 r_2 \cos\theta_{12},$$

one gets

$$d^3r_2 = \frac{r_2 dr_2 r_{12} dr_{12}}{r_1} d\phi_{12}.$$

Using this in general expression for the integrals and carrying out the angular integrations, one gets for the integral (Patil, 2004)

$$I = 8\pi^2 \int F(r_1, r_2)\, r_1 dr_1\, r_2 dr_2 \int_{|r_1 - r_2|}^{(r_1+r_2)} f(r_{12}) r_{12} dr_{12} \tag{4.2.16}$$

in terms of $r_1$, $r_2$, $r_{12}$, known as the Hylleraas coordinates.

The general procedure for the evaluation of integrals in the matrix elements while working with wavefunctions expressed in Hylleraas coordinates is to use the Equation 4.2.16.

The aim of this thesis work is avoid of integration over Hylleraas coordinates and perform most of the integrals analytically over single-particle coordinates. In this thesis unlike the general procedure mentioned above, the Fourier transforms have been used for the terms including interparticle distance $r_{12}$.

### *4.2.2 Integral Representations*

In order to study only with single-particle coordinates instead of Hylleraas coordinates we can pass by using Delta function. Taking $r_{12} = |\vec{r}_1 - r_2|$ we can write this expression with the aid of delta function as follows

$$\begin{aligned} \Lambda(r_{12}) &= \int d|\vec{r}_1 - \vec{r}_2| \delta(|\vec{r}_1 - \vec{r}_2| - r_{12}) \Lambda(|\vec{r}_1 - \vec{r}_2|) \\ 1 &= \int d|\vec{r}_1 - \vec{r}_2| \delta(|\vec{r}_1 - \vec{r}_2| - r_{12}) \end{aligned} \tag{4.2.17}$$

The Fourier transforms for three-dimensional system are defined as (Deb, 1994; Bhattacharyya et al., 1996)

$$\frac{e^{-\lambda r}}{r} = \frac{1}{2\pi^2}\int \frac{e^{i\vec{q}\cdot\vec{r}}}{(\lambda^2+q^2)}\, d\vec{q} \tag{4.2.18}$$

and

$$\frac{1}{r_{12}} = \frac{1}{2\pi^2}\int \frac{e^{i\vec{R}\cdot(\vec{r}_1-\vec{r}_2)}}{R^2}\, d\vec{R}. \tag{4.2.19}$$

Using this definitions we can obtain the general expression for the terms as $r^p \exp{-\lambda r}$. This can be done by the consecutive derivative of the terms given above as

$$\begin{aligned}
e^{-\lambda r} = -\frac{\partial}{\partial\lambda}\left(\frac{e^{-\lambda r}}{r}\right) &= \frac{2}{(2\pi)^2}\int d\vec{q}(-1)\,\frac{\partial}{\partial\lambda}\left(\frac{1}{q^2+\lambda^2}\right)e^{i\vec{q}\cdot\vec{r}} \\
r\,e^{-\lambda r} = (-1)\frac{\partial}{\partial\lambda}(e^{-\lambda r}) &= \frac{2}{(2\pi)^2}\int d\vec{q}(-1)^2\,\frac{\partial^2}{\partial\lambda^2}\left(\frac{1}{q^2+\lambda^2}\right)e^{i\vec{q}\cdot\vec{r}} \\
r^2\,e^{-\lambda r} = (-)\frac{\partial}{\partial\lambda}(r\,e^{-\lambda r}) &= \frac{2}{(2\pi)^2}\int d\vec{q}(-1)^3\,\frac{\partial^3}{\partial\lambda^3}\left(\frac{1}{q^2+\lambda^2}\right)e^{i\vec{q}\cdot\vec{r}}
\end{aligned} \tag{4.2.20}$$

So for $p \in \mathbf{Z}$ and $p = 0, 1, 2, ...$ we obtain

$$r^{(p-1)}\,\mathrm{e}^{-\lambda\,\mathrm{r}} = (-1)^p\frac{2}{(2\pi)^2}\int d\vec{q}(-1)^p\,\frac{\partial^p}{\partial\lambda^p}\left(\frac{1}{q^2+\lambda^2}\right)e^{i\vec{q}\cdot\vec{r}} \qquad ; p = 0, 1, 2, ... \tag{4.2.21}$$

Using the definition of delta function we can find the explicit expression for terms including interparticle distance:

$$e^{-\lambda|\vec{r}_1-\vec{r}_2|}\,|\vec{r}_1-\vec{r}_2|^{(p-1)} = \frac{2}{(2\pi)^2}\int_0^\infty dq\,q^2\int d\Omega_q\, e^{i\vec{q}\cdot\vec{r}_1}\,e^{i\vec{q}\cdot\vec{r}_2}(-1)^p\frac{\partial^p}{\partial\lambda^p}\left[\frac{1}{(q^2+\lambda^2)}\right] \tag{4.2.22}$$

We define new expression

$$Q_{3D}[q,\lambda,p] = (-1)^p\frac{\partial^p}{\partial\lambda^p}\left[\frac{1}{(q^2+\lambda^2)}\right] \qquad , \quad p \geq 0 \tag{4.2.23}$$

To find more compact form for this expression we use the Rayleigh equation for the terms as $e^{i\vec{q}\cdot\vec{r}}$ (Arfken, & Weber, 2005; Abramowitz, & Stegun, 1972). The Rayleigh equation states that a plane wave may be expanded in a series of spherical waves:

$$e^{i\,q\,r\,\cos\gamma} = \sum_{l=0}^{\infty} i^l\,(2\,l+1) j_l(q\,r)\,P_l(\cos\gamma) \tag{4.2.24}$$

where $j_l(q\,r)$ are spherical Bessel functions and $P_l(\cos\gamma)$ are Legendre polynomials.

In spherical coordinate system let's $(\theta_1, \varphi_1)$ and $(\theta_2, \varphi_2)$ indicate two different directions separated by an angle $\gamma$. There is a trigonometric expression between these angles

$$\cos\gamma = \cos\theta_1\cos\theta_2 + \sin\theta_1\sin\theta_2\cos(\varphi_1 - \varphi_2)$$

According to the Addition Theorem for spherical harmonics Legendre Polynomial can be written as

$$P_l(\cos\gamma) = \frac{4\pi}{(2l+1)} \sum_{m=-l}^{l} Y^{\star}_{l,m}(\theta_1,\varphi_1) Y_{l,m}(\theta_2,\varphi_2) \tag{4.2.25}$$

Using the 4.2.24

$$\begin{aligned} e^{i\,q\,r\,\cos\gamma} &= \sum_{l=0}^{\infty} i^l\,(2\,l+1) j_l(q\,r)\,P_l(\cos\gamma) \\ \Rightarrow \quad e^{i\vec{q}\cdot\vec{r}} &= 4\pi \sum_{l=0}^{\infty}\sum_{m=-l}^{l} i^l j_l(qr) Y^{\star}_{lm}(\Omega_q) Y_{lm}(\Omega_r) \qquad (4.2.26) \\ j_l(x) &= \left(\frac{\pi}{2x}\right)^{1/2} J_{l+\frac{1}{2}}(x) \quad ; \quad l = 0, 1, 2, ... \end{aligned}$$

By using the definitions given above we find an expression for the terms including

interparticle coordinate

$$
\begin{aligned}
e^{-\lambda r_{12}}\, r_{12}^{(p-1)} &= \frac{2}{(2\pi)^2}\int_0^\infty dq\, q^2 \int d\Omega_q Q[q,\lambda,p] \\
&\cdot \quad (4\pi)\sum_{l_1=0}^{\infty}\sum_{m_1=-l_e}^{l_1} (i)^{l_1} j_{l_1}(qr_1) Y^{\star}_{l_1,m_1}(\Omega_q) Y_{l_1,m_1}(\Omega_1) \\
&\cdot \quad (4\pi)\sum_{l_2=0}^{\infty}\sum_{m_2=-l_2}^{l_2} (-i)^{l_2} j_{l_2}(qr_2) Y_{l_2,m_2}(\Omega_q) Y_{l_2,m_2}(\Omega_2)^{\star}
\end{aligned}
\tag{4.2.27}
$$

Orthogonality relations between Spherical Harmonics would lead to the

$$\int d\Omega_q Y^{\star}_{l_1,m_1}(\Omega_q) Y_{l_2,m_2}(\Omega_q) = \delta_{l_1,l_2}\delta_{m_1,m_2}$$

$$\int d\Omega_i Y_{l_i,m_i} = \sqrt{4\pi}\delta_{l_i,0}\delta_{m_i,0}$$

After some simple arrangements we arrive to the integral representations for the terms like $e^{-\lambda r_{12}}\, r_{12}^{p}$:

$$
\begin{aligned}
\int d\Omega_1 \int d\Omega_2\, e^{-\lambda r_{12}}\, r_{12}^{(p-1)} &= 32\pi \int_0^\infty dq. \frac{\sin(qr_1)}{r_1}\,\frac{\sin(qr_2)}{r_2}\, Q[q,\lambda,p] \\
Q_{3D}[q,\lambda,p] &= (-1)^p \frac{\partial^p}{\partial\lambda^p}\left[\frac{1}{(q^2+\lambda^2)}\right]
\end{aligned}
\tag{4.2.28}
$$

Similar derivation can be obtained for the two-dimensional system. Fourier transform for two-dimension is given as

$$\frac{e^{-\lambda r}}{r} = \frac{1}{(2\pi)}\int_0^\infty d\vec{q}\frac{e^{i\vec{q}\cdot\vec{r}}}{\sqrt{q^2+\lambda^2}} \tag{4.2.29}$$

Following the same steps as for three-dimension

$$e^{-\lambda r} = -\frac{\partial}{\partial\lambda}\left(\frac{e^{-\lambda r}}{r}\right) = \frac{1}{(2\pi)}\int d\vec{q}(-1)\,\frac{\partial}{\partial\lambda}\left(\frac{1}{\sqrt{q^2+\lambda^2}}\right)e^{i\vec{q}\cdot\vec{r}}$$

$$r\,e^{-\lambda r} = (-1)\frac{\partial}{\partial\lambda}(e^{-\lambda r}) = \frac{1}{(2\pi)}\int d\vec{q}(-1)^2\,\frac{\partial^2}{\partial\lambda^2}\left(\frac{1}{\sqrt{q^2+\lambda^2}}\right)e^{i\vec{q}\cdot\vec{r}} \quad (4.2.30)$$

$$r^2\,e^{-\lambda r} = (-)\frac{\partial}{\partial\lambda}(r\,e^{-\lambda r}) = \frac{1}{(2\pi)}\int d\vec{q}(-1)^3\,\frac{\partial^3}{\partial\lambda^3}\left(\frac{1}{\sqrt{q^2+\lambda^2}}\right)e^{i\vec{q}\cdot\vec{r}}$$

So for $p \in \mathbf{Z}$ and $p = 0, 1, 2, ...$ we obtain

$$\mathrm{e}^{-\lambda\,\mathrm{r}}\,r^{(p-1)} = (-1)^p\frac{1}{(2\pi)}\int d\vec{q}(-1)^p\,\frac{\partial^p}{\partial\lambda^p}\left(\frac{1}{\sqrt{q^2+\lambda^2}}\right)e^{i\vec{q}\cdot\vec{r}} \quad ; \quad p = 0, 1, 2, ... \quad (4.2.31)$$

Using the definition 4.2.17 we can find the explicit expression for terms including interparticle distance.

$$e^{-\lambda|\vec{r}_1-\vec{r}_2|}\,|\vec{r}_1-\vec{r}_2|^{(p-1)} = \frac{1}{(2\pi)}\int_0^\infty dq\,q\int d\Omega_q\,e^{i\vec{q}\cdot\vec{r}_1}\,e^{i\vec{q}\cdot\vec{r}_2}(-1)^p\frac{\partial^p}{\partial\lambda^p}\left[\frac{1}{\sqrt{q^2+\lambda^2}}\right] \quad (4.2.32)$$

and we define new expression

$$Q_{2D}[q,\lambda,p] = (-1)^p\frac{\partial^p}{\partial\lambda^p}\left[\frac{1}{\sqrt{q^2+\lambda^2}}\right] \quad , p \geq 0 \quad (4.2.33)$$

According to Jacobi-Anger expansion, a plane wave may be expanded in a series of cylindrical waves (Arfken, & Weber, 2005).

$$e^{i\,z\,\cos\theta} = \sum_{m=-\infty}^{\infty} i^m\,J_m(z)\,e^{i\,m\,\theta} \quad (4.2.34)$$

where $J_m(z)$ are Bessel functions of the first kind. With the assistance of 4.2.34 and orthogonality relations we can express the terms as $r_{12}^p\,\mathrm{e}^{-\lambda\,r_{12}}$ in more compact

form. Expansion for the exponential in two-dimension is given as

$$e^{i\vec{q}\cdot\vec{r}} = e^{iqr\cos(\theta_q-\theta_r)} = \sum_{n=-\infty}^{\infty}(i)^n.J_n(qr).e^{in(\theta_q-\theta_r)} \tag{4.2.35}$$

$$\begin{aligned} e^{i\vec{q}\cdot\vec{r}_{12}} &= e^{i\vec{q}\cdot\vec{r}_1}.e^{-i\vec{q}\cdot\vec{r}_2} \\ &= \sum_{n=-\infty}^{\infty}(i)^n.J_n(qr_1).e^{in(\theta_q-\theta_{r_1})}\cdot\sum_{n'=-\infty}^{\infty}(-i)^n.J_{n'}(qr_2).e^{-in'(\theta_q-\theta_{r_2})} \end{aligned} \tag{4.2.36}$$

Using the integral definitions of delta function and Equation 4.2.33

$$\begin{aligned} &\frac{1}{2\pi}\int d\theta_q.e^{i(n-n')\theta_q} = \delta_{n,n'} \\ &\int d\theta_1.e^{-in\theta_1} = 2\pi\delta_{n,0} \qquad ; \qquad \int d\theta_2 \mathrm{e}^{i\theta_2} = 2\pi\delta_{n,0} \end{aligned} \tag{4.2.37}$$

we obtain the integral representations for the terms like $e^{-\lambda r_{12}}\, r_{12}^{p}$

$$\begin{aligned} \int_0^{\infty}d\theta_1\int_0^{\infty}d\theta_2\, e^{-\lambda r_{12}}\, r_{12}^{(p-1)} &= (2\pi)^2\int_0^{\infty}dq\, q\, Q_{2D}[q,\lambda,p]\, J_0(qr_1)\, J_0(qr_2) \\ Q_{2D}[q,\lambda,p] &= (-1)^p\frac{\partial^p}{\partial\lambda^p}\left[\frac{1}{\sqrt{q^2+\lambda^2}}\right] \qquad ,p\geq 0 \end{aligned} \tag{4.2.38}$$

Utilization of this integral representations for the terms in the form of $r_{12}^k\exp(-\lambda\, r_{12})$, ($k\in\mathbb{Z}$ and $\lambda$ is a parameter) avoid the use of general integration technique for Hylleraas coordinates. This approach provides the calculation of most of integrals to be done analytically over single-particle coordinates instead of Hylleraas coordinates

# CHAPTER FIVE
# NUMERICAL RESULTS

## 5.1 Ground State Energy of He Isoelectronic Sequence

### *5.1.1 Brief Overview*

The theory of two-electron atoms has played an important role on development of theoretical physics since the early days of quantum mechanics. He and helium like atoms in which the electron-electron correlation has an important effect, do not have analytical solutions; for this reason these systems have been a field of intensive study since the early times of quantum mechanics (Kleinekathofer et al., 1996; Aquino, 1996). Complete understanding of these two electron systems would guide to the solution of more complicated many-electron systems. Although several methods have been proposed to solve the problem (Styszynski, & Karwowski, 1988; Braun et al., 1993; Rodriguez et al., 2007), variational method is still a standard technique applied in the study of atomic properties (Frankowski, & Pekeris, 1966; Freund et al., 1984; Bhattacharyya et al., 1996; Le Sech, 1997; Patil, 2004; Otranto et al., 2004). Determination of accurate and simple wavefunctions is not only important for understanding of single-particle properties but also for understanding of physical processes like double ionization (Ancarani et al., 2004; Rodriguez, & Gasaneo, 2005). Calculation of cross section of inelastic collision processes involves evaluation of multidimensional integrals (Le Sech, 1997). The use of simple wavefunctions allows partial analytical development of double ionization amplitudes which reduces the difficulty of the calculations (Otranto et al., 2004; Ancarani et al., 2004).

Efforts related to the determination of accurate wavefunctions for atomic bound

states could be divided into two main approaches: first one is based on sophisticated calculations where many variational parameter wavefunctions are used to produce highly precise approximations (Frankowski, & Pekeris, 1966; Freund et al., 1984; Pekeris, 1959; Goldman, 1998; Korobov, 2000). More recently, by using wavefunction depending on exponential-type functions with complex variational parameters chosen in a quasirandom manner, Korobov (2000) obtained highly accurate energies for helium and positive hydrogen molecular ion with 2200 number of basis set. Drake et al. (2002) used triple basis set in Hylleraas coordinates including 2300 terms and obtained 22-figure accuracy for non relativistic energy of He. Increment in the number of variational parameters and utilization of huge basis sets needed to improve the wavefunction, generally not only results in more time-consuming calculations (Otranto et al., 2004), but also it is not realistic for the use in scattering calculations (Ghoshal et al., 2003). Within the second approach trial wavefunction generally is constructed to fulfill the correct asymptotic behavior and involves relatively low number of variational parameters (Kleinekathofer et al., 1996; Le Sech, 1997; Patil, 2004; Otranto et al., 2004; Ancarani et al., 2007; David, 2006). Le Sech (1997) reported an accuracy for two-parameter wavefunction which fulfill the cusp conditions at singularities and correct behavior for large interparticle separations to be about $10^{-3}$. Patil (2004) brought out the structural importance of the correlation property of two-electron systems in terms of simple zero- and one-parameter wave functions. Lateen Ancarani et al. (2007) proposed parameter free simple wave function satisfying all two-particle cusp conditions that given fully analytical expressions for energy and other mean values. The shortage of this approach is that the energies are not good enough to describe the system (Rodriguez et al., 2007). Hylleraas-type wavefunctions can be considered as an intermediate approach (Rodriguez, & Gasaneo, 2005). After the manifestation of explicitly correlated basis set at the end of 1920s, several works for the calculation of ground state energy of He atom and He-isoelectronic sequence using different derivatives of

Hylleraas basis set have been published (Goldman, 1998; Korobov, 2000; Bartlett et al., 1935; Chandrasekhar et al., 1953; Green et al., 1953; Thakkar, & Koga, 1994). Following the method applied by Hylleraas, Schwartz (1956) allowed an half-integer powers of the Hylleraas variables while Kinoshita (1957) extended the domain of powers of three Hylleraas coordinates to negative integers. After introduction of atomic wavefunction closely related to the Hylleraas ansatz by Coolidge, & James, (1936) successful application of wavefunction depending on perimetric coordinates had been done by (Pekeris, 1959). Frankowski, et al.(1966) suggested the inclusion of terms with logarithmic dependence.

In this part of the thesis we focus our work on the determination of ground state energy for helium and He-like ions with nuclear charges $Z = 1-6$. Relatively simple wavefunction for obtaining the ground state energy of two-electron atoms is constructed in terms of exponential and power series. In order to to fulfill conditions for coalescence points special care is taken. Our work, with low number of parameters, is based on modifying and extending the wavefunction proposed by Bhattacharyya et al. (1996) with Hylleraas-like basis set to get improved accuracy than the work done by them for He atom and apply the same wavefunction for He-like ions. Variational parameters for improved versions of ground state wavefunction have been determined.

### *5.1.2 Theory and Method*

The non-relativistic three-body (two electrons and nucleus) Coulomb Hamiltonian in the infinitely heavy nucleus approximation is given as

$$\hat{H} = -\frac{1}{2}\vec{\nabla}^2_{r_1} - \frac{1}{2}\vec{\nabla}^2_{r_2} - \frac{Z}{r_1} - \frac{Z}{r_2} + \frac{1}{r_{12}} \tag{5.1.1}$$

where $j = (1, 2)$, $r_j$, indicates the location of $j^{th}$ electron relative to the nucleus and $r_{12}$ is interelectronic distance. The Hamiltonian in 5.1.1 includes six

independent electronic spherical coordinates. Using coordinate system which explicitly includes $r_{12}$ interelectronic distance render possible to treat the electron-electron correlation effects. The most used is $r_1$, $r_2$, $r_{12}$, $\alpha$, $\beta$ and $\gamma$ basis set where $\alpha$, $\beta$ and $\gamma$ are three Euler angles (Forrey, 2004). After taking away the Euler angles, Schrödinger equation reduces to Hylleraas equation which leads to the reduction of six-dimensional system to the three-dimensional system. For complete description of S-states these three independent coordinates are sufficient (Ancarani et al., 2007; Myers et al., 1991).Thus the Hamiltonian of the system expressed in Hylleraas coordinates can be written as (Aquino et al., 2006)

$$\begin{aligned}\hat{H} &= -\frac{1}{2}\left(\frac{\partial^2}{\partial r_1^2}+\frac{2}{r_1}\frac{\partial}{\partial r_1}+\frac{\partial^2}{\partial r_{12}^2}+\frac{2}{r_{12}}\frac{\partial}{\partial r_{12}}+2\hat{r}_1\cdot\hat{r}_{12}\frac{\partial^2}{\partial r_1 r_{12}}\right)\\ &\quad -\frac{1}{2}\left(\frac{\partial^2}{\partial r_2^2}+\frac{2}{r_2}\frac{\partial}{\partial r_2}+\frac{\partial^2}{\partial r_{12}^2}+\frac{2}{r_{12}}\frac{\partial}{\partial r_{12}}-2\hat{r}_2\cdot\hat{r}_{12}\frac{\partial^2}{\partial r_2 r_{12}}\right) \qquad (5.1.2)\\ &\quad -\frac{Z}{r_1}-\frac{Z}{r_2}+\frac{1}{r_{12}}\end{aligned}$$

$\hat{r}_1$, $\hat{r}_2$ stands for the unit vectors for electron-nucleus distance and $\hat{r}_{12}$ denotes the unit vector of interelectronic distance.

One of the most important point in the works on two-electron systems is the choice of wavefunction which satisfies proper symmetry under the interchange of the electron coordinates and correct cusp conditions that are responsible for the two-body Coulomb singularities. The ground state wavefunctions of He and He-like ions are expressed as a product of wavefunction describing the orbital motion of free-particles in the field of nucleus area and a correlation function depending on the interelectronic distance $r_{12}$ (Bhattacharyya et al., 1996; Le Sech, 1997). Following these ideas we proposed here in this article wavefunction, without inclusion of Hylleraas basis set, that ensures the

conditions: the separability of the wavefunction when the two electrons are far apart $r_{12} \to \infty$ and requirement of small finite value of correlation function in $r_{12} \to 0$ limits. The wavefunction proposed in this connection is constructed as a product of Slater-type orbitals that are solutions of non-interacting system and $(1 - \lambda e^{-\mu r_{12}})$ term which defines two-electron correlation. Our ansatz for finding the appropriate wavefunction describing the ground state of atom (ions) in He isoelectronic sequence is chosen in the form of

$$\phi(r_1, r_2, r_{12}) = e^{-Z\alpha(r_1+r_2)} e^{-\beta r_{12}} (1 - \lambda e^{-\mu r_{12}}) \tag{5.1.3}$$

where $\alpha$, $\beta$, $\lambda$ and $\mu$ are adjustable variational parameters and $Z$ denotes the nuclear charge. The difference between wavefunction of Bhattacharyya et al. (1996) and ours is the $e^{-\beta r_{12}}$ term that is important for the evaluation of integrals by means of integral representations obtained for the terms containing powers of $r_{12}$ coordinates. The approximate solution is built by expanding the wavefunction expressed in analytical form with Hylleraas-like basis set

$$\Phi(r_1, r_2, r_{12}) = \sum_N C_N \, \Psi^N(r_1, r_2, r_{12}) \tag{5.1.4}$$

where

$$\Psi^N(r_1, r_2, r_{12}) = \phi(r_1, r_2, r_{12})(1 + P_{12}) r_1^{n_1} r_2^{n_2} r_{12}^{n_{12}} \tag{5.1.5}$$

Here $n_i, (i = 1, 2, 12)$ are integers and $N \equiv \{n_1, n_2, n_{12}\}$ are sets of all parameters incorporated in wavefunction. $P_{12}$ denotes permutation operator of coordinates $r_1$ and $r_2$. Factor $(1 + P_{12})$ accounts for spatial symmetric combinations associated with singlet state. For simplicity, in what follows we shall drop the $(r_1, r_2, r_{12})$ dependence of $\Psi^N(r_1, r_2, r_{12})$. As a consequence of $S = 0$ (antisymmetric spin function) for the ground state of the systems, spatial function $\Psi$ has to be symmetric under the exchange of electron coordinates imposing the constraint $C_{n_1,n_2,n_{12}} = C_{n_2,n_1,n_{12}}$. To fulfill with that symmetry the series on 5.1.4 has to include terms up to the same value of the indices $n_1$ and $n_2$.

In order to investigate the convergence of each form of a given excitation level all possible combinations of variables have been considered. Optimization with respect to the $C_N$ linear expansion coefficients in 5.1.4 is a generalized eigenvalue problem, consisting in diagonalization of matrix

$$\mathbf{H}\,\mathbf{C} = E\,\mathbf{S}\,\mathbf{C}. \tag{5.1.6}$$

Here matrix $\mathbf{H}$ denotes kinetic energy, energy from Coulomb interaction and interaction with nucleus whereas matrix $\mathbf{S}$ denotes the norm with respect to the basis function. $C_N$ stands for column matrix of $C_{n_1,n_2,n_{12}}$ coefficients. Elements of overlap matrix $\mathbf{S}$ are given as

$$S_{M,N} = \langle \Psi^M | \Psi^N \rangle = \int\int d\vec{r}_1 d\vec{r}_2 \Psi^{M*} \Psi^N \tag{5.1.7}$$

and elements of $\mathbf{H}$ Hamiltonian matrix are

$$\begin{aligned} H_{M,N} &= \langle \Psi^M | \hat{H} | \Psi^N \rangle \\ &= \frac{1}{2}\int\int d\vec{r}_1 d\vec{r}_2 \left( \vec{\nabla}_{r_1} \Psi^{M*} \cdot \vec{\nabla}_{r_1} \Psi^N + \vec{\nabla}_{r_2} \Psi^{M*} \cdot \vec{\nabla}_{r_2} \Psi^N \right) \\ &\quad -Z \int\int d\vec{r}_1 d\vec{r}_2 \Psi^{M*} \left( \frac{1}{r_1} + \frac{1}{r_2} \right) \Psi^N \\ &\quad + \int\int d\vec{r}_1 d\vec{r}_2 \Psi^{M*} \frac{1}{r_{12}} \Psi^N \end{aligned} \tag{5.1.8}$$

Matrix elements are calculated using integral representations obtained for 3D in Equation 4.2.28. Since these integral representations separate coordinates of each electron from other one, integrals in similar form are obtained for each electron. These separated integrals are calculated analytically in terms of gamma and trigonometric functions. Integrations over $r_1$ and $r_2$ coordinates are performed analytically whereas numerical procedure is applied for the integrations over $q$ variable coming from the integral representations.

### *5.1.3 Results and Discussion*

We have performed calculations for ground state energy of He atom and He-like ions by means of wavefunction expressed as Hylleraas-like basis set 5.1.4, which spans powers $\{n_1, n_2, n_{12}\}$ for the corresponding coordinates $r_1$, $r_2$ and $r_{12}$ and commensurate with the condition $n_1 + n_2 + n_{12} \leq 8$. Calculation of ground state energies have been actualized in two stages. The first one is getting $\alpha$, $\lambda$ and $\mu$ variational parameters which minimizes energy by using 5.1.3, in other words without using Hylleraas-like series expansion with $\beta \simeq 0$, $n_{1\max} = 0$, $n_{2\max} = 0$ and $n_{12\max} = 0$ we obtained optimal values of variational parameters. Here the notation $n_{(i)_{\max}}$, where $(i = 1, 2, 12)$, indicates the maximum power of corresponding coordinate. Columns three, four and five of Table 5.1 present the optimized values of variational parameters. The corresponding calculated energies of the systems $H^-$, He, $Li^+$, $Be^{2+}$, $B^{3+}$ and $C^{4+}$ are given at the last column of Table 5.1.

Table 5.1 Ground state energies of $H^-$, He, $Li^+$, $Be^{2+}$, $B^{3+}$, $C^{4+}$ calculated using the wavefunction given in 5.1.3 and values of the corresponding optimized parameters. All obtained energies are in atomic units.

| System | Z | $\alpha$ | $\lambda$ | $\mu$ | $-$ Energy |
|---|---|---|---|---|---|
| $H^-$ | 1 | 0.81 | 0.89 | 0.07 | 0.5076 |
| He | 2 | 0.92 | 0.95 | 0.02 | 2.8911 |
| $Li^+$ | 3 | 0.94 | 0.44 | 0.60 | 7.2669 |
| $Be^{2+}$ | 4 | 0.96 | 0.61 | 0.22 | 13.6443 |
| $B^{3+}$ | 5 | 0.96 | 0.22 | 1.52 | 22.0167 |
| $C^{4+}$ | 6 | 0.98 | 0.46 | 0.45 | 32.3951 |

Table 5.2 Ground state energy of He atom (in atomic units) for different number of maximum degrees of $n_1$, $n_2$ and $n_{12}$ corresponding to the coordinates $r_1$, $r_2$ and $r_{12}$ respectively.

| $n_{1\max}(n_{2\max})$ | $n_{12\max}$ | $-$ Energy |
|---|---|---|
| 1 | 1 | 2.8969 |
| 2 | 1 | 2.9030 |
| 3 | 1 | 2.9033 |
| 1 | 2 | 2.9028 |
| 2 | 2 | 2.9032 |
| 3 | 2 | 2.9034 |

Second stage of the calculation is the incorporating Hylleraas-like series expansion by using the values of parameters obtained at the first stage. We introduced the exponential factor $e^{-\beta r_{12}}$ in the wavefunction 5.1.3 in order to calculate the integrals related to interelectronic distance analytically by using Fourier transforms. Also we fixed the parameter $\beta$ to $10^{-2}$ for all two-electron systems since, it showed a little sensitivity to the evaluated energy value. Expansion of different powers, $(n_1, n_2, n_{12})$, of all coordinates is performed by putting into account the values for non-linear variational parameters obtained in the first stage of the calculation. By using the wavefunction as in 5.1.4, relatively low expansions are sufficient to accomplish reasonably accurate energies describing the ground state of the systems. To illustrate the appreciable improvement on the energy of adding more terms to the expansion, we show dependency of energy with different number of maximum degrees of $n_1$, $n_2$ and $n_{12}$ only for He atom in Table 5.2.

Inclusion of higher degrees of $r_1$, $r_2$ and $r_{12}$ coordinates into the expansion leads to an considerable improvement in variational energy for the systems considered in this work. This situation is evident in Table 5.3 in comparison

to the energies given in Table 5.1.

The conditions that measure the quality of the approximate wavefunction at singular points of potentials have been tested. Parameters related to the electron-nucleus coalescence point are not far from their exact values. Expected value for this coalescence point is equal to the negative value of nuclear charge of the two-electron system. So in our calculations the value of non-linear $\alpha$ parameter should be equal to 1. As seen in Table 5.1 $\alpha$ parameter approaches to its exact value with increase in nuclear charge. Parameters related to the electron-electron coalescence point, $R_{ee}$, are presented in Table 5.3. Except the case of $H^-$, obtained values for $R_{ee}$ are smaller than the expected value which is 0.5. This can be interpreted as underestimation of interelectronic repulsion by the proposed wavefunction. But more significantly ground state energies of isoelectronic sequence have been found to be within reasonable accuracy. The wavefunction proposed in this work yields ground-state energies for the helium-like atoms with $Z = 1$ ($H^-$) to $Z = 6$ ($C^{4+}$) within $0.0009-0.0002$ au of the *exact* energies of Ref. (Pekeris, 1958) which is widely used in literature as a reference work. These results are significantly better than the results obtained with previous models. Rodriguez et al. (2007) reported angular correlated configuration-interaction method to analyze n-parameter Hylleraas wavefunctions satisfying all cusp conditions. Results obtained by Rodriguez (Rodriguez et al., 2007) are given in Table 5.3 for comparison. We also compared energies with the energies found by Otranto et al. (2004). They used relatively simple analytical wavefunctions, by modifying the wavefunctions used by (Bonham, & Kohl, 1966) and Le Sech (1997). In spite of a little complexity, relative to the Ref. (Otranto et al., 2004), wavefunction proposed in this work gave slightly closer values for energy. This can be interpreted as the wavefunction proposed in this work describes better the ground state of the systems under consideration.

Table 5.3 Ground state energies calculated using the wavefunction given in 5.1.4 and electron-electron cusp condition. Exact energies are taken from Ref.(Pekeris, 1958). All energies are in atomic units.

| System | Z | − Energy | − $\text{Energy}_{\text{exact}}$ | $R_{\text{ee}}$ |
|---|---|---|---|---|
| $H^-$ | 1 | 0.5268 [a] | 0.5277 | 0.5564 |
| | | 0.5258 [b] | | |
| | | 0.5259 [c] | | |
| He | 2 | 2.9034 [a] | 2.9037 | 0.3700 |
| | | 2.9020 [b] | | |
| | | 2.9019 [c] | | |
| $Li^+$ | 3 | 7.2797 [a] | 7.2799 | 0.4614 |
| | | 7.2778 [b] | | |
| | | 7.2780 [c] | | |
| $Be^{2+}$ | 4 | 13.6551 [a] | 13.6555 | 0.3440 |
| | | 13.6534 [b] | | |
| | | 13.6536 [c] | | |
| $B^{3+}$ | 5 | 22.0307 [a] | 22.0309 | 0.3781 |
| | | 22.0287 [b] | | |
| | | 22.0290 [c] | | |
| $C^{4+}$ | 6 | 32.4056 [a] | 32.4062 | 0.3733 |
| | | 32.4039 [b] | | |
| | | 32.4043 [c] | | |

[a] this study
[b] Ref. (Rodriguez et al., 2007)
[c] Ref. (Otranto et al., 2004)

## 5.2 Ground State Energy of Two-electrons in Parabolic Quantum Dot

### *5.2.1 Introduction and Motivation*

The progress in nanofabrication technology makes it possible to fabricate low-dimensional nanostructures with controllable chemical composition and geometric structure. Quantum dots (QDs), quasi-zero dimensional systems, are nanostructures where the strong confinement is imposed in all three spatial dimensions (Pino, & Villalba, 2001). In these systems, finite number of electrons are confined in a small spatial region whose dimensions are comparable to the de Broglie wavelength of carriers (El-Said, 2000; Drouvelis et al., 2004; Dineykhan et al., 2005). Due to the nanoscale extensions in all spatial dimensions, QDs possess discrete energy levels that can be tuned (El-Said, 1995). As a consequence of reduced dimensionality with design flexibility, the singular nature ($\delta$-function like) of density of states, presence of several comparable energy and length scales, QDs show new physical phenomena quite different from those of the bulk (Peeters, & Schweigert, 1996).

There is an increasing interest in this extremely fascinating field in the last two decades which is motivated by the physical effects and potential novel device applications of QDs (Boyaciglu et al., 2007), such as electronic memories, single-electron transistors, quantum dot lasers and ultrafast computers (El-Said, 1995; El-Said, 2007. The capability of control over the properties of QDs in semiconductors has attracted great attention both for experimental (Sikorski, & Merkt, 1989; Tarucha et al., 1996; Ellenberger et al., 2006; Ihn et al., 2006) and theoretical works (Pino, & Villalba, 2001; Merkt et al., 1991; Pfannkuche, & Gerhardts, 1991; Taut, 1993; Zhu et al., 1997; Lamouche, & Fishman, 1998; McKinney, & Watson, 2000; Adamowski et al., 2000; Ciftja, & Faruk, 2005; Ciftja, & Faruk).

Various theoretical approaches have been employed to study the energy spectra and correlation effects of interacting electrons confined in QDs. Widely used methods include numerical diagonalization (Pfannkuche, & Gerhardts, 1991; Lamouche, & Fishman, 1998; Sun et al., 2003), variational method (Ciftja, & Kumar, 2004; Szafran et al., 1999; Vazquez et al., 2004), Monte Carlo simulations (Harju et al., 2002; Siljamaki et al., 2005), shifted 1/N method (Pino, & Villalba, 2001; El-Said, 2007), series expansion method (Zhu et al., 1997) and configuration interaction method (Bielinska-Waz et al., 2001; Sako, & Diercksen, 2003a; Sako, & Diercksen, 2003b). Most of these theoretical studies have assumed the model electron confinement usually described by a parabolic potential due to the fact that the pronounced shell structure measured in the addition energy spectra of QDs is a direct consequence of it (Tarucha et al., 1996; Brey et al., 1989; Peeters, 1990).

Experimental investigations have allowed the characterization of the energy spectra of a few-electron QDs where interesting phenomena like singlet-triplet transitions, charge quantization and Coulomb blockade have been observed (Maksym, & Chakraborty, 1990; Lin, & Jiang, 2001). But from a theoretical point of view these few-body systems represent a challenging problem. Inability of exact analytical solution of this problem leads works to resort to numerical methods or approximation schemes (Gu, 2006). However a fully quantum mechanical treatment requires numerical calculations which could be computationally expensive and time-consuming as the number of electrons grow. The simplest example of a few-electron QDs is a system consisting of two electrons, interacting via Coulomb force, where carriers are trapped by parabolic confinement potential. But nevertheless an exact analytical solution of this two-electron problem is not attainable (El-Said, 2007). The insights provided by the studies of this minimal system may be the first step on the understanding of the many fundamental properties of systems with a larger number of particles.

In the present part, we calculated the ground state energy of a two-electron quantum dot confined by a two-dimensional (2D) and three-dimensional (3D) isotropic harmonic potential by using variational method with Hylleraas-like trial wavefunction.

### *5.2.2 Model and Method*

The effective mass Hamiltonian for an interacting pair of electrons confined in a quantum dot by a parabolic potential is given as

$$\hat{H} = \sum_{i=1}^{2} \left( -\frac{\hbar^2}{2m^*} \vec{\nabla}_i^2 + \frac{1}{2} m^* \omega_0^2 r_i^2 \right) + \frac{e^2}{4\pi\varepsilon r_{12}}. \tag{5.2.1}$$

Here $\omega_0$ is the confining frequency and $\varepsilon$ is the dielectric constant of the medium where the particles move. The location of each electron, with effective mass $m^*$, relative to the center of QD is labeled by $\vec{r}_1$ and $\vec{r}_2$ for the first and the second electron, respectively. $\vec{r}_{12}$ represents the interelectronic distance. In terms of simplicity distortion of Coulomb interaction formed due to the difference between dielectric constants of quantum dot and matrix material has been neglected.

In order to express the Hamiltonian in dimensionless form, we define

$$a^* = \frac{4\pi\varepsilon\hbar^2}{m^* e^2} \qquad \text{and} \qquad l_0 = \sqrt{\frac{\hbar}{m^*\omega_0}} \tag{5.2.2}$$

where $a^*$ is the effective Bohr radius and $l_0$ is the characteristic length of quantum dot. The effective Rydberg $\mathrm{Ry}^* = \hbar^2/2m^*a^*$ and the effective Bohr radius $a^*$ are taken as the energy and length scales, respectively. The introduced dimensionless parameter $\mathrm{W} = 2\left(a^*/l_0\right)^2$ describes the relative magnitude of the confinement energy and Coulombic energy scales. $\mathrm{W}^{-1/2}$ is related to the confinement region of electrons in QD which later will be used to investigate the quantum size effects. Upon the definitions introduced above, dimensionless Hamiltonian of parabolic

quantum dot with two electrons is written as

$$\hat{H} = \sum_{i=1}^{2} \left( -\vec{\nabla}_i^2 + \frac{1}{4}\mathrm{W}^2 r_i^2 \right) + \frac{2}{r_{12}}. \tag{5.2.3}$$

The Hamiltonian in 5.2.3 includes six independent spherical coordinates. Using Hylleraas coordinate system Hamiltonian can be expressed in terms of $r_1$, $r_2$ and $r_{12}$ which render possible to treat electron-electron correlation effects (Myers et al., 1991; Forrey, 2004). One of the most important point in the variational works on two electron systems is the choice of appropriate wavefunction. In variational treatment of three-body Coulomb systems, functions expanded in terms of generalized Hylleraas basis set are widely used (Aquino et al., 2006). The built-in correlated character of these functions render possible to ensure accurate energies for ground state of two-electron and three-body molecular systems over relatively low expansions. Having this in mind, our ansatz for wavefunction describing the ground state of two electron QD confined by parabolic potential is chosen in the form of

$$\Phi\left(r_1, r_2, r_{12}\right) = \sum_N C_N \Psi^N\left(r_1, r_2, r_{12}\right) \tag{5.2.4}$$

where

$$\Psi^N\left(r_1, r_2, r_{12}\right) = \phi\left(r_1\right)\phi\left(r_2\right)\, \mathrm{e}^{-\lambda r_{12}}\, r_1^{n_1}\, r_2^{n_2}\, r_{12}^{n_{12}}. \tag{5.2.5}$$

Basis function $\phi\left(r_i\right)$ has been chosen to be the solution of the non-interacting system in the form of

$$\phi\left(r_i\right) = \mathrm{e}^{-\gamma \mathrm{W} \frac{r_i^2}{2}} \quad , \quad (i = 1, 2). \tag{5.2.6}$$

Here, $\gamma$ and $\lambda$ are adjustable variational parameters varied so as to minimize the expectation value of energy. Product $\phi\left(r_1\right)\phi\left(r_2\right)$ defines the ground state of uncorrelated electron pair in parabolic confinement with strength W. Exponential term $\mathrm{e}^{-\lambda r_{12}}$, which defines the correlation between electrons, not

only has physical meaning but also has crucial role in the perspective of this study. The main importance of this term is to yield the evaluation of integrals by means of integral representations obtained for the terms like $r_{12}^{k}\,\exp\left(-\lambda\, r_{12}\right)$. And finally, $r_1^{n_1}\, r_2^{n_2}\, r_{12}^{n_{12}}$ product in 5.2.5 is introduced in order to take into account the spatial correlations. Proposed wavefunction is spanned by $N \equiv \{n_1, n_2, n_{12}\}$, where integers, $n_i\,(i = 1, 2, 12)$, in the series expansion part of the wavefunction corresponds to the powers of coordinates $r_1$, $r_2$ and $r_{12}$, respectively and are positive or equal to zero. For simplicity, in what follows we shall drop the $(r_1, r_2, r_{12})$ dependence of $\Psi^N\,(r_1, r_2, r_{12})$.

Having the trial wavefunction 5.2.4, the standard energy eigenvalue problem arising out of the Ritz's variational principle for determination of correlated basis $\Psi_N$ takes the form

$$\mathbf{H}\,\mathbf{C} = E\,\mathbf{S}\,\mathbf{C}. \tag{5.2.7}$$

Here $\mathbf{H}$ consists of kinetic term, Coulomb interaction, and interaction with confinement potential, $\mathbf{S}$ denotes the norm with respect to the basis function $\Psi^N$, and $\mathbf{C}$ stands for column matrix of $C_{n_1,n_2,n_{12}}$ coefficients.

Elements of $\mathbf{S}$ overlap matrix are given as

$$S_{M,N} = \langle \Psi^M \,|\, \Psi^N \rangle = \int\int d\vec{r}_1 d\vec{r}_2 \Psi^{M^*} \Psi^N \tag{5.2.8}$$

In order to express Hamiltonian of the system in Hylleraas coordinates we use the definition of vector operator del in Hylleraas-type coordinates as

$$\vec{\nabla}_i = \hat{r}_i \frac{\partial}{\partial r_i} + \sum_{j \neq i} \hat{r}_{ij} \frac{\partial}{\partial r_{ij}}. \tag{5.2.9}$$

After a simple arrangement, the elements of Hamiltonian matrix $\mathbf{H}$ can be

evaluated as follows:

$$
\begin{aligned}
H_{M,N} = \; & \langle \Psi^M | \hat{H} | \Psi^N \rangle \\
= \; & \int\int d\vec{r}_1 d\vec{r}_2 \left[ \vec{\nabla}_{r_1} \Psi^{M\star} \cdot \vec{\nabla}_{r_1} \Psi^N + \Psi^{M\star} \frac{1}{4} \mathrm{W}^2 r_1^2 \, \Psi^N \right] \\
+ \; & \int\int d\vec{r}_1 d\vec{r}_2 \frac{(r_1^2 - r_2^2 + r_{12}^2)}{2 r_1 r_{12}} \left( \frac{\partial \Psi^{M\star}}{\partial r_1} \frac{\partial \Psi^N}{\partial r_{12}} + \frac{\partial \Psi^{M\star}}{\partial r_{12}} \frac{\partial \Psi^N}{\partial r_1} \right) \\
+ \; & \int\int d\vec{r}_1 d\vec{r}_2 \left[ \vec{\nabla}_{r_2} \Psi^{M\star} \cdot \vec{\nabla}_{r_2} \Psi^N + \Psi^{M\star} \frac{1}{4} \mathrm{W}^2 r_2^2 \, \Psi^N \right] \\
+ \; & \int\int d\vec{r}_1 d\vec{r}_2 \frac{(r_2^2 - r_1^2 + r_{12}^2)}{2 r_2 r_{12}} \left( \frac{\partial \Psi^{M\star}}{\partial r_2} \frac{\partial \Psi^N}{\partial r_{12}} + \frac{\partial \Psi^{M\star}}{\partial r_{12}} \frac{\partial \Psi^N}{\partial r_2} \right) \\
+ \; & \int\int d\vec{r}_1 d\vec{r}_2 \left[ 2 \, \vec{\nabla}_{r_{12}} \Psi^{M\star} \cdot \vec{\nabla}_{r_{12}} + \Psi^{M\star} \frac{2}{r_{12}} (r_{12}) \, \Psi^N \right]
\end{aligned}
\tag{5.2.10}
$$

Evaluation of the matrix elements is achieved by using integral representations for 3D:

$$
\int d\Omega_1 \int d\Omega_2 \; \mathrm{e}^{-\lambda r_{12}} \, r_{12}^{(p-1)} = 32\pi \int_0^\infty dq \; \frac{\sin(q r_1)}{r_1} \; \frac{\sin(q r_2)}{r_2} \, Q_{3D}[q, \lambda, p]
\tag{5.2.11}
$$

where

$$
Q_{3D}[q, \lambda, p] = (-1)^p \frac{\partial^p}{\partial \lambda^p} \left[ \frac{1}{(q^2 + \lambda^2)} \right] \qquad p = 0, 1, 2, ...
$$

and $\Omega_i, (i = 1, 2)$ are solid angles describing spatial orientation of each electron. Since these integral representations separate coordinates of the electrons from each other, the integrations over $r_1$ and $r_2$ in 5.2.8 and 5.2.10 leads to the integrals in similar form for each electron. These separated integrals, let's name them $G_{3D}$, are calculated analytically and have the general form in terms of hypergeometric

$({}_1F_1)$ and gamma $(\Gamma)$ functions as

$$\begin{aligned} G_{3D}(q,\gamma,\mathrm{W},m,n,k) &= \frac{1}{2}q(\mathrm{W}\gamma)^{\frac{1}{2}(-k-m-n-2)}\Gamma\left(\frac{1}{2}(k+m+n+2)\right) \\ &\quad \times {}_1F_1\left(\frac{1}{2}(k+m+n+2);\frac{3}{2};-\frac{q^2}{4\mathrm{W}\gamma}\right) \end{aligned} \tag{5.2.12}$$

Initially integrations over $r_1$ and $r_2$ coordinates are performed analytically for $H_{MN}$ and $S_{MN}$, then the numerical procedure is applied for the integrations over $q$ variable introduced in 5.2.11.

Under these definitions, 5.2.11 and 5.2.12, the elements of **S** matrix for 3D are obtained according to the expression given below

$$\begin{aligned} S^{3D}_{M,N} &= 32\pi \int_0^\infty dq\, Q_{3D}(q,2\lambda,m_{12}+n_{12}+1) \\ &\quad \times G_{3D}(q,\gamma,\mathrm{W},m1,n1,1)G_{3D}(q,\gamma,\mathrm{W},m2,n2,1). \end{aligned} \tag{5.2.13}$$

By using the lengthly definitions of $A_{nd}$, $B_{nd}$, $C_{nd}$ and $D_{nd}$ given below, the elements of **H** matrix are calculated as follows:

$$\begin{aligned} H^{3D}_{M,N} &= 32\pi \int_0^\infty dq\, [Q_{3D}(q,2\lambda,m_{12}+n_{12}-1)A_{3D} + Q_{3D}(q,2\lambda,m_{12}+n_{12})B_{3D} \\ &\quad + Q_{3D}(q,2\lambda,m_{12}+n_{12}+1)C_{3D} + Q_{3D}(q,2\lambda,m_{12}+n_{12}+2)D_{3D}] \end{aligned} \tag{5.2.14}$$

Procedure similar to the Fourier transforms in three-dimension can be applied to

two-dimensional disk-like QD (2D). Integral representations are obtained as:

$$\int_0^\infty d\theta_1 \int_0^\infty d\theta_2 . \mathrm{e}^{-\lambda r_{12}} r_{12}^{(p-1)} = (2\pi)^2 \int_0^\infty dq\, q\, J_0(qr_1)\, J_0(qr_2) Q_{2D}[q,\lambda,p]$$

where (5.2.15)

$$Q_{2D}[q,\lambda,p] = (-1)^p \frac{\partial^p}{\partial \lambda^p}\left[\frac{1}{\sqrt{q^2+\lambda^2}}\right] \qquad p = 0,1,2,...$$

where $J_0$ is Bessel function. The analytical expression for the integrals in similar form over the separated electron coordinates is found in terms of hypergeometric ${}_1F_1$ and gamma ($\Gamma$) functions as follows:

$$\begin{aligned} G_{2D}(q,\gamma,\mathrm{W},m,n,k) &= \frac{1}{2}(\mathrm{W}\gamma)^{\frac{1}{2}(-k-m-n-1)}\Gamma\left(\frac{1}{2}(k+m+n+1)\right) \\ &\quad \times {}_1F_1\left(\frac{1}{2}(k+m+n+1);1;-\frac{q^2}{4\mathrm{W}\gamma}\right) \end{aligned} \tag{5.2.16}$$

The evaluation of the matrix elements in 2D is similar to the calculation in 3D. Using the definitions for $A_{nd}$, $B_{nd}$, $C_{nd}$ and $D_{nd}$ given below, the matrix elements of **S** and **H** for 2D are

$$\begin{aligned} S^{2D}_{M,N} &= (2\pi)^2 \int_0^\infty q\, dq\, Q_{2D}(q, 2\lambda, m_{12}+n_{12}+1) \\ &\quad \times G_{2D}(q,\gamma,\mathrm{W},m_1,n_1,1) G_{2D}(q,\gamma,\mathrm{W},m_2,n_2,1) \end{aligned} \tag{5.2.17}$$

$$H^{2D}_{M,N} = (2\pi)^2 \int_0^\infty q\,dq\ [Q_{2D}(q,2\lambda,m_{12}+n_{12}-1)A_{2D} + Q_{2D}(q,2\lambda,m_{12}+n_{12})B_{2D}$$

$$+ Q_{2D}(q,2\lambda,m_{12}+n_{12}+1)C_{2D} + Q_{2D}(q,2\lambda,m_{12}+n_{12}+2)D_{2D}]\,. \tag{5.2.18}$$

**Auxiliary definitions:**

If the subscript $nd$ indicates dimension of space, 2D or 3D, definitions used for calculation of the elements of matrix $\mathbf{H}$ are given below:

$$\begin{aligned} A_{nd} = \frac{1}{2}\,&(-(m_2 n_{12} + m_{12} n_2)\, G_{nd}(q,\gamma,\mathrm{W},m_1,n_1,3) G_{nd}(q,\gamma,\mathrm{W},m_2,n_2,-1) \\ &+ ((m_1+m_2)\,n_{12} + m_{12}\,(n_1 + 4\,n_{12} + n_2)) \\ &\quad \times G_{nd}(q,\gamma,\mathrm{W},m_1,n_1,1) G_{nd}(q,\gamma,\mathrm{W},m_2,n_2,1) \\ &- (m_{12} n_1 + m_1 n_{12})\, G_{nd}(q,\gamma,\mathrm{W},m_1,n_1,-1) G_{nd}(q,\gamma,\mathrm{W},m_2,n_2,3)) \end{aligned} \tag{5.2.19}$$

$$\begin{aligned} B_{nd} = \frac{1}{2}\,&((m_2+n_2)\,\lambda G_{nd}(q,\gamma,\mathrm{W},m_1,n_1,3) G_{nd}(q,\gamma,\mathrm{W},m_2,n_2,-1) \\ &- (-4 + (m_1 + 4\,m_{12} + m_2 + n_1 + 4\,n_{12} + n_2)\,\lambda) \\ &\quad \times G_{nd}(q,\gamma,\mathrm{W},m_1,n_1,1) G_{nd}(q,\gamma,\mathrm{W},m_2,n_2,1) \\ &+ (m_1+n_1)\,\lambda G_{nd}(q,\gamma,\mathrm{W},m_1,n_1,-1) G_{nd}(q,\gamma,\mathrm{W},m_2,n_2,3)) \end{aligned} \tag{5.2.20}$$

$$
\begin{aligned}
C_{nd} &= \frac{1}{4}\left(\left(2\left(m_{12}n_1 + m_1\left(2\,n_1 + n_{12}\right)\right)G_{nd}(q,\gamma,\mathrm{W},m_1,n_1,-1)\right.\right.\\
&\quad + \mathrm{W}^2\left(1+4\,\gamma^2\right)G_{nd}(q,\gamma,\mathrm{W},m_1,n_1,3)\Big)\\
&\quad \times G_{nd}(q,\gamma,\mathrm{W},m_2,n_2,1) + G_{nd}(q,\gamma,\mathrm{W},m_1,n_1,1)\\
&\quad \times\left(2\left(m_{12}n_2 + m_2\left(n_{12}+2\,n_2\right)\right)G_{nd}(q,\gamma,\mathrm{W},m_2,n_2,-1)\right.\\
&\quad -4\left(\left(m_1+m_{12}+m_2+n_1+n_{12}+n_2\right)\mathrm{W}\gamma - 2\,\lambda^2\right)G_{nd}(q,\gamma,\mathrm{W},m_2,n_2,1)\\
&\quad \left.\left.+\ \mathrm{W}^2\left(1+4\,\gamma^2\right)G_{nd}(q,\gamma,\mathrm{W},m_2,n_2,3)\right)\right)
\end{aligned}
\tag{5.2.21}
$$

$$
\begin{aligned}
D_{nd} &= -\frac{1}{2}\lambda\left(\left(m_1+n_1\right)G_{nd}(q,\gamma,\mathrm{W},m_1,n_1,-1)G_{nd}(q,\gamma,\mathrm{W},m_2,n_2,1)\right.\\
&\quad +G_{nd}(q,\gamma,\mathrm{W},m_1,n_1,1)\left(\left(m_2+n_2\right)G_{nd}(q,\gamma,\mathrm{W},m_2,n_2,-1)\right.\\
&\quad \left.\left.-\ 4\,\mathrm{W}\,\gamma\,G_{nd}(q,\gamma,\mathrm{W},m_2,n_2,1)\right)\right)
\end{aligned}
\tag{5.2.22}
$$

### *5.2.3 Results and Discussion*

We have performed calculations for the ground state energy of two-electron in parabolic quantum dot by means of Hylleraas-like wavefunction in 5.2.4, which spans powers of $\{n_1, n_2, n_{12}\}$ for the corresponding coordinates $r_1$, $r_2$ and $r_{12}$ and commensurate with the condition $(n_1 + n_2 + n_{12}) \leq 6$. Due to the built-in correlated character of the wavefunction, relatively low expansions are sufficient to ensure a good accuracy without lengthening calculation time. We have calculated the ground state energies for the strengths of dimensionless parameter W between 0.05 and 60.0, which describes the relative magnitude of the

confinement energy and Coulombic energy scales. Also the effects of parabolic confinement for the different quantum dot shapes (3D spherical and 2D disk-like) have been investigated.

In Figure 5.1 we present our variational calculation results for the ground state energy of two electrons in two-dimensional and three-dimensional parabolic quantum dot. In order to show the quantum-size effects and compare with the works have been done previously, we have plotted energies normalized by W as a function of $W^{-1/2}$.

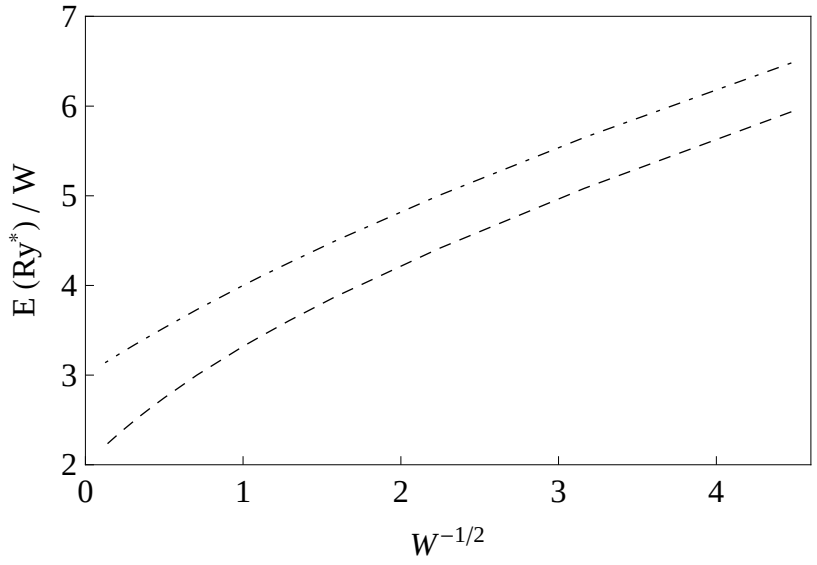


Figure 5.1 Ground state energy, E, normalized by W vs $W^{-1/2}$. The dashed curve represents the results of 2D system while dot dashed curve represents the results of 3D.

The prominent feature of the variational parameters for the two-dimensional QD is that in the weak confinement region, $\lambda$ parameter takes the same value 0.01, whereas the $\gamma$ changes in the range $0.33 - 0.48$. For the intermediate and strong regimes the situation is opposite, i.e., $\gamma$ takes the same value 0.5, whereas the parameter $\lambda$ varies in the range $0.01 - 0.56$. Similar situation is observed also for the three-dimensional system. In the weak confinement regime, $\lambda$ is fixed to

0.01 whereas the range for the $\gamma$ is $0.40 - 0.50$. Redound the value of W from 1.0 to 60.0, the $\gamma$ is fixed to 0.5 despite $\lambda$ varies in the range $0.02 - 0.40$. The values of the parameters $\gamma$ and $\lambda$ for each confinement strength W's are presented in Table 5.4 and Table 5.5. Another important indication of the calculation is that, for the intermediate and strong confinement cases, the convergency is achieved for the small number of expansions both for the 2D and 3D QDs.

Figure 5.1 shows that the qualitative property of the ground state energy level for the 2D and 3D systems are similar with the change of the confinement region of the system, $W^{-1/2}$. However, the quantitative differences are also visible: the normalized ground state energies for the two electrons in 2D QD are located slightly below the corresponding energies for those in 3D QD. This is due to the enhanced effective confinement of electrons in the 2D nanostructure. Also the energies dramatically changed as the $W^{-1/2}$ changes from 0 to 4.4721. It means that the ground state energy depends not only on the dot sizes but also on the dot shapes. Adamowski et al. (2000) studied two electrons confined in 2D and 3D quantum dot under an assumption of Gaussian confining potential and its parabolic approximation. They needed 55 number of basis elements in trial wavefunction which explicitly includes interparticle distance to achieve the required accuracy. In order to investigate the energy spectra of two electrons in 2D harmonic QD, Merkt et al. (1991) applied the numerical diagonalization by using a two-particle wavefunction. They reported that for fixed angular momentum, matrices of size $50 \times 50$ are needed to obtain convergent eigenenergies. It is readily seen that our results, obtained with relatively low number of expansions, are in good agreement with those in Refs. (Merkt et al., 1991; Zhu et al., 1997; Elsaid, 2002), which we can find to compare with. This indicates that the chosen trial wavefunction 5.2.4 is suitable to describe accurately the two-electron states confined in parabolic QDs.

To demonstrate the efficiency of our method with respect to the QD dimensionality and to investigate the details of size effect, it is interesting to study the electron-electron interaction energies, $E_{e-e} = \langle 2/r_{12} \rangle$. The electron-electron interaction energies, calculated at particular confinement frequency W, may be obtained simply by substituting out the energies of noninteracting electrons in parabolic potential from the total energy of the system.

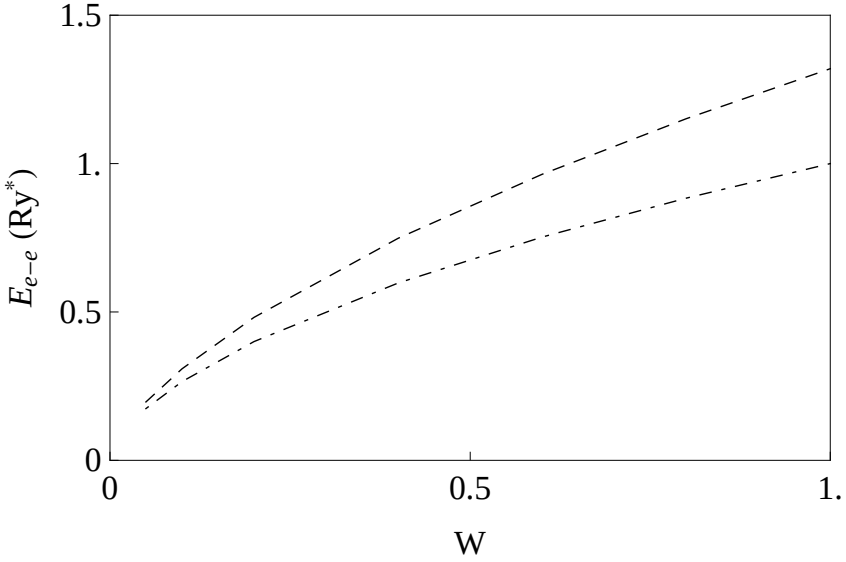


Figure 5.2 Comparison of the Coulomb interaction energy, $E_{e-e}$, vs W for 2D and 3D quantum dot. The dashed curve indicate the two-electron system in 2D while dot-dashed curve indicate the 3D system.

In Figure 5.2, we show the behaviour of the Coulombic energies of the ground state for the two-electron system in a spherical and disk-like QD as W increases. Figure 5.2 is also in good agreement with the energies predicted by the calculations done in Refs. (Zhu et al., 1997; McKinney, & Watson, 2000; Elsaid, 2002). We show the comparison for the ground state energies as well as Coulomb energies at various confinement strengths of two electrons in 2D QDs with those in 3D QDs in Table 5.4 and Table 5.5. It's important to give an attention to the results for the W = 0.05 and W = 1.0 that are frequently given in literature.

Table 5.4 Electron-electron interaction energy for 2D quantum dot calculated using the wavefunction given in 5.2.4 compared with results given in literature. Energies are in units of effective Rydbergs (Ry*).

| W | $\gamma$ | $\lambda$ | E | $E_{e-e}$ |
|---|---|---|---|---|
| 0.05 | 0.33 | 0.01 | 0.2966[a] | 0.1966[a] |
| | | | 0.2952[b] | 0.1951[b] |
| | | | 0.2962[c] | |
| 0.1 | 0.38 | 0.01 | 0.5082[a] | 0.3082[a] |
| | | | | 0.3048[b] |
| 0.2 | 0.42 | 0.01 | 0.8816[a] | 0.4816[a] |
| | | | | 0.4732[b] |
| 0.4 | 0.45 | 0.01 | 1.5479[a] | 0.7479[a] |
| | | | | 0.7290[b] |
| 0.6 | 0.47 | 0.01 | 2.1637[a] | 0.9637[a] |
| | | | | 0.9345[b] |
| 0.8 | 0.48 | 0.01 | 2.7511[a] | 1.1511[a] |
| 1.0 | 0.49 | 0.01 | 3.3195[a] | 1.3195[a] |
| | | | 3.2703[b] | 1.2715[b] |
| | | | 3.3196[c] | |
| 2.0 | 0.50 | 0.01 | 6.0000[a] | 2.0000[a] |
| 4.0 | 0.50 | 0.06 | 10.9930[a] | 2.9930[a] |
| 6.0 | 0.50 | 0.11 | 15.7675[a] | 3.7675[a] |
| 8.0 | 0.50 | 0.15 | 20.4252[a] | 4.4252[a] |
| 10.0 | 0.50 | 0.18 | 25.0071[a] | 5.0071[a] |
| | | | 24.744[b] | |
| 20.0 | 0.50 | 0.31 | 47.3033[a] | 7.3033[a] |
| 40.0 | 0.50 | 0.45 | 90.5677[a] | 10.5677[a] |
| 60.0 | 0.50 | 0.56 | 133.0785[a] | 13.0785[a] |

[a] Present work
[b] Ref. (Elsaid, 2002)
[c] Ref. (Zhu et al., 1997)

Table 5.5 Electron-electron interaction energy for 3D quantum dot calculated using the wavefunction given in 5.2.4 compared with results given in literature. Energies are in units of effective Rydbergs (Ry$^*$).

| W | $\gamma$ | $\lambda$ | E | $E_{e-e}$ |
|---|---|---|---|---|
| 0.05 | 0.40 | 0.01 | 0.3239[a] | 0.1739[a] |
| | | | | 0.1732[b] |
| 0.1 | 0.43 | 0.01 | 0.5650[a] | 0.2650[a] |
| | | | | 0.2634[b] |
| 0.2 | 0.46 | 0.01 | 1.0000[a] | 0.4000[a] |
| | | | | 0.3969[b] |
| 0.4 | 0.48 | 0.01 | 1.7975[a] | 0.5975[a] |
| | | | | 0.5921[b] |
| 0.6 | 0.49 | 0.01 | 2.5521[a] | 0.7521[a] |
| | | | | 0.7447[b] |
| 0.8 | 0.50 | 0.01 | 3.2835[a] | 0.8835[a] |
| 1.0 | 0.50 | 0.02 | 4.0000[a] | 1.0000[a] |
| | | | 3.9896[b] | 0.9896[b] |
| 2.0 | 0.50 | 0.04 | 7.4602[a] | 1.4602[a] |
| 4.0 | 0.50 | 0.08 | 14.1157[a] | 2.1157[a] |
| 6.0 | 0.50 | 0.12 | 20.6204[a] | 2.6204[a] |
| 8.0 | 0.50 | 0.15 | 27.0464[a] | 3.0464[a] |
| 10.0 | 0.50 | 0.17 | 33.4220[a] | 3.4220[a] |
| | | | 33.385[b] | |
| 20.0 | 0.50 | 0.25 | 64.8973[a] | 4.8973[a] |
| 40.0 | 0.50 | 0.34 | 126.9856[a] | 6.9856[a] |
| 60.0 | 0.50 | 0.40 | 188.5886[a] | 8.5886[a] |

[a] Present work
[b] Ref. (Elsaid, 2002)

W = 1.0 is an intermediate regime where neither the confinement energy nor the Coulombic energy scale dominates the other, whereas W = 0.05 is the weak confinement regime. For both of these cases our results are in good agreement with the references given in Table 5.4 and Table 5.5. In addition to this, as the confinement strength strongly increases, i.e. $W \to \infty$ ($W^{-1/2} \to 0$), the energy values approach to the exact results of the harmonic oscillator energies: $E/W = 2.0$ and 3.0, in 2D and 3D, respectively. Thus we can say that our method and variational wavefunction is applicable to the entire range of W. Another important conclusion seen from Tables 5.4 and 5.5 is that the energies enhance as the dimensionality of the quantum dot increases.

## 5.3 Ground State Energy of Excitons in Parabolic Quantum Dot

### *5.3.1 Introduction and Motivation*

Progress in modern nanofabrication techniques made it possible the growth of low-dimensional semiconductor systems where the size and composition could be controlled well. Structures where the strong confinement is imposed in all three spatial dimensions are referred as quantum dot (QD) (Hui, 2004). Dynamical confinement by application of external field on electrons and holes implements of complete quantization of their free motion (Wen-Fang, 2006) that make possible to observe Quantum size effect (QSE) in these quasi-zero-dimensional systems (Kayanuma, 1991). Because of the quantum size effect, quantum dots show many new physical features which differs from bulk systems.

Modern technologies, such as self-organized growth or molecular beam epitaxy, allow scientists to fabricate QDs up to 10 nm where size, shape and properties are well controlled in experiments (Tkach, & Seti, 2007). Since the natural length scale of QDs is about a few nanometers they contain finite number of carriers.

Thus QDs have discontinuous energy spectra (Nair, & Takagahara, 1997). So the increased interest has been focused on Coulomb states of few-particles where quantum mechanical effect can be strongly observed (Thao, & Viet, 2004). This is an attractive area not only for technological application in optoelectronic devices, such as quantum dot lasers, but also for the fundamental researches.

Optical methods are convenient experimental tools for studying the properties of quantum dots. One type of elementary excitations in quantum dots are excitons which play a central role on semiconductor optical properties (Jaziri, & Bennaceur, 1995; Gammon et al., 1996; Xie, 2005). In quasi-zero-dimensional quantum dot systems, the different quantum confinement dramatically changes the optical and electronic properties of the system. Correspondingly, the excitonic spectrum is expected to be strongly affected which improves the electron-hole interaction (Takagahara, 1993).

Theoretical investigations of excitons in QDs have been in strong interest of researches in last two decades. Many studies have been carried out on the electron-hole pair in nanocrystals from various points of view. Among these, variational studies assuming a model of a spherical quantum dot with an effective-mass approximation have been widely used to gain insight into the essential features of quantum size effects (Laheld et al., 1993; Bryant, 1988; Nair et al., 1987; Marin et al., 1998). Generally infinite barriers have been considered as a confinement potential of excitons. Exact numerical analysis of the exciton problem has been done by Hu et al. (1990) where excitonic ground state wavefunction is expanded in terms of single-particle wavefunctions. There are also papers where non-spherical quantum dots, such as boxes, square flat plates and cylindrical shapes, have been investigated (Kayanuma, 1991; Song, & Ulloa, 1995; Bryant, 1988; Marin et al., 2007).

In contrast to various works done on excitonic states in spherical quantum

dots, the works on parabolic confinement are relatively low in numbers (Garm, 1996; Jaziri, & Bennaceur, 1995; Halonen et al., 1992; Xie, 2000). It has been demonstrated theoretically that Far-Infrared light is strongly absorbed for bare parabola frequencies for electrons confined in quantum dot (Brey et al., 1989; Peeters, 1990; Yip, 1991). These theoretical predictions are consistent with experimental measurements done on QDs (Johnson, & Payne, 1991). The evidence that bare potential in many quantum dots has a parabolic form is basic electrostatic models (Dempsey et al., 1990). Sikorksi ,& Merkt (1989) envisaged that the parabolic model is suitable approach for a few electron quantum dots.

In this part of the thesis, we calculated the ground state energy of an exciton in two-dimensional (2D) and three-dimensional (3D) quantum dot by using variational method with Hylleraas-like trial wavefunction.

### *5.3.2 Model and Calculation*

Within the framework of the effective mass approximation, Hamiltonian of a system composed of electron and hole pair confined in a spherical or disk-like quantum dot can be written as

$$\hat{H} = -\frac{\hbar^2}{2m_e}\vec{\nabla}_e^2 - \frac{\hbar^2}{2m_h}\vec{\nabla}_h^2 + V\left(r_e\right) + V\left(r_h\right) - \frac{e^2}{4\pi\varepsilon r_{eh}}\,. \tag{5.3.1}$$

Here $m_e(m_h)$ and $\vec{r}_e(\vec{r}_h)$ are isotropic effective mass of electron (hole) and position vectors, respectively and $r_{eh} = |\vec{r}_e - \vec{r}_h|$ indicates the distance between electron and hole. Also here, $\varepsilon$ is the dielectric constant of the medium where particles move. In terms of simplicity distortion of Coulomb interaction formed due to difference between dielectric constants of quantum dot and matrix material has been neglected. In the model presented in this work unscreened $V(r_i)$, $(i = e, h)$, confinement potential with strength $\omega_0$ for $i^{th}$ particle has been considered as parabolic. So the spherical symmetric potential experienced by both of electron

and hole is chosen to be

$$V(r_i) = \frac{1}{2} m_i \omega_0^2 r_i^2 \quad , \quad (i = e, h). \tag{5.3.2}$$

Assumption of identical parabola frequency for the different charge carriers indicates that the range of electron and hole potentials are approximately the same. This is not a bad approximation for the materials like GaAs (Garm, 1996). Therefore it's expected great overlap between electron and hole wavefunctions and strong Coulomb interaction.

By defining new parameters; $\mu = 1/(m_e^{-1} + m_h^{-1})$ as the reduced effective mass, $\sigma_i = m_i/\mu$ as the dimensionless effective mass of electron $(i = e)$ and hole $(i = h)$, we choose effective Bohr radius $a_{\mathrm{x}}^{\star} = 4\pi\varepsilon\hbar^2/\mu e^2$ as the length scale and effective Hartree energy $E_H^{\star} = \hbar^2/\mu a_{\mathrm{x}}^{\star 2}$ as the energy scale. These new definitions lead to the dimensionless Hamiltonian of the system to be

$$\frac{\hat{H}}{E_H^{\star}} = -\frac{1}{2\sigma_e}\vec{\nabla}^2_{\tilde{r}_e} - \frac{1}{2\sigma_h}\vec{\nabla}^2_{\tilde{r}_h} + \tilde{V}(\tilde{r}_e) + \tilde{V}(\tilde{r}_h) - \frac{1}{\tilde{r}_{eh}}, \tag{5.3.3}$$

where $\tilde{V}(\tilde{r}_i) = \frac{1}{2}\sigma_i \mathrm{W}^2 \tilde{r}_i^2, \quad (i = e, h)$ is dimensionless confinement potential and $\tilde{r}_j\,(j = e, h, eh)$ represent dimensionless coordinates. For simplicity, in what follows we shall use "tildeless" representation of coordinates unless otherwise is stated. $l_0 = \sqrt{\hbar/\mu\omega_0}$ is the characteristic length of quantum dot and dimensionless parameter W is defined as $\mathrm{W} = (a_{\mathrm{x}}^{\star}/l_0)^2$. It's clear that $\mathrm{W}^{-1/2}$ is related with the confinement region of the exciton in a parabolic quantum dot.

The Hamiltonian in 5.3.3 includes six independent spherical coordinates. Using Hylleraas coordinate system which explicitly includes $r_{eh}$ interparticle distance is very convenient for this problem (Kayanuma, 1988). In this coordinate system six degree of freedom are classified into two groups named "*inner*" and "*outer*". Outer coordinates are chosen as three Euler angles that denotes the plane spanned

by $\vec{r}_e$ and $\vec{r}_h$ vectors. It is appropriate to adopt $r_e \equiv |\vec{r}_e|$, $r_h \equiv |\vec{r}_h|$ and $r_{eh} \equiv |\vec{r}_e - \vec{r}_h|$ as the inner coordinates. After taking away the outer coordinates, Schrödinger equation reduces to the form including only inner coordinates (Uozumi et al., 1999; Forrey, 2004). Due to the spherical symmetry of the system, complete description of the ground state can be obtained by these inner coordinates.

The wavefunction expanded in terms of generalized Hylleraas basis set have been used in variational treatment of three-body Coulomb systems with optimization techniques chosen according to the desired accuracy (Aquino et al., 2006). Owing to the correlated character of these functions it's sufficient to use rather low expansions to reach the accurate energies of free two-electron and three-body molecular systems for describing their ground state. In this connection the accuracy of both energy and wavefunctions can be improved by systematic increase of expansion. Our ansatz to find the appropriate wavefunction describing exciton in quantum dot confined by parabolic potential is chosen in the form of

$$\Phi\left(r_e, r_h, r_{eh}\right) = \sum_N C_N \Psi^N\left(r_e, r_h, r_{eh}\right) \tag{5.3.4}$$

where

$$\Psi^N\left(r_e, r_h, r_{eh}\right) = \phi\left(r_e\right)\phi\left(r_h\right) e^{-\lambda r_{eh}}\, r_e^{n_e}\, r_h^{n_h}\, r_{eh}^{n_{eh}}. \tag{5.3.5}$$

The basis function $\phi\left(r_i\right)$ is chosen to be solution of the non-interacting system in the form of

$$\phi\left(r_i\right) = e^{-\gamma \mathrm{W} \sigma_i \frac{r_i^2}{2}} \quad , \quad (i = e, h). \tag{5.3.6}$$

The trial wavefunction, 5.3.4, is spanned by $\mathrm{N} \equiv \{n_e, n_h, n_{eh}\}$ which corresponds to the powers of coordinates $r_e$, $r_h$ and $r_{eh}$, respectively. $\phi\left(r_e\right)\phi\left(r_h\right)$ product in 5.3.5 defines the ground state of uncorrelated electron-hole pair in parabolic confinement with strength W. The next term, $e^{-\lambda r_{eh}}$, describes the Coulombic correlation between electron and hole. And finally $r_e^{n_e} r_h^{n_h} r_{eh}^{n_{eh}}$

product is introduced in order to take into account the spatial correlations where the integers $n_e, n_h, n_{eh}$ are positive or equal to zero. $\lambda$ and $\gamma$ are used as the variational parameters. For simplicity, in what follows we shall drop the $(r_e, r_h, r_{eh})$ dependence of $\Psi^N(r_e, r_h, r_{eh})$.

Having this trial wavefunction, the ground state energy of an exciton in 3D and 2D QD system can be found by using Ritz's variational principle. The linear $C_{n_e,n_h,n_{eh}}$ expansion coefficients and nonlinear $\gamma$ and $\lambda$ parameters in the wavefunction are defined to minimize the average value of energy:

$$< E(\gamma,\lambda) >=< \Phi|\hat{H}|\Phi > / < \Phi|\Phi > \tag{5.3.7}$$

Optimization with respect to the $C_N$ linear expansion coefficients in 5.3.4 is a generalized eigenvalue problem, $\mathbf{H}\,\mathbf{C} = E\ \mathbf{S}\,\mathbf{C}$. Here $\mathbf{H}$ consists of kinetic term, Coulomb interaction and confinement potential, and $\mathbf{S}$ is the norm with respect to the $\Psi^N$. $\mathbf{C}$ stands for the column matrix of $C_{n_e,n_h,n_{eh}}$ coefficients.

Elements of $\mathbf{S}$ overlap matrix are given as

$$S_{M,N} \;=\; \langle \Psi^M|\Psi^N\rangle = \int\int d\vec{r}_e d\vec{r}_h \Psi^{M\star}\Psi^N. \tag{5.3.8}$$

Using the definition of vector operator del expressed in Hylleraas-type coordinates as

$$\vec{\nabla}_i = \hat{r}_i \frac{\partial}{\partial r_i} + \sum_{j\neq i} \hat{r}_{ij} \frac{\partial}{\partial r_{ij}} \tag{5.3.9}$$

and interaction potential $U(r_{eh}) = -1/r_{eh}$, elements of $\mathbf{H}$ Hamiltonian matrix

can be evaluated as follows:

$$
\begin{aligned}
H_{M,N} = & \quad \langle \Psi^M | \hat{H} | \Psi^N \rangle \\
= & \int\int d\vec{r}_e d\vec{r}_h \left[ \frac{1}{2\sigma_e} \vec{\nabla}_{r_e} \Psi^{M\star} \cdot \vec{\nabla}_{r_e} \Psi^N + \Psi^{M\star} V(r_e) \Psi^N \right] \\
+ & \int\int d\vec{r}_e d\vec{r}_h \frac{1}{2\sigma_e} \frac{(r_e^2 - r_h^2 + r_{eh}^2)}{2 r_e r_{eh}} \left( \frac{\partial \Psi^{M\star}}{\partial r_e} \frac{\partial \Psi^N}{\partial r_{eh}} + \frac{\partial \Psi^{M\star}}{\partial r_{eh}} \frac{\partial \Psi^N}{\partial r_e} \right) \\
+ & \int\int d\vec{r}_e d\vec{r}_h \left[ \frac{1}{2\sigma_h} \vec{\nabla}_{r_h} \Psi^{M\star} \cdot \vec{\nabla}_{r_h} \Psi^N + \Psi^{M\star} V(r_h) \Psi^N \right] \\
+ & \int\int d\vec{r}_e d\vec{r}_h \frac{1}{2\sigma_h} \frac{(r_h^2 - r_e^2 + r_{eh}^2)}{2 r_h r_{eh}} \left( \frac{\partial \Psi^{M\star}}{\partial r_h} \frac{\partial \Psi^N}{\partial r_{eh}} + \frac{\partial \Psi^{M\star}}{\partial r_{eh}} \frac{\partial \Psi^N}{\partial r_h} \right) \\
+ & \int\int d\vec{r}_e d\vec{r}_h \left[ \frac{1}{2} \vec{\nabla}_{r_{eh}} \Psi^{M\star} \cdot \vec{\nabla}_{r_{eh}} + \Psi^{M\star} U(r_{eh}) \Psi^N \right]
\end{aligned}
\tag{5.3.10}
$$

Evaluation of matrix elements is performed by using Fourier transforms of the terms like $(e^{-\lambda r_{eh}} r_{eh}^k)$. The obtained integral representations are

$$
\int d\Omega_e \int d\Omega_h \; e^{-\lambda r_{eh}} \; r_{eh}^{(p-1)} = 32\pi \int_0^\infty dq \; \frac{\sin(q r_e)}{r_e} \; \frac{\sin(q r_h)}{r_h} \, Q_{3D}[q, \lambda, p]
\tag{5.3.11}
$$

where

$$
Q_{3D}[q, \lambda, p] = (-1)^p \frac{\partial^p}{\partial \lambda^p} \left[ \frac{1}{(q^2 + \lambda^2)} \right] \qquad p = 0, 1, 2, ...
$$

and $\Omega_i, (i = e, h)$ are solid angles describing spatial orientation of electron and hole. Since these integral representations separate coordinates of electron and hole from each other, the integrations over $r_e$ and $r_h$ in 5.3.8 and 5.3.10 leads to the integrals in similar form for each carrier. These separated integrals, let's name them $G_{3D}$, are calculated analytically and have the general form in terms

of hypergeometric ($_1F_1$) and gamma ($\Gamma$) functions as

$$\begin{aligned} G_{3D}(q,\gamma,\sigma,\mathrm{W},m,n,k) &= \frac{1}{2}q(\mathrm{W}\gamma\sigma)^{\frac{1}{2}(-k-m-n-2)}\Gamma\left(\frac{1}{2}(k+m+n+2)\right) \\ &\quad \times {}_1F_1\left(\frac{1}{2}(k+m+n+2);\frac{3}{2};-\frac{q^2}{4\mathrm{W}\gamma\sigma}\right). \end{aligned} \tag{5.3.12}$$

Initially, integrations over $r_e$ and $r_h$ coordinates are performed analytically for $S_{M,N}$ and $H_{M,N}$, then the numerical procedure is applied for the integrations over $q$ variable introduced in 5.3.11.

Under these definitions, 5.3.11 and 5.3.12, the elements of **S** matrix for 3D are obtained according to the expression given below

$$\begin{aligned} S^{3D}_{M,N} &= 32\pi\int_0^\infty dq\, Q_{3D}(q,2\lambda,m_{eh}+n_{eh}+1) \\ &\quad \times G_{3D}(q,\gamma,\sigma_e,\mathrm{W},m_e,n_e,1)G_{3D}(q,\gamma,\sigma_h,\mathrm{W},m_h,n_h,1). \end{aligned} \tag{5.3.13}$$

By using the lengthly definitions of $A_{nd}$, $B_{nd}$, $C_{nd}$ and $D_{nd}$ given below, the elements of **H** matrix are calculated as follows:

$$\begin{aligned} H^{3D}_{M,N} &= 32\pi\int_0^\infty dq\ [Q_{3D}(q,2\lambda,m_{eh}+n_{eh}-1)D_{3D}+Q_{3D}(q,2\lambda,m_{eh}+n_{eh})C_{3D} \\ &\quad +Q_{3D}(q,2\lambda,m_{eh}+n_{eh}+1)B_{3D}+Q_{3D}(q,2\lambda,m_{eh}+n_{eh}+2)A_{3D}] \end{aligned} \tag{5.3.14}$$

Procedure similar to the Fourier transforms in three-dimension can be applied to

two-dimensional disk-like QD (2D). Using the integral representations,

$$\int d\theta_e \int d\theta_h \, e^{-\lambda r_{eh}} r_{eh}^{(p-1)} = (2\pi)^2 \int_0^\infty dq \; q \; J_0(qr_e) \; J_0(qr_h) Q_{2D}[q, \lambda, p]$$

where (5.3.15)

$$Q_{2D}[q, \lambda, p] = (-1)^p \frac{\partial^p}{\partial \lambda^p} \left[ \frac{1}{\sqrt{q^2 + \lambda^2}} \right] \qquad p = 0, 1, 2, ...$$

and $J_0$ is Bessel function. Analytical expression for the integrals in similar form over the separated electron and hole coordinates is found in terms of hypergeometric ($_1F_1$) and gamma ($\Gamma$) functions as follows:

$$\begin{aligned} G_{2D}(q, \gamma, \sigma, \mathrm{W}, m, n, k) &= \frac{1}{2} (\mathrm{W}\gamma\sigma)^{\frac{1}{2}(-k-m-n-1)} \Gamma\left( \frac{1}{2}(k+m+n+1) \right) \\ &\quad \times {}_1F_1\left( \frac{1}{2}(k+m+n+1); 1; -\frac{q^2}{4\mathrm{W}\gamma\sigma} \right) \end{aligned} \tag{5.3.16}$$

The evaluation of the matrix elements in 2D is similar to the calculation in 3D. Using the definitions for $A_{nd}$, $B_{nd}$, $C_{nd}$ and $D_{nd}$ given below, the matrix elements of **S** and **H** for 2D are

$$\begin{aligned} S_{M,N}^{2D} &= (2\pi)^2 \int_0^\infty dq \; q \, Q_{2D}(q, 2\lambda, m_{eh} + n_{eh} + 1) \\ &\quad \times G_{2D}(q, \gamma, \sigma_e, \mathrm{W}, m_e, n_e, 1) G_{2D}(q, \gamma, \sigma_h, \mathrm{W}, m_h, n_h, 1) \end{aligned} \tag{5.3.17}$$

$$\begin{aligned} H_{M,N}^{2D} &= (2\pi)^2 \int_0^\infty dq \, q \; [Q_{2D}(q, 2\lambda, m_{eh} + n_{eh} - 1) D_{2D} + Q_{2D}(q, 2\lambda, m_{eh} + n_{eh}) C_{2D} \\ &\quad + Q_{2D}(q, 2\lambda, m_{eh} + n_{eh} + 1) B_{2D} + Q_{2D}(q, 2\lambda, m_{eh} + n_{eh} + 2) A_{2D}] \, . \end{aligned} \tag{5.3.18}$$

**Auxiliary definitions:**

If the subscript $nd$ indicates dimension of space, 2D or 3D, definitions used for calculation of the elements of matrix $\mathbf{H}$ are given below:

$$\begin{aligned}
A_{nd} &= \left(-\frac{m_h}{4\sigma_h}-\frac{n_h}{4\sigma_h}\right)\lambda G_{nd}(q,\gamma,\sigma_e,\mathrm{W},m_e,n_e,1)G_{nd}(q,\gamma,\sigma_h,\mathrm{W},m_h,n_h,-1) \\
&+\left(-\frac{m_e}{4\sigma_e}-\frac{n_e}{4\sigma_e}\right)\lambda G_{nd}(q,\gamma,\sigma_e,\mathrm{W},m_e,n_e,-1)G_{nd}(q,\gamma,\sigma_h,\mathrm{W},m_h,n_h,1) \\
&+\mathrm{W}\gamma\lambda G_{nd}(q,\gamma,\sigma_e,\mathrm{W},m_e,n_e,1)G_{nd}(q,\gamma,\sigma_h,\mathrm{W},m_h,n_h,1)
\end{aligned} \tag{5.3.19}$$

$$\begin{aligned}
B_{nd} &= \left(-\frac{m_e\mathrm{W}\gamma}{2}-\frac{m_{eh}\mathrm{W}\gamma}{2}-\frac{m_h\mathrm{W}\gamma}{2}-\frac{n_e\mathrm{W}\gamma}{2}-\frac{n_{eh}\mathrm{W}\gamma}{2}-\frac{n_h\mathrm{W}\gamma}{2}+\frac{\lambda^2}{2}\right) \\
&\times G_{nd}(q,\gamma,\sigma_e,\mathrm{W},m_e,n_e,1)G_{nd}(q,\gamma,\sigma_h,\mathrm{W},m_h,n_h,1) \\
&+\left(\frac{m_en_e}{2\sigma_e}+\frac{m_{eh}n_e}{4\sigma_e}+\frac{m_en_{eh}}{4\sigma_e}\right) \\
&\times G_{nd}(q,\gamma,\sigma_e,\mathrm{W},m_e,n_e,-1)G_{nd}(q,\gamma,\sigma_h,\mathrm{W},m_h,n_h,1) \\
&+\left(\frac{1}{2}\mathrm{W}^2\sigma_e+\frac{1}{2}\mathrm{W}^2\gamma^2\sigma_e\right) \\
&\times G_{nd}(q,\gamma,\sigma_e,\mathrm{W},m_e,n_e,3)G_{nd}(q,\gamma,\sigma_h,\mathrm{W},m_h,n_h,1) \\
&+\left(\frac{m_hn_h}{2\sigma_h}+\frac{m_{eh}n_h}{4\sigma_h}+\frac{m_hn_{eh}}{4\sigma_h}\right) \\
&\times G_{nd}(q,\gamma,\sigma_e,\mathrm{W},m_e,n_e,1)G_{nd}(q,\gamma,\sigma_h,\mathrm{W},m_h,n_h,-1) \\
&+\left(\frac{1}{2}\mathrm{W}^2\sigma_h+\frac{1}{2}\mathrm{W}^2\gamma^2\sigma_h\right) \\
&\times G_{nd}(q,\gamma,\sigma_e,\mathrm{W},m_e,n_e,1)G_{nd}(q,\gamma,\sigma_h,\mathrm{W},m_h,n_h,3)
\end{aligned} \tag{5.3.20}$$

$$
\begin{aligned}
C_{nd} &= \left(-\kappa - \frac{m_{eh}\lambda}{2} - \frac{n_{eh}\lambda}{2} - \frac{m_e\lambda}{4\sigma_e} - \frac{n_e\lambda}{4\sigma_e} - \frac{m_h\lambda}{4\sigma_h} - \frac{n_h\lambda}{4\sigma_h}\right) \\
&\times G_{nd}(q,\gamma,\sigma_e,\mathrm{W},m_e,n_e,1)G_{nd}(q,\gamma,\sigma_h,\mathrm{W},m_h,n_h,1) \\
&+ \left(\frac{m_e\lambda}{4\sigma_e} + \frac{n_e\lambda}{4\sigma_e}\right) G_{nd}(q,\gamma,\sigma_e,\mathrm{W},m_e,n_e,-1)G_{nd}(q,\gamma,\sigma_h,\mathrm{W},m_h,n_h,3) \\
&+ \left(\frac{m_h\lambda}{4\sigma_h} + \frac{n_h\lambda}{4\sigma_h}\right) G_{nd}(q,\gamma,\sigma_e,\mathrm{W},m_e,n_e,3)G_{nd}(q,\gamma,\sigma_h,\mathrm{W},m_h,n_h,-1)
\end{aligned} \tag{5.3.21}
$$

$$
\begin{aligned}
D_{nd} &= \left(\frac{m_{eh}n_{eh}}{2} + \frac{m_{eh}n_e}{4\sigma_e} + \frac{m_en_{eh}}{4\sigma_e} + \frac{m_{eh}n_h}{4\sigma_h} + \frac{m_hn_{eh}}{4\sigma_h}\right) \\
&\times G_{nd}(q,\gamma,\sigma_e,\mathrm{W},m_e,n_e,1)G_{nd}(q,\gamma,\sigma_h,\mathrm{W},m_h,n_h,1) \\
&+ \left(-\frac{m_{eh}n_e}{4\sigma_e} - \frac{m_en_{eh}}{4\sigma_e}\right) \\
&\times G_{nd}(q,\gamma,\sigma_e,\mathrm{W},m_e,n_e,-1)G_{nd}(q,\gamma,\sigma_h,\mathrm{W},m_h,n_h,3) \\
&+ \left(-\frac{m_{eh}n_h}{4\sigma_h} - \frac{m_hn_{eh}}{4\sigma_h}\right) \\
&\times G_{nd}(q,\gamma,\sigma_e,\mathrm{W},m_e,n_e,3)G_{nd}(q,\gamma,\sigma_h,\mathrm{W},m_h,n_h,-1)
\end{aligned} \tag{5.3.22}
$$

### *5.3.3 Results and Discussion*

We have performed calculations for ground state energy of exciton in parabolic quantum dot by means of Hylleraas-like wavefunction in 5.3.4, which spans powers of $\{n_e, n_h, n_{eh}\}$ for the corresponding coordinates $r_e$, $r_h$ and $r_{eh}$ and commensurate with the condition $(n_e + n_h + n_{eh}) \leq 3$. Due to the built-in correlated character of the wavefunction, relatively low expansions are sufficient to

ensure a good accuracy without lengthening calculation time. We have calculated the ground state energies for different radii of quantum dot for both heavy- and light-hole. Also the effects of parabolic confinement potential for different quantum dot shapes (3D spherical and 2D disk-like) have been investigated.

In this section we present the numerical results for the parameters appropriate to GaAs quantum dot. We chose dielectric constant $\varepsilon = 13.1$, electron effective mass $m_e = 0.067\, m_0$, and hole effective mass $m_{lh} = 0.090\, m_0$ for light-hole (lh) and $m_{hh} = 0.377\, m_0$ for heavy-hole (hh) where $m_0$ indicates free electron mass (Jaziri, & Bennaceur, 1995; Halonen et al., 1992).

In Figure 5.3 we present our variational calculation results for the light- and heavy-hole exciton ground state energies in two-dimensional (disk-like) quantum dot as a function of single-particle confinement potential energy, $\hbar\omega_0$. The variational parameters $\lambda$ and $\gamma$ vary in the ranges between $1.9 - 2.0$ and $0.9 - 1.0$, respectively. In principle, for more realistic calculations one should consider the finite thickness of disk-like QD. However, we assumed that the confinement in vertical direction is very strong, so the small corrections arisen from the finite thickness can be ignored.

Decrease in confinement potential, in other words increase in quantum dot radius, leads to monotonically decrease in ground state energy of the exciton. This is due to the decrease of individual confinement energies of the electron and hole states. The confinement of exciton for larger quantum dot radius is getting weaker and behaviour of the exciton resemble to the bulk material.

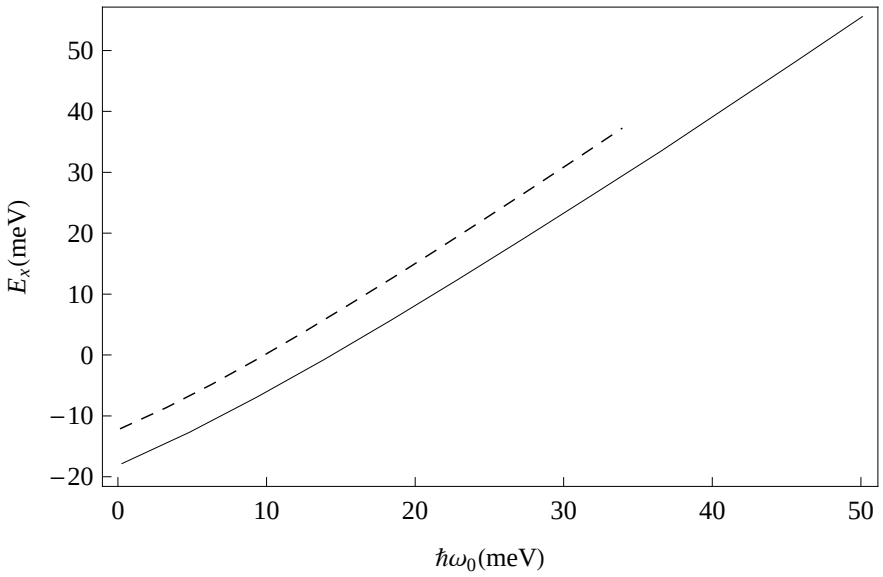


Figure 5.3 Ground state energy of 2D exciton in GaAs quantum dot as a function of a single-particle confinement potential energy. The solid curve here is for heavy-hole exciton while dashed curve is for light-hole exciton.

As seen in Figure 5.3, the energy of light-hole exciton for the same quantum dot radius is greater than that of heavy-hole. The effect of quantum confinement appears more for the electron and light-hole pair than the electron and heavy-hole pair, as expected from lighter charge carriers (Jaziri, et al., 1995). Halonen et al. (1992) calculated the ground state energies for 2D hydrogenic heavy-hole exciton in GaAs by the method of numerical diagonalization. They needed 500 basis states for the expansion of the wavefunction of the system in terms of the eigenfunctions of the non-interacting electron-hole pair to describe accurately the ground state of the system. Que (1992) reported the results for the energies for the exciton in 2D disk-like QD obtained by configuration interaction method, where more than 20 basis states were used. Our results, obtained with relatively low number of expansions, are in good agreement with these previous theoretical calculations of Refs. (Halonen et al., 1992; Que, 1992; El-Said, 1994; Xie, 2005), indicating that the chosen variational wavefunction 5.3.4 is suitable for the exciton states

confined in parabolic QDs.

To further our investigation of the behaviour of the exciton ground state trapped in GaAs QD, in Figure 5.4, we plot the ground state energy of the exciton in 3D spherical parabolic QD as a function of confinement potential. We found the variational parameters $\lambda$ and $\gamma$ of 3D exciton in the range of $0.6 - 0.8$ and $0.8 - 1.1$, respectively. Although the general behaviour of 3D exciton is similar to the 2D disk-like system, there is an obvious quantitative difference in energy values. It's clear that the effect of the effective mass of hole on the system energy is less than that of the 2D exciton. As seen in Figure 5.3 and Figure 5.4 the light-hole exciton calculation stops earlier than the heavy-hole exciton. The reason for that is, simply, we used the same W value for both calculation.

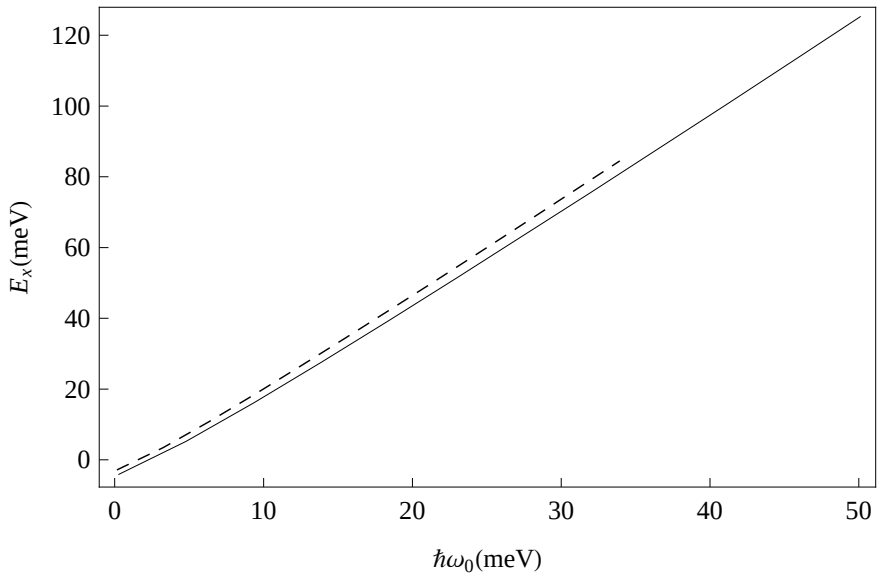


Figure 5.4 Ground state energy of 3D exciton in GaAs quantum dot as a function of a single-particle confinement potential energy. The solid curve is for heavy-hole exciton while dashed curve is for light hole exciton.

Additionally, in order to compare the effect of confinement on the shape of excitonic systems, we present the behaviour of ground state energy of the heavy-hole exciton in parabolic quantum dot for 2D disk-like and 3D spherical

quantum dot as a function of radius of nanocrystal in Figure 5.5. The energy decreases rapidly with increasing QD radius both for 2D and 3D excitons with a quantitative differences.

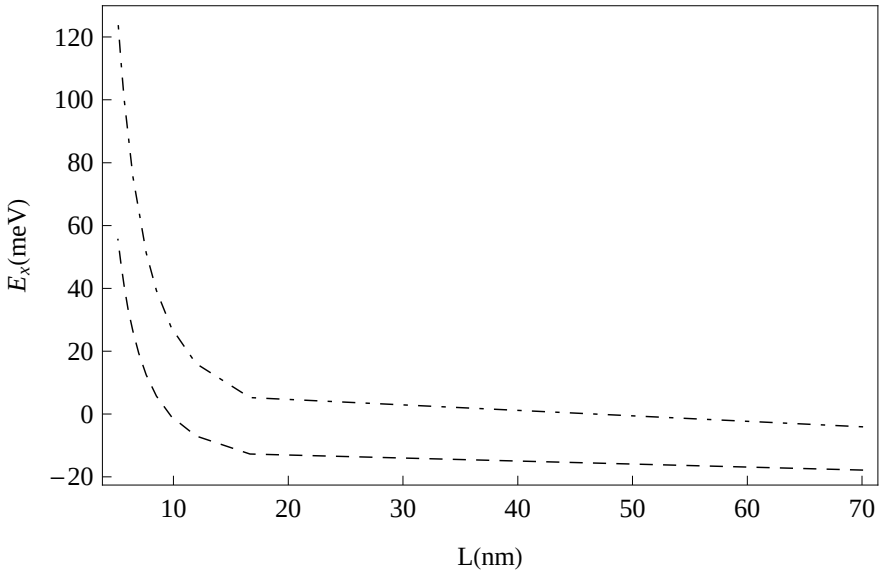


Figure 5.5 Ground state energy of 2D and 3D heavy-hole exciton in GaAs as a function of quantum dot radius. Dashed curve shows the results for 2D exciton and the dot-dashed curve for 3D exciton.

For smaller values of radius, the energy of exciton is more sensitive to the size of the dot. Increasing exciton energies are obtained in the case of narrower QD where the effect of quantum confinement is more pronounced. In this case spatial overlap between electron and hole increases which leads to the enhancement of Coulomb binding energy. Against of this for larger QD radius confinement comes weaker so the energy of the exciton resembles to its bulk value.

The energy of 2D disk-like QD is lower than the value of 3D spherical QD for the same radius. The reason of this situation is the enhanced effective confinement of electron and hole in 2D disk-like QD. This result is in agreement with the results given by Xie (2005).

# CHAPTER SIX
# CONCLUSION

The main objectives of this work have been the variational calculations of the ground state energy of two-particle systems by using Hylleraas-like wavefunctions. Emphasis has also been set on developing and testing the computational method which is useful and essential in these calculations.

In this thesis it has been introduced an computationally efficient approach for the calculation of the expectation value of ground state energy. The choice of explicitly correlated trial wavefunction has an crucial role in application of the introduced method. Hylleraas-like wavefunctions have been used in variational calculations. In this work unlike general numerical integration procedure for Hylleraas coordinates, integral representations obtained from the Fourier transforms for the terms like $e^{-\lambda r_{12}} r_{12}^k$ have been used. This representations provide the calculation of the most of the integrations in matrix elements to be done analytically over single-particle coordinates instead of Hylleraas coordinates, without time-consuming numerical calculations. Inevitable numerical procedure has been invoked at the last stage of the calculations.

In present work, to ensure the validity of our method, ground state energy of three different types of systems composing of two particles have been examined. Firstly, ground state energies of He-like ions have been calculated via Hylleraas like wavefunction. Utilizing minimization parameters obtained from the three parameter simple wavefunction, series expansion leads to the significant improvement on the energy. The accuracy for all two-electron atomic systems which have been investigated in this work have been obtained to be better than $1 \times 10^{-3}$ au. As a second problem, size and shape effects of quantum dot on the ground state energy of electron pair have been investigated. Calculations for the two-electron system in two-dimensional disk-like and three-dimensional spherical

quantum dot lead to qualitatively similar but quantitatively different results for the ground state energies as well as electron-electron energies as expected. Finally ground state energy of exciton in parabolic quantum dot has been considered. Dependencies of the ground state energy as a function of confinement potential and effective mass ratios for the exciton in 2D disk-like and 3D spherical quantum dot have been investigated. Calculations for an exciton in 2D and 3D quantum dot lead to qualitatively similar but quantitatively different results for ground state energies as expected. Comparison with the previous theoretical works both for the excitons and two-electron systems, revealed a good agreement for ground state energies.

Explicit incorporation of interparticle distance in the wavefunction made it possible to accomplish reasonable accurate energies with relatively low number of expansions. Appropriately chosen build-in correlated trial wavefunction describes accurately the ground state energies of the two-particle systems confined in a parabolic quantum dot as well as atomic systems like He isoelectronic sequence. Results on artificial atoms and real atomic systems confirm that the method introduced in this work provides a powerful tool for variational calculations by means of suitable chosen correlated wavefunction. This suggests that the presented method could be used successfully to address the other problems, especially those where a small number of particles are existing.

Application of the introduced method is extendable to many electron quantum dots. However calculations are no so straight forward due to the limitations arising from the inclusion of all interparticle distances in Hylleraas-like wavefunction. As a subsequent work, we are planning to apply the method to the trions and exciton-ionized donor complexes in quantum dots.

The main results of the thesis have been published elsewhere as follows:

1. S. Şakiroğlu, Ü. Doğan, A. Yıldız, K. Akgüngör, H. Epik, Y. Ergün, H. Sarı and İ. Sökmen, (2009). Ground state energy of excitons in quantum dot treated variationally via Hylleraas-like wavefunction. *Chin. Phys. B, 18*, (04), 1-08.

2. S. Şakiroğlu, K. Akgüngör and İ. Sökmen, (2008). Ground state energy of He isoelectronic sequence treated variationally via Hylleraas-like wavefunction. *Chin. Phys. B*, accepted.

3. S. Şakiroğlu, A. Yıldız, Ü. Doğan, K. Akgüngör, H. Epik, Y. Ergün, H. Sarı and İ. Sökmen, (2008). Fourier Transform Technique in variational treatment of two-electron parabolic quantum dot. *Chin. Phys. B*, under review.

## REFERENCES

Abramowitz, M., & Stegun, I. A. (1972). *Handbook of mathematical functions with formulas, graphs, and mathematical tables* (10th ed.).Washinton D.C.: National Bureau of Standards.

Adamowski, J., Sobkowicz, M, Szafran, B., & Bednarek, S. (2000). Electron pair in a Gaussian confining potential. *Phys. Rev. B, 62* (7), 4234–4237.

Ancarani, L. U., Montagnese, T., & Dal Cappello, C. (2004). Role of the helium ground state in (e,3e) processes. *Phys. Rev. A, 70*, 012711.

Ancarani, L.U., Rodriguez, K. V., & Gasaneo, G. (2007). A simple parameter-free wavefunction for the ground state of two-electron atoms. *J. Phys. B: At. Mol. Opt. Phys., 40* (13), 2695–2702.

Aquino, N. (1996). Rational wavefunctions for helium-like ions. *Eur. J. Phys., 17*, 327–330.

Aquino, N., Flores-Riveros, A., & Rivas-Silva, J. F. (2003). The compressed helium atom variationally treated via a correlated Hylleraas wave function. *Phys. Lett. A, 307*, 326–336.

Aquino, N, Garza, J., Flores-Riveros, A., Rivas-Silva, J. F., & Sen, K. D. (2006). Confined helium atom low-lying S states analyzed through correlated Hylleraas wave functions and the Kohn-Sham model. *J. Chem. Phys., 124*, 054311.

Arfken, G. B., & Weber, H. J. (2005). *Mathematical methods for physicists* (6th ed.). USA: Elsevier Academic Press.

Baboczi, K. (2005). *Characterization of II-VI semiconductor nanostructures by low wavenumber Raman- and Four-Wave-Mixing specroscopy.* Würzburg: Ph.D. Thesis.

Bartlett, Jr. J. H., Gobbons, Jr. J. J., & Dunn, C. G. (1935). The normal helium atom. *Phys. Rev., 47*, 679–680.

Baym, G. (1974). *Lecture on Quantum Mechanics* (3th ed.). Mento Park, CA: Benjamin / Cummings.

Bellucci, D. (2005). *Correlated electronic states in artificial molecules under magnetic fields*. Modena: Ph.D. Thesis.

Bianucci, P. (2007). *Optical resonators and quantum dots: An excursion into quantum optics, quantum information and photonics*. Austin: Ph.D. Thesis.

Bhattacharyya, S., Bahttacharyya, A., Talukdar, B., & Deb, N. C. (1996). Analytical approach to the helium-atom ground state using correlated wavefunctions. *J. Phys. B: At. Mol. Opt. Phys., 29*, L147–L150.

Bielinska-Waz, D., Karwowski, J., & Diercksen, G. H. F. (2001). Spectra of confined two-electron atoms. *J. Phys. B: At. Mol. Opt. Phys., 34*, 1987–2000.

Bonham, R. A., & Kohl, D. A. (1966). Simple correlated wavefunctions for the ground state of Heliumlike atoms. *J. Chem. Phys., 45*,2471.

Boyaciglu, B., Saglam, M., & Chatterjee, A. (2007). Two-electron singlet states in semiconductor quantum dots with Gaussian confinement: a single-parameter variational calculation. *J. Phys.: Condens. Matter, 19*, 456217.

Braun, M., Schweizer, W., & Herold, H. (1993). Finite-element calculations for the S states of helium. *Phys. Rev. A, 48* (3), 1916–1920.

Brey, L., Johnson, N. F., & Halperin, B. I. (1989). Optical and magneto-optical absorption in parabolic quantum wells. *Phys. Rev. B, 40* (15), 10647–10649.

Bryant, G. W. (1988). Excitons in quantum boxes: Correlation effects and quantum confinement. *Phys. Rev. B, 37* (15), 8763–8772.

Cassar, M. M. (1998). *Variational calculations for genreal three-body systems.* Ontario: M.Sc. Thesis.

Cassar, M. M. (2004). *High precision theoretical study of* $H_2^+$. Ontario: Ph.D. Thesis.

Chandrasekhar, S., Elbert, D., & Herzberg, G. (1953). Shift of the $1^{1S}$ state of helium. *Phys. Rev., 91* (5), 1172–1173.

Ciftja, O., & Kumar, A. A. (2004). Ground state of tw-dimensional quantum-dot helium in zero magnetic field: Perturbation, diagonalization, and variational theory. *Phys. Rev. B, 70*, 205326.

Ciftja, O., & Faruk, M. G. (2005). Two-dimensional quantum-dot helium in a magnetic field: Variational theory. *Phys. Rev. B, 72*, 205334.

Ciftja, O. & Faruk, M. G. (2006). Two interacting electrons in a one-dimensional parabolic quantum dot: exact numerical diagonalization. *J. Phys.: Condens. Matter, 18*, 2623–2633.

Coolidge, A. S., & James, H. M. (1936). Wave functions for 1s2s $^1S$ helium. *Phys. Rev., 49*, 676–687.

David, C. W. (2006). Compact $1^1S$ helium wave functions. *Phys. Rev. A, 74*, 014501.

Deb, N. C. (1994). Fourier transform technique to calculate matrix elements in the basis of hydrogenic wave functions. *Phys. Scr., 49*, 550–552.

Dempsey, J., Johnson, N. F., Brey, L., & Halperin, B. I. (1990). Collective modes in quantum-dot arrays in magnetic fields. *Phys. Rev. B, 42* (18), 11708–11713.

Dineykhan, M., Zhaugasheva, S. A., & Kalkozova, Zh. K. (2005). Stark splitting of the energy spectrum in a two-electron quantum dot. *Russian Physics Journal, 48* (5), 446–459.

Drake, G. W. F., Cassar, M. M., & Nostor, R. A. (2002). Ground-state energies for helium, $H^-$, and $Ps^-$. *Phys. Rev. A, 65*, 054501.

Dreizler, R. M., & Gross, E. K. U. (1990). *Density functional theory: An approach to the Quantum many-body problem.* Germany: Springer-Verlag.

Drouvelis, P. S., Schmelcher, P., & Diakonos, F. K. (2004). Effects of anisotropy and magnetic fields on two-electron parabolic quantum dots. *J. Phys.: Condens. Matter, 16*, 3633–3646.

El-Said, M. (1994). The ground-state energy of an exciton in a parabolic quantum dot. *Semicond. Sci. Technol., 9*, 272-274.

El-Said, M. (1995). Two-electron quantum dots in a magnetic field. *Semicond. Sci. Technol., 10*, 1310–1314.

El-Said, M. (2000). Spectroscopic structure of two interacting electrons in a quantum dot by the shifted 1/N expansion method. *Phys. Rev. B, 61* (19), 13026–13031.

Ellenberger, C., Ihn, T., Yannouleeas, C., Landman, U., Ensslin, K., Driscoll, D., et al. (2006). Excitation spectrum of two correlated electrons in a lateral quantum dot with neglible Zeeman splitting. *Phys. Rev. Lett., 96*, 126806.

Elsaid, M. K. (2002). The effects of dimensionality on the spectral properties of a two-electron quantum dot. *Chin. J. Phys., 40* (3), 315–324.

Elsaid, M. K. (2007). The ground-state electronic properties of a quantum dot with a magnetic field. *Phys. Scr., 75*, 436–438.

Forrey, R. C. (2004). Compact representation of helium wave functions in perimetric and hyperspherical coordinates. *Phys. Rev. A, 69*, 022504.

Frankowski, K., & Pekeris, C. I. (1966). Logarithmic terms in the wave functions of the ground state of two-electron atoms. *Phys. Rev, 146* (1), 46–49.

Freund, D. E., Huxtable, B. D., & Morgan III, J. D. (1984). Variational calculations on the helium isoelectronic sequence. *Phys. Rev. A, 29* (2), 980–982.

Gammon, D., Snow, E. S., Shanabrook, B. V., Katzer, D. S., & Park, D. (1996). Fine structure splitting in the optical spectra of single GaAs quantum dots. *Phys. Rev. Lett., 76* (16), 3005–3008.

Garm, T. (1996). Exciton states in spherical parabolic GaAs quantum dots. *J. Phys.: Condens. Matter, 8*, 5725-5735.

Ghoshal, A., Kar, S., & Mandal, P. (2003). Correlation functions of types $e^{-\mu r_{12}}$ and $\frac{1}{a+b\,r_{12}}$ for normal two-electron systems. *Phys. Scrp., 67*, 7-22.

Goldman, S. P. (1998). Uncoupling correlated calculations in atomic physics: Very high accuracy and ease. *Phys. Rev. A: At., Mol., and Opt. Phys., 57* (2), R677–R680.

Green, L. C., Mulder, M. M., & Milner, P. C. (1953). Correlation energy in the ground state of He I. *Phys. Rev., 91* (1), 35–39.

Gu, X. Y. (2006). Energy of two-electron quantum dots: The quantization rule approach. *Foundations of Physics, 36* (12), 1884–1892.

Halonen, V., Chakraborty, T., & Pietilainen, P. (1992). Excitons in a parabolic quantum dot in magnetic field. *Phys. Rev. B, 45* (11), 5980–5985.

Harju, A., Siljamaki, S., & Nieminen, R. M. (2002). Wigner molecules in quantum dots: A quantum Monte Carlo study. *Phys. Rev. B, 65*, 075309.

Heeb, E. (1994). *A new variational method with application to strongly correlated electrons*. Zürich: Ph.D. Thesis .

Helle, M. (2006). *Few-electron quantum dot molecules*. Espoo: Ph.D. Thesis.

Hu, Y. Z., Lindberg, M, & Koch, S. W. (1990). Theory of optically excited intrinsic semiconductor quantum dots. *Phys. Rev. B, 42* (3), 1713–1723.

Hui, P. (2004). Quantum-confinement effects on binding energies and optical properties of excitons in quantum dots. *Chin. Phys. Lett., 21* (1), 160–163.

Hylleraas, E. A. (1929). On the ground state of the helium atom. *Z. Phys., 54*, 347.

Ihn, T., Ellenberger, C., Ensslin, K., Yannouleas, C., Landaman, U., Drscoll, D. C., et al. (2006). Quantum dots based on parabolic quantum wells: importance of electronic correlations. *Int. J. Modern Phys. B*, 1-10.

Inci, L. (2004). *Test of cusp conditions and integral recursion relations for helium wave functions*. Ontario: M.Sc. Thesis.

Jacak, L., Hawrylak, P., & Wojs, A. (1998). *Quantum dots*. Heidelberg: Springer.

Jaziri, S. & Bennaceur, R. (1995). Excitonic properties in GaAs parabolic quantum dots. *J. Phys. III France, 5*, 1565–1572.

Johnson, N. F., & Payne, M. C. (1991). Exactly solvable model of interacting particles in a quantum dot. *Phys. Rev. Lett., 67* (9), 1157–1160.

Kayanuma, Y. (1988). Quantum-size effects of interacting electrons and holes in semiconductor microcrystals with spherical shape. *Phys. Rev. B, 38* (14), 9797–9805.

Kayanuma, Y. (1991). Wannier excitons in low-dimensional microstructures: shape dependence of the quantum size effect. *Phys. Rev. B, 44* (23), 13085–13088.

Kent, P. R. C. (1999). *Techniques and applications of Quantum Monte Carlo*. Cambridge: Ph.D. Thesis.

Kimani, P. B. N. (2008). *Electronic structure and electron correlation in weakly confining spherical quantum dot potentials*. Reno: Ph.D. Thesis.

Kinoshita, T. (1957). Ground state of the helium atom. *Phys. Rev., 105* (5), 1490–1502.

Kleinekathofer, U., Patil, S. H., Tang, K. T.,& Toennies, J. P. (1996). Boundary-condition-determined wave function for the ground state of helium and
isoelectronic sequence. *Phys. Rev. A, 54* (4), 2840–2849.

Koga, T. (1990). Hylleraas six-term wave function: Correction. *J. Chem. Phys., 93*, 3720.

Kohanoff, J. (2006). *Electronic structure calculations for solids and molecules: theory and computational methods*. Cambridge: Cambridge Press.

Korobov, V. I. (2000). Coulomb three-body bound-state problem: Variational calculations of nonrelativistic energies. *Phys. Rev. A, 61*, 064503.

Kouwenhoven, L. P., Austing, D. G., & Tarucha, S. (2001). Few-electron quantum dots. *Rep. Prog. Phys., 64*, 701-736.

Laheld, U. E. H., Pedersen, F. B., & Hemmer, P. C. (1993). Excitons in type-II quantum dots: Binding of spatially separated electron and hole. *Phys. Rev. B, 48* (7), 4659–4665.

Lamouche, G., & Fishman, G. (1998). Two interacting electrons in a three-dimensional parabolic quantum dot: a simple solution. *J. Phys.: Condens. Matter, 10*, 7857–7867.

Le Sech, C. (1997). Accurate analytic wavefunctions for two-electron atoms. *J. Phys. B: At. Mol. Opt. Phys., 30*, L47–L50.

Lee, S. (2002). *Optically excited and multiply charged semiconductor quantum dots modeled by empirical tight binding*. Ohio: Ph.D. Thesis.

Lehtonen, O. (2007). *Quantum chemical studies of supramolecular complexex and nanoclusters*. Espoo: Ph.D. Thesis.

Lin, J. T., & Jiang, T. F. (2001). Two interacting electrons in a vertical quantum dot with magnetic fields. *Phys. Rev. B, 64*, 195323.

Maksym, P. A., & Chakraborty, T. (1990). Quantum dots in a magnetic field: Role of electron-electron interactions. *Phys. Rev. Lett., 65* (1), 108–111.

Marin, J. L., Riera, R., & Cruz, S. A. (1998). Confinement of excitons in spherical quantum dots. *J. Phys. Condens. Matter, 10*, 1349–1361.

Marin, J. H., Mikhailov, I. D., & Garcia, L.F. (2007). Charge distribution in quantum dot with trapped exciton. *Physica B, 398*, 135–143.

Masumoto, Y., & Takagahara, T. (2002). *Semiconductor quantum dots: Physics, spectroscopy and applications*. Heidelberg: Springer-Verlag.

McKinney, B. A. & Watson, D. K. (2000). Semiclassical perturbation theory for two electrons in a D-dimensional quantum dot. *Phys. Rev. B, 61* (7), 4958–4962.

Merkt, U., Huser, J., & Wagner, M. (1991). Energy spectra of two electrons in a harmonic quantum dot. *Phys. Rev. B, 43* (9), 7320–7323.

Michler, P. (2003). *Single quantum dots: Fundamentals, applications and new concepts*. Heidelberg: Springer-Verlag.

Mlinar, V. (2007). *Electronic Structure Calculation of Single and Coupled Self-Assembled Quantum Dots*. Belgium: Ph.D. Thesis.

Myers, C. R., Umrigar, C. J., Sethna, J. P., & Morgan III, J. D. (1991). Fock's expansion, Kato's cusp conditions, and the exponential ansatz. *Phys. Rev. A, 44* (9), 5537–5546.

Nair, S. V., Sinha, S., & Rustagi, K. C. (1987). Quantum size effects in spherical semiconductor microcrystals. *Phys. Rev. B, 35* (8), 4098–4101.

Nair, V. S. & Takagahara, T. (1997). Theory of exciton pair states and their nonlinear optical properties in semiconductor quantum dots. *Phys. Rev. B, 55* (8), 5153–5170.

Nistor, R. A. (2004). *Improved strategies for variational calculations for Helium.* Ontario: M.Sc. Thesis.

Otranto, S., Gasaneo, G., & Garibotti, C. R. (2004). Energy and cusp-conditions study for the He isoelectronic sequence. *Nuclear Instruments and Methods in Physics Research B, 217*, 12–17.

Pekeris, C. L. (1958). Ground state of two-electron atoms. *Phys. Rev., 112* (5), 1649–1658.

Pekeris, C. L. (1959). $1^1S$ and $2^3S$ states of helium. *Phys. Rev., 115* (5), 1216–1221.

Patil, S. H. (2004). Electron correlation in He and isoelectronic ions. *Eur. J. Phys., 25*, 91–100.

Pauncz, R. (1979). *Spin eigenfunctions: Construction and use.* New York: Plenum Press.

Peeters, F. M. (1990). Magneto-optics in parabolic quantum dots. *Phys. Rev. B, 42* (2), 1486–1487.

Peeters, F. M., & Schweigert, V. A. (1996). Two-electron quantum discs. *Phys. Rev. B., 53* (3), 1468–1474.

Pfannkuche, D., & Gerhardts, R. R. (1991). Quantum-dot helium: Effects of deviations from a parabolic onfinement potential. *Phys. Rev. B, 44* (23), 13 132–13 135.

Pino, R., & Villalba, V. M. (2001). Calculation of the energy spectrum of a two-electron spherical quantum dot. *J. Phys.: Condend. Matter, 13*, 11651–11660.

Que, W. (1992). Excitons in quantum dots with parabolic confinement. *Phys. Rev. B, 45* (19), 11036–11041.

R*äsä*nen, E. (2004). *Electronic properties of non-circular quantum dots*. Espoo: Ph.D. Thesis.

Reusch, B. (2003). *Quantum simulations of semiconductor quantum dots: From artificial atoms to Wigner molecules*. Düsseldorf: Ph.D. Thesis.

Rodriguez, K. V., & Gasaneo, G. (2005). Accurate Hylleraas-like functions for the He atom with correct cusp conditions. *J. Phys. B: At. Mol. Opt. Phys., 38*, L259–L267.

Rodriguez, K. V., Gasaneo, G., & Mitnik, D. M. (2007). Accurate and simple wavefunctions for the helium isoelectronic sequence with correct cusp conditions. *J. Phys. B: At. Mol. Opt. Phys., 40*, 3923–3939.

Rychlewski, J. (2004). *Explicitly correlated wave functions in chemistry and physics: theory and applications*. Netherlands: Kluwer Acedemic Publishers.

Saarikoski, H. (2003). *Density-functional approaches to interacting electrons in quantum dots*. Espoo: Ph.D. Thesis.

Sako, T., & Diercksen, G. H. F. (2003). Confined quantum systems: a comparison of the spectral properties of the two-electron quantum dot, the negative hydrogen ion and the helium atom. *J. Phys. B: At. Mol. Opt. Phys., 36*, 1681–1702.

Sako, T., & Diercksen, G. H. F. (2003). Confined quantum systems: spectral properties of two-electron quantum dots. *J. Phys.: Condens. Matter, 15*, 5487–5509.

Schwartz, H. M. (1956). Ground-state solution of the nonrelativistic equation for helium. *Phys. Rev., 103* (1), 110–111.

Sikorski, Ch., & Merkt, U. (1989). Specroscopy of electronic states in InSb quantum dots. *Phys. Rev. Lett., 62* (18), 2164–2167.

Siljamaki, S. (2003). *Wave function methods for quantum dots in magnetic field.* Espoo: Ph.D. Thesis.

Siljamaki, S., Harju, A., Rasanen, E., Suorsa, J., & Nieminen, R. M. (2005). Diagonalizations on a correlated basis. *Physica E, 26*, 441–445.

Song, J., & Ulloa, S. E. (1995). Geometrical-confinement effects on excitons in quantum discs. *Phys. Rev. B, 52* (12), 9015–9022.

Styszynski, J., & Karwowski, J. (1988). Multiconfiguration Dirac-Fock study on the ground-state energies of two-electron atoms. *J. Phys. B: At. Mol. Opt. Phys., 21*, 2389–2397.

Sun, L. L., Ma, F. C., & Li S. S. (2003). Energy spectra of two-electron two-dimensional quantum dots confined by elliptical and bowl-like potentials. *Journal of Applied Physics, 94* (9), 5844–5849.

Szabo, A., & Ostlund, N. S. (1989). *Modern Quantum Chemistry: Introduction to advanced electronic structure theory* (1st ed.). USA: McGraw-Hill.

Szafran, B., Adamowski, J., & Bednarek, S. (1999). Ground and excited states of few-electron systems in spherical quantum dots. *Physica E, 4*, 1–10.

Takagahara, T. (1993). Effects of dielectric confinement and electron-hole exchange interaction on excitonic states in semiconductor quantum dots. *Phys. Rev. B, 47* (8), 4569–4584.

Tarucha, S., Austing, D. G., & Honda, T. (1996). Shell filling and spin effects in a few electron quantum dot. *Phys. Rev. Lett., 77* (17), 3613–3616.

Taut, M. (1993). Two electrons in an external oscillator potential: Particular analytic solutions of a Coulomb correlation problem. *Phys. Rev. A, 48* (5), 3561–3566.

Thakkar, A. J., & Koga, T. (1994). Ground-state energies for the helium isoelectronic series. *Phys. Rev. A, 50* (1), 854–856.

Thao, T. T., & Viet, N. A. (2004). Binding energy of exciton in quantum dots with the central-cell correction depending on the dot size. *Commun. Phys., 14* (2), 95–99.

Tkach, M. V., & Seti, J. O. (2007). Exciton in closed and opened quantum dot. *Cond. Matt. Phys., 10* (1(49)), 23–31.

Torsti, T. (2003). *Real-space electronic structure calculations for nanoscale systems*. Espoo: Ph.D. Thesis.

Uozumi, T., Kayanuma, Y., Yamanaka, K., Edamatsu, K., & Itoh, T. (1999). Excited-state absorption of excitons confined in spherical quantum dots. *Phys. Rev. B, 59* (15), 9826–9829.

Uozumi, T., & Kayanuma, Y. (2002). Excited states of an electron-hole pair in spherical quantum dots and their optical properties. *Phys. Rev. B, 65*, 165318.

Vazquez, G. J., del Castillo-Mussot, M., Mendoza, C. I., & Spector, H. N. (2004). Spherical quantum dot under an electric field. *phys. stat. sol. (c), 1* (S1), S54–S57.

Wen-Fang, X. (2006). Binding energies of an exciton in a Gaussian potential quantum dot. *Chin. Phys., 15* (1), 203–208.

Williamson, A. J. (1996). *Quantum Monte Carlo calculations of electronic excitations*. Cambridge: Ph.D. Thesis.

Xie, W. (2000). Exciton states in a disk-like quantum dot. *Physica B, 279*, 253–256.

Xie, Wenfang (2005). Exciton states trapped by a parabolic quantum dot. *Physica B, 358*, 109–113.

Yip, S. K. (1991). Magneto-optical absorption by electrons in the presence of parabolic confinement potentails. *Phys. Rev. B, 43* (2), 1707–1718.

Zhu, J. L., Li, Z. Q., Yu, J. Z., Ohno, K., & Kawazoe, Y. (1997). Size and shape effects of quantum dots on two-electron spectra. *Phys. Rev. B, 55* (23), 15 819–15 823.

# APPENDIX

## FOURIER TRANSFORMS FOR $\exp(-\lambda r)/r$ in 3D and 2D

### A. FOURIER TRANSFORMS FOR $\exp(-\lambda r)/r$ in 3D

**Method A. 1:**

$$I = \frac{2}{(2\pi)^2}\int d\vec{q}\frac{e^{i\vec{q}\cdot\vec{r}}}{(q^2+\lambda^2)} = \frac{e^{-\lambda r}}{r}$$

$$= \frac{2}{(2\pi)^2}\int_0^\infty dq q^2 \int d\Omega_q \frac{1}{(q^2+\lambda^2)}$$

$$\times \quad 4\pi\sum_{l=0}^{\infty}\sum_{m=-l}^{l}(i^l) j_l(qr) Y^\star_{lm}(\Omega_q) Y_{lm}(\Omega_r)$$

since $Y_{l'=0,m'=0}(\Omega_q) = \frac{1}{\sqrt{4\pi}}$

$$I_1 = \sqrt{4\pi}\int d\Omega_q Y^\star_{l,m}(\Omega_q) Y_{0,0}(\Omega_q) = \sqrt{4\pi}\delta_{l,0}\delta_{m,0}$$

$$I = \frac{2}{(2\pi)^2}\int_0^\infty dq \frac{q^2}{(q^2+\lambda^2)} 4\pi\, j_0(qr)\sqrt{4\pi}\frac{1}{\sqrt{4\pi}}$$

$$= \frac{2}{\pi}\int_0^\infty dq \frac{q^2}{(q^2+\lambda^2)} j_0(qr)$$

Spherical Bessel functions are defined as

$$J_0(x) = \sqrt{\frac{\pi}{2x}} J_{1/2}(x) = \frac{\sin(x)}{x} \quad ; J_{1/2}(x) = \sqrt{\frac{2}{\pi x}}\sin(x)$$

$$I = \frac{2}{\pi r}\int_0^\infty dq \frac{q\sin(qr)}{(q^2+\lambda^2)} = \frac{2}{\pi r}.\frac{1}{2}\int_{-\infty}^\infty dq \frac{q\sin(qr)}{(q^2+\lambda^2)}$$

$$= \frac{2}{\pi r}.\frac{1}{4i}\int_{-\infty}^\infty dq \frac{q(e^{iqr}-e^{-iqr})}{(q^2+\lambda^2)} = \frac{2}{\pi r}.\frac{1}{2i}\int_{-\infty}^\infty dq \frac{qe^{iqr}}{(q^2+\lambda^2)}$$

Using residue theorem for the integration in complex plane

$$\int_{-\infty}^\infty dq \frac{qe^{iqr}}{(q^2+\lambda^2)} = 2\pi i \left.\frac{qe^{iqr}}{(q+i\lambda)}\right|_{q=i\lambda} = 2\pi i \frac{i\lambda}{2\lambda i}e^{-\lambda r} = \pi i.e^{-\lambda q}$$

in this situation

$$I = \frac{2}{\pi r}\frac{1}{2i}\pi i.e^{-\lambda r} = \frac{e^{-\lambda r}}{r}$$

**Method A. 2:**

If we assume $\vec{q} = q\hat{z}$ , and $\theta$ is the angle between $\vec{q}$ and $\vec{r}$, then $\vec{q}\cdot\vec{r} = qr\cos\theta$.

$$\begin{aligned}
I &= \frac{2}{(2\pi)^2}\int d\vec{q}\frac{e^{i\vec{q}\cdot\vec{r}}}{(q^2+\lambda^2)} \\
&= \frac{2}{(2\pi)^2}\int_0^\infty dq q^2 \int_0^\pi \sin\theta d\theta \int_0^{2\pi} d\varphi \frac{e^{iqr\cos\theta}}{(q^2+\lambda^2)} \\
&= \frac{1}{\pi}\int_0^\infty dq \frac{q^2}{(q^2+\lambda^2)}.\int_{-1}^{+1} d(\cos\theta)e^{iqr\cos\theta} \\
&= \frac{1}{\pi}\int_0^\infty dq \frac{q^2}{(q^2+\lambda^2)}.\frac{1}{iqr}(e^{iqr}-e^{-iqr}) \\
&= \frac{1}{r\pi i}\int_{-\infty}^\infty dq \frac{qe^{iqr}}{(q^2+\lambda^2)} = \frac{1}{r\pi i}.2\pi i.\left.\frac{qe^{iqr}}{(q+i\lambda)}\right|_{q=i\lambda} \\
&= \frac{e^{-\lambda r}}{r}
\end{aligned}$$

## B. FOURIER TRANSFORMS FOR $\exp(-\lambda r)/r$ in 2D

**Method B. 1:**

$$I = \frac{1}{2\pi}\int d\vec{q}\frac{1}{\sqrt{q^2+\lambda^2}}.e^{i\vec{q}\cdot\vec{r}}$$

$$= \frac{1}{2\pi}\int dq.q.\frac{1}{\sqrt{q^2+\lambda^2}}\int_0^{2\pi} d\theta.e^{iqr\cos\theta}$$

$$e^{iz\cos\varphi} = \sum_{n=-\infty}^{\infty} i^n.J_n(z).e^{in\varphi}$$

By using Rayleigh equation we can perform the integration over $d\theta$ as

$$e^{iqr\cos\theta} = \sum_{n=-\infty}^{\infty} i^n.J_n(qr).e^{in\theta}$$

The integral I is obtained

$$I = \int dq\frac{q}{\sqrt{q^2+\lambda^2}}\sum_{n=-\infty}^{\infty} i^n.J_n(qr)\int_0^{2\pi}\frac{d\theta}{2\pi}e^{in\theta}$$

By using the expression

$$\int_0^{2\pi}\frac{d\theta}{2\pi}e^{in\theta} = \delta_{n,0}$$

we obtain

$$I = \int_0^{2\pi} dq.\frac{q}{\sqrt{q^2+\lambda^2}}J_0(qr) = \frac{e^{-\lambda r}}{r}$$

This integral can be evaluated in Mathematica. In this situation we can write

$$I = \frac{e^{-\lambda r}}{r} = \frac{1}{2\pi}\int d\vec{q}\frac{1}{\sqrt{q^2+\lambda^2}}.e^{i\vec{q}\cdot\vec{r}}$$

**Method B. 2:**

$$\frac{e^{-\lambda r}}{r} = \frac{1}{2\pi}\int d\vec{q}\frac{1}{\sqrt{q^2+\lambda^2}}e^{i\vec{q}\cdot\vec{r}}$$

With aid of Hankel-Nicholson type

$$\int_0^\infty dx\frac{x^{\nu+1}}{(x^2+y^2)^{\mu+1}}J_\nu(ax) = \frac{a^\mu y^{\nu-\mu}K_{\nu-\mu}(ay)}{2^\mu\Gamma(\mu+1)} \qquad ;(a>0,\mathbb{R}y>0,-1<\mathbb{R}\nu<2\mathbb{R}\mu+\frac{3}{2})$$

integral expressions we can easily show that

$$I = \int_0^\infty dq\frac{q}{\sqrt{q^2+\lambda^2}}J_0(qr) = \frac{e^{-\lambda r}}{r}$$

Here $\nu = 0, \mu = -1/2, x = q, y = \lambda, a = r, \Gamma(1/2) = \sqrt{\pi}, K_{1/2}(z) = \sqrt{\frac{\pi}{2z}}e^{-z}$

$$I = \frac{r^{-1/2}\lambda^{1/2}K_{1/2(r\lambda)}}{2^{-1/2}\Gamma(1/2)} = \sqrt{\frac{2}{\pi r}}\sqrt{\lambda}\sqrt{\frac{\pi}{2\lambda r}}e^{-\lambda r} = \frac{e^{-\lambda r}}{r}$$